Susana Luísa Casegas de Carvalho Gomez
Licenciada em Ciências da Engenharia Química e Bioquímica

Taste Masking of Bitter Drugs

Dissertação para obtenção do Grau de Mestre em
Engenharia Química e Bioquímica

Orientador: Doutora Constança Filomena Cacela Pesquinha da Silva, Hovione
FarmaCiência, SA.
Co-orientadores:
Prof. Doutora Ana Isabel Nobre Martins Aguiar de Oliveira Ricardo, FCT-UNL
Doutor Márcio Milton Nunes Temtem, Hovione FarmaCiência, SA.

Júri:

Presidente: Prof. Doutor Mário Fernando José Eusébio, FCT-UNL
Arguente: Prof. Doutora Teresa Maria Alves Casimiro, FCT-UNL
Vogal: Doutora Constança Filomena Cacela Pesquinha da Silva, Hovione FarmaCiência, SA.

FACULDADE DE
CIÊNCIAS E TECNOLOGIA
UNIVERSIDADE NOVA DE LISBOA

Março 2017

Taste Masking of Bitter Drugs

"Derrota tras derrota hasta la victoria final."
Ernesto Che Guevara

Agradecimentos / Acknowledgements

Resumo

O disfarce do sabor de princípios farmacêuticos ativos é crítico no desenvolvimento de formas de dosagem orais sólidas, especialmente para populações pediátricas, mais sensíveis ao gosto dos medicamentos. Assim, é essencial melhorar as metodologias existentes e desenvolver novas abordagens para avaliação da eficácia do disfarce do sabor.

Este trabalho focou-se na produção de formulações de sabor mascarado dum fármaco modelo amargo e um excipiente apropriado, utilizando diferentes processos de co-precipitação: Reactor Agitado, tecnologia AFA (Acústica Focada e Adaptável) e Microfluidização, para comparação no que diz respeito às propriedades de disfarce de sabor. Assim, realizou-se um desenho de experiências para estudar o efeito de diferentes variáveis de formulação (percentagem de droga, concentração de sólidos na alimentação e rácio solvente/antisolvente) nos atributos críticos da qualidade (estado sólido da droga, morfologia e tamanho de partícula e dissolução). A eficiência de encapsulação foi seguidamente determinada utilizando diferentes métodos de dissolução e também técnicas de caracterização superficial (Microscópio Electrónico de Varrimento – Espectroscopia de Energia Dispersiva de Raios-X (SEM-EDS) e Espectroscopia de Fotoelectrão de Raios-X (XPS)).

O sabor das formulações foi mascarado por qualquer um dos processos de co-precipitação utilizados. Uma das formulações produzida pela tecnologia de Microfluidização, foi a melhor atendendo à eficiência de encapsulação, apresentando menor libertação de droga no fluído salivar simulado nos primeiros 5 minutos e melhor eficiência de encapsulação estimada por XPS. Tal, pode dever-se à elevada taxa de mistura fornecida pela tecnologia de Microfluidização. Além disso, os resultados dos estudos de dissolução com alteração de pH de certas formulações e do produto comercial (comprimido revestido) revelaram perfis de dissolução idênticos, indicando que a solubilidade da droga no estômago e intestino superior parece não ter sido influenciada pelos processos utilizados. Relativamente às técnicas utilizadas para avaliação do disfarce do sabor, a análise EDS apresentou algumas limitações enquanto o XPS deu resultados que corroboraram com os dos estudos de dissolução.

Termos-chave: encobrimento de sabor, eficiência de encapsulação, processos de co-precipitação, dissolução, técnicas de caracterização de superfície

Abstract

Taste masking of Active Pharmaceutical Ingredients (APIs) is critical in the development of solid oral dosage forms, since it is related to patient compliance, especially for pediatric populations. Therefore, it is essential to improve the existing methodologies and to develop new approaches that allow assessment of taste-masking efficacy.

The current work focused on the production of taste-masked formulations of a bitter model drug substance and an appropriate excipient, using different co-precipitation processes: Stirred Reactor, Adaptive Focused Acoustics (AFA) technology and Microfluidization, for benchmarking purposes regarding taste masking properties. Thus, an experimental design of experiments was conducted to study the effect of different formulation variables (drug loading, feed solids concentration and solvent/antisolvent volume ratio) in the critical quality attributes of the spray-dried co-precipitated powders (drug's solid state, morphology and particle size and dissolution performance). The encapsulation efficiency (EE) was then evaluated by using different dissolution methods and also surface characterization techniques (Scanning Electron Microscopy – Energy Dispersive X-ray Spectroscopy (SEM-EDS) and X-ray Photoelectron Spectroscopy (XPS)).

Formulations were taste masked using any of the processes disclosed in this work. One of the formulations produced by Microfluidization technology, was the best regarding encapsulation efficiency, presenting a lower drug release in simulated salivary fluid within the first 5 minutes and the best encapsulation efficiency estimated by means of XPS. This can be explained by a high shear rate mixture provided by Microfluidization technology. Moreover, the pH shifts dissolution results for specific formulations and a commercial product (coated tablet) revealed similar dissolution profiles, meaning that the solubility of the drug substance (in the stomach and the upper intestine) seems not to be impacted by the processes used. According with the taste masking assessment techniques, EDS analysis presented some limitations and, in this case, it was proved not to be adequate, contrary to XPS which results corroborated the dissolution ones.

Keywords: taste masking, encapsulation efficiency, co-precipitation processes, dissolution, surface characterization techniques

List of Contents

List of Figures

List of Tables

List of Abbreviations

AAPS	American Association of Pharmaceutical Sciences
ACP	Antisolvent Controlled Precipitation
AES	Auger Electron Spectroscopy
AFA	Adaptive Focused Acoustics
API	Active Pharmaceutical Ingredient
ASD	Amorphous Solid Dispersion
CAM	clarithromycin
CD	Cyclodextrins
CPB	Cycles per burst
CQA	Critical Quality Attributes
CSTR	Continuous Stirred-Tank Reactor
DEX	dextromethorphan
DF	Duty Factor
DoE	Design of Experiments
DMA	Dimethylacetamide
DMF	Dimethylformamide
DMSO	Dimethylsulfoxide
DSC	Differential Scanning Calorimetry
EE	Encapsulation Efficiency
FAT	Fixed Analyzer Transmission
FDT	Fast Disintegrating Tablet
FeSSIF	Fed State Simulated Intestinal Fluid
FIP	International Pharmaceutical Federation
GHP	Hydrophilic Polypropylene
GPCR	G-Protein-Coupled Receptor
HCl	Hydrochloride Acid
HME	Hot Melt Extrusion
HPLC	High-Performance Liquid Chromatography
HREELS	High Resolution Electron Energy Loss Spectroscopy
MCED	Mean Circular Equivalent Diameter
MeOH	Methanol
MRT	Microfluidics Reaction Technology
NCE	New Chemical Entity
NPs	Nanoparticles
ODT	Orally Dispersible Tablet
OSH	ondansetron hydrochloride
PBS	Phosphate Buffer Solution
PIP	Peak Incident Power

PS	Particle Size
PSD	Particle Size Distribution
RDT	Rapid Disintegrating Tablet
RZBT	rizatriptan benzoate
SAS	Supercritical Antisolvent Precipitation
SAS volume ratio	Solvent/Antisolvent volume ratio
SC	Spray Congealing
SD	Spray Drying
SEM(-EDS)	Scanning Electron Microscopy (-Energy Dispersive Spectroscopy)
SHL	shellac
SPFX	sparfloxacin
SSF	Simulated Salivary Fluid
TGA	Thermogravimetric Analysis
TOA	Take-Off Angle
UPLC	Ultra-Performance Liquid Chromatography
UV	Ultaviolet
XPS	X-Ray Photoelectron Spectroscopy
XRD	X-Ray Diffraction
XRPD	X-Ray Powder Diffraction

1. Introduction

1.1. Taste

Taste is defined as the ability of certain cells called taste buds, present all over the surface of the tongue, to percept the flavor of different substances such as food, poisons, minerals and medications (Chirag et al., 2013; Vummaneni and Nagpal, 2012). The mechanism of taste transduction can be conducted by two different forms: the first, based on electrical changes within taste cells, promoted by the diffusion of given ions in the ion channels and the other, involves a complex process of the activation of G-protein-coupled receptors (GPCRs) on the apical surface of taste cells, where the tastants bind (Purves et al., 2001).

According to the chemical structure of the compound, the type of the ions produced in saliva, solubility and the degree of ionization, the sensation interpreted by the brain is different (Shet and Vaidya, 2013). For that reason, there are four primary sensations of taste (sour, salty, sweet and bitter) and a fifth called umami.

The localization of the bitter taste buds is toward the back of the tongue. The bitter taste sensation is caused by almost all organic substances, in particular very long chains ones and alkaloids (for example, quinine, caffeine, strychnine and nicotine). Also, high molecular weight salts may have a bitter taste (Guyton, 1977; Shet and Vaidya, 2013).

1.2. Relevance of Taste Masking

Taste masking has been gaining importance since the majority of APIs found on oral dosage forms present a bitter taste. Examples include macrolide antibiotics, non-steroidal inflammatory and penicillins (Karaman et al. 2014; Maniruzzaman et al. 2014; Karaman et al., 2015).

The need to improve palatability during the development of oral dosage forms has been rising in the last few years. It has become a focus of attention and study, due to patient compliance, especially for people that suffer from chronic diseases, generally geriatric population (Bhalekar et al., 2014; Pawar and Joshi, 2014) and in particular, for children, since they are more sensitive to the bitter taste, presenting a higher number of taste buds than in adults (Pandey et al. 2010).

In fact, the American Academy of Pediatrics estimates that the average compliance in children was approximately 50% in the beginning of the 21st century, in other words 50 in 100 children failed when it came to take the medication (Winnick et al., 2005).

Thus, for medication to be effective it is necessary to be taken appropriately (Matsui, 1997). If this is not the case, it can result in the persistence of the patient's disease symptoms, requiring the use of additional drugs, the need for additional medical appointments and even hospitalizations, which increase healthcare costs, both for the patient and the state. The development of drug-resistant organisms is also a huge concern related to this issue (Suthar and Patel, 2010).

Therefore, taste masking is essential allowing a reduction on the perception of the bitter taste. In general, taste making can be achieved by two different modes: reduce the solubility of the drug in the pH of saliva

or change the nature and affinity of the drug, which will interact with the taste bud receptor (Sagar et al., 2012; Tripathi et al., 2011).

1.3. Overview of Taste Masking Approaches

In the last decades, innumerous approaches were proposed for taste masking purposes, such as addition of sweeteners, coating, solid dispersions, inclusion complexes, granulation, ion exchange resins and microencapsulation (Vummaneni and Nagpal, 2012).

In regards to the evolution of the number of published patents, related with taste masking technologies along the years, which is illustrated in figure 1.1, it is possible to conclude that there is a tendency, since the beginning of the millennium, for the stabilization of the number of published patents related with the addition of sweetener agents. Beyond that, coating technology shows the biggest development in terms of studies with published patents in the last decades. Other technologies, such as microencapsulation and granulation, have also shown merit resulting in new published patents.
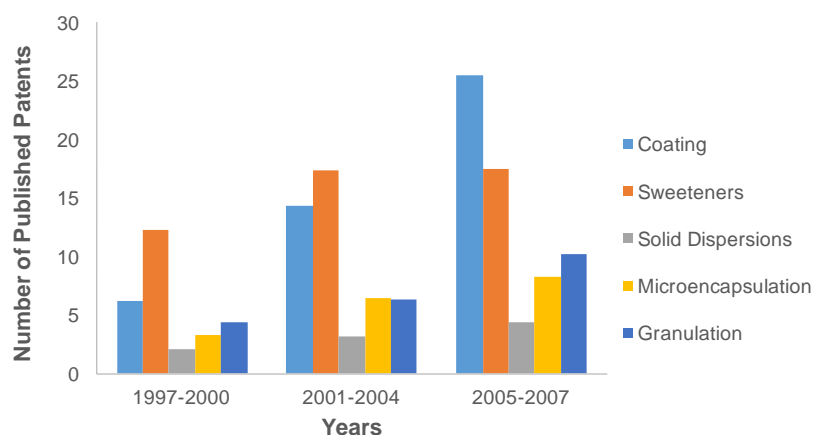
Figure 1.1 Evolution of the number of published patents related to taste masking technologies between 1997 to 2007 (adapted from Ayenew et al. 2009).

To select the most appropriate approach, it is necessary to take into consideration factors like:
- ✓ dose of API - usually, with high doses the coating approach is used while with small doses, sweeteners and flavoring agents are added to the formulation (P. Kumar, 2015);
- ✓ intensity of the drug's bitter taste - for extremely bitter drugs, the use of simple techniques, like the addition of sweeteners, may be insufficient by itself to achieve taste masking, therefore complementary techniques like coating and microencapsulation are used to improve the efficiency of taste masking (Chirag et al. 2013; Karaman 2012);
- ✓ type of dosage form;
- ✓ drug solubility;
- ✓ ionic characteristic of drug;
- ✓ drug particle shape and size distribution - if the final particles have core materials with irregular shapes and small particle size (PS), it may result on poor efficiency of taste masking (Chirag et al., 2013).

In this thesis, a new microencapsulation approach was used for taste masking purposes of a bitter taste antibiotic selected as model compound. By coating the particles, a physical barrier is created between

the drug and the taste buds receptors, resulting on the reduction on drug solubility and consequent taste improvement (Sourabh et al., 2012). In table 1.1 it is presented the taste masking state of the art, using microencapsulation as the main approach.

Table 1.1 List of several drugs that were taste masked through microencapsulation process.

Drug	Polymer	Aim of the study	Techniques used	References
beclamide	Gelatin, anhydrous sodium sulfate	Mask the bitter taste	Simple coacervation	(Ozer and Hincal, 1990)
cefuroxime axetil	CAT,BP MCP-55 UPMCP 50	Mask the bitter taste and assure its release in the intestinal cavity	Solvent evaporation and solvent extraction	(Cuña et al., 1997)
diclofenac sodium	Ethyl cellulose	Mask the bitter taste, without affecting the drug release rate	Precipitation	(Al-Omran et al., 2002)
flucloxacilin	17 % Ethyl Cellulose	Assure the availability for taste abatement of the drug from the tablet as the raw unprocessed antibiotic	n.s.	(Maccari et al. 1980)
ibuprofen	Methacylic acid copolymer	To obtain chewable taste masked tablet with release characteristics.	Fluid Bed Coating	(Shen, 1991)
indeloxazine	Hydrogenated oil and surfactant	Assure the taste masking of the drug and the bioavailability by heat treatment.	Fluidized bed using the side-spray method	(Sugao et al., 1998)

1.4. Motivations and Objectives

The microencapsulation of the particles can be achieved using different techniques, namely spray drying (SD), spray congealing (SC), fluid bed coating, coacervation phase separation, among others. The focus of the current work was to develop and study alternative processes for the microencapsulation of active ingredients and enhance taste masking properties.

Thus, this thesis discloses alternative processes that are based on co-precipitation principles, in particular liquid antisolvent precipitation, with the main goal of producing taste masked formulations of a model drug.

Several goals were defined for this thesis:

I. To investigate the conventional antisolvent precipitation process in a stirred batch reactor, producing taste masked formulations of the model drug, according to the design of experiments (DoE), and to study the impact of the formulation variables on the critical quality attributes

(CQAs) (solid state, particle size and morphology and *in vitro* performance), as well as taste masking properties;

II. To develop a novel antisolvent precipitation process based on microfluidization, using a new setup PureNano™, producing taste masked formulations of a model drug and studying the impact of the aforementioned formulation variables in taste masking properties and CQAs;

III. To study through an innovative technology called Adaptive Focused Acoustics™ (AFA) system based on ultrasound treatment, developed by Covaris® (company that provides technologies that allow to improve sample preparation and novel drug formulations), the same formulations produced by PureNano and stirred batch reactor approaches;

IV. To benchmark the different technologies used in this thesis, by comparing and studying the impact that the use of each technology has in the critical quality attributes and more important, in taste masking properties;

V. To develop and apply analytical characterization techniques to assess the efficiency of encapsulation of the produced formulations.

1.5. Thesis Layout

In *Chapter 2*, a literature review is given, presenting the main work related with existing taste masking technologies, with special focus on the co-precipitation method.

Chapter 3 presents a selection of current literature on the existing taste masking assessment technologies, with particular reference to *in vitro* dissolution studies and also characterization surface techniques, since those will be the methods of particular relevance in this project.

Chapter 4 describes the materials and methods applied in this research, as well as the methodology or protocol followed for each laboratory experiment or analytical characterization.

The results and discussion of the experimental work developed in the laboratory and analytical characterization of the powders produced are presented in *Chapter 5*, with the main purpose of benchmarking co-precipitation technologies regarding the taste masking properties. This chapter is divided in six subchapters: the first four are related with general aspects of analytical characterization of the spray-dried co-precipitated powders - morphology, particle size, drug's solid state and also drug content in the formulations -, while the last two subchapters are related to the determination of encapsulation efficiency and taste masking properties – *in vitro* dissolution studies, determination of encapsulation efficiency using SEM-EDS (Scanning Electron Microscopy-Energy Dispersive Spectroscopy) and XPS (X-Ray Photoelectron Spectroscopy) analysis.

Chapter 6 presents the general conclusions obtained in this work and also provides some recommendations for further research and work.

2. Overview of Taste Masking Technologies

2.1. Spray Drying (SD)

SD emerged during World War II with the necessity to reduce the transport weight of foods, e.g. the production of powder milk, and other materials (Patel et al. 2009). It is a powerful technique for particle engineering used in many applications in the pharmaceutical industry, and among the different taste masking technologies is one of the most simple and viable approaches (Dobry et al., 2009; Kaushik and Dureja, 2015).

In SD, a stream - solution, suspension or emulsion - is fed, at controlled rate flow, to an atomizer, located inside the chamber, concurrently or counter currently with a hot drying gas. The atomizer will transform the solution into very fine droplets, and the hot drying gas is responsible for the drying of the particles. These are then collected and separated from the hot drying gas, through a cyclone, usually followed by a bag-filter, that will collect the fine particles existing in the system (Dobry et al. 2009; Gil et al. 2010). Spray dryers can operate in different configurations. Generally, laboratory SD's operate in an open cycle mode, where drying gas passes to the chamber and then is exhausted to the appropriate waste stream (BETE Fog Nozzle, 2005; Dobry et al., 2009). Many large pilot-scale and production-scale SD's operate in a closed-loop mode, characterized by a gas recycle unit. The hot gas passes through a condenser to remove the residual solvent and then, is reheated in a heat exchanger, to obtain the initial operational conditions, being reinserted in the drying chamber (Dobry et al. 2009; Gil et al. 2010), as illustrated in figure 2.1.
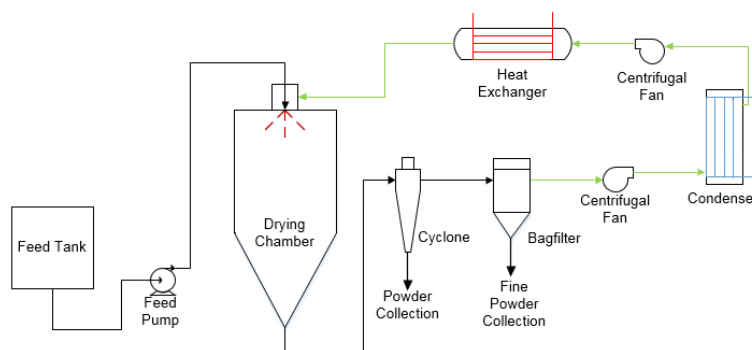
Figure 2.1 Closed cycle Spray Drying equipment configuration, at green is represented the gas recycle unit (adapted from Dobry et al. 2009).

The atomization is an essential step, since it controls the droplets size and consequently the particle size. There are several types of nozzles used for atomization and the most commonly used are rotary, pressure, two-fluids and ultrasonic nozzles (Gil et al. 2010; Kaushik and Dureja 2015). The selection of the suitable type of nozzle has to take into consideration the intended morphology and particle size (e.g., a narrow particle size distribution (PSD) is obtained using a pressure nozzle instead of two fluid nozzle), as well as the viscosity of the liquid stream (e.g., two fluid nozzle has a lower sensitivity to viscosity when compared to pressure nozzle).

Sollohub et al. (2011) used SD to obtain microparticles of roxithromycin with high taste masking efficiency. These authors concluded, through an electronic tongue study, that in water the taste masking effect remained at least several dozen hours.

Bora et al. (2008) studied the use of three different polymers (Chitosan, Methocel E15 LV and Eudragit E100) for the formation of taste-masked microspheres of intensely bitter drug ondansetron hydrochloride (OSH) by SD. The authors concluded that in Methocel microspheres the taste masking was absent for all the drug-polymer ratios. The Chitosan microspheres showed taste masking at 1:1 drug-polymer ratio, whereas Eudragit microspheres displayed taste masking at 1:2 drug-polymer ratio. Dissolution studies reveal, for Eudragit microspheres, 97 % of drug release within 15 min, while for Chitosan microspheres was verified a drug release of 40 %. Thus, the selection of the suitable polymer and also the proportion between polymer and drug is very important since it can affect the properties of the final product, namely the dissolution of the drug and taste masking properties.

Lukas et al. (1997) developed paracetamol taste masked formulation by SD method using ethyl cellulose as the coating material. According to this study, the use of coating material with less than 23 % of the total weight of the formulation, provides taste masking characteristics. The authors proved that the coated paracetamol composition, prepared in a first phase as a powder and then transformed into tablets, exhibits immediate release properties, maintaining the taste masking properties.

2.2. Spray Congealing (SC)

Another technique used for microencapsulation, is spray congealing or spray chilling. This technique relies on the same principle as SD, however the API is dissolved (or suspended) in a melted excipient (typically, matrix material), forming a molten mixture that is atomized into a cooling air, where the molten droplets are congealed leading to the particle formation (Mackaplow et al. 2006). Matos and Duarte (2016) and Qiyun (2008) consider that the transformation of molten droplets from liquid to solid occurs with the removal of energy from the droplets.

Yajima et al. (1996) assessed the palatability and taste of clarithromycin (CAM) formulation through SC technique. Results were significantly better when compared with conventional coated granules. Moreover, the *in vitro* dissolution studies showed that in a buffer solution at pH=6.5, the amount of CAM released was less than the threshold concentration of the bitter taste (14 mg/L).

Maschke et al. (2007) reported that the application of SC technique for the preparation of insulin-loaded lipid microparticles led to a good EE, since the microparticles did not show a burst release in the dissolution test. Thus, an efficient encapsulation can inhibit the escape of API from microparticles, enabling a lower perception of the bitter taste.

Similarly, Cordeiro et al. (2014) analyzed the taste masking efficiency of a model drug (quinine sulphate) produced through SC and Hot Melt Extrusion (HME) techniques by SEM-EDS and fluorescence microscopy. By SEM-EDS, the sulphur element peaks were not detected (characteristic from API molecule) in the surface of the particles produced by SC, while these peaks were detected in the surface of particles produced by HME. Regarding the fluorescence microscopy trials, the extruded material revealed a higher intensity of fluorescence when compared with spray congealed particles. Therefore, in terms of taste masking better results were obtained with the SC technique then with HME.

2.3. Hot Melt Extrusion (HME)

Joseph Brama established the HME process in the end of the eighteenth century. It can be applied to a large range of pharmaceutical dosage forms such as capsules, tablets, films and implants for drug delivery via oral, transdermal and trans mucosal (R.V. Tiwari et al. 2016). For that reason, HME is a good alternative to other conventional methods, such as SD (Maniruzzaman et al. 2012).

HME allows to melt blends of polymer, excipients and API, forcing the material to pass by an hole, compressing it and converting it into a uniform shape product (Maniruzzaman et al. 2012; Particle Sciences Inc. 2011). The process requires a premixing step, where the API, polymer and excipients are blended and then inserted into the rotating screw by an hopper (Patel et al. 2013). The extruder is mainly divided into three zones: feeding, melting or compression, and metering, as shown in figure 2.2.
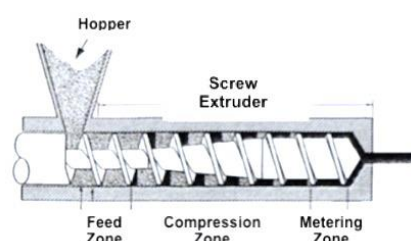
Figure 2.2 Schematic representation of mainly sections along a single screw extruder (adapted from (Patel et al. 2013)).

The process requires downstream auxiliary equipment to finish, shape and analyze the extruded material, being necessary to cool, cut and/or collect the finished product, and obtain it in the desired shaped (Kolter et al., 2012).

Pimparade et al. (2015) developed taste masked caffeine citrate formulations using HME. They performed an *in vitro* study, which revealed an insignificant amount of drug release in the salivary medium, while in 0.1 N Hydrochloride Acid (HCl) a drug release over 80 % within the first 30 min was obtained. Likewise, Petereit et al. (2014) produced taste masked verapamil HCl granules via HME using Eudragit® L100/L100-55. They identified as responsible for taste masking, the strong hydrogen bonding interaction with the functional group of the API-polymer mixture. The efficiency of taste masking formulations with different drug loads was evaluated, concluding that for drug loadings about 30-50% a neutral taste was verified. However, when the drug load was increased to 70% a slightly bitter taste perceived. In addition, taste masking efficiency can be improved by increasing the temperature and the screw rotation speeds.

2.4. Co-precipitation

According to Simonelli et al. (1969) the co-precipitation arises in pharmaceutical industry to produce amorphous solid dispersions (ASD's), based on the simultaneous precipitation of drug and polymer by changing the solubility conditions.

It occurs when two components, simultaneously, exceed their solubility, resulting in the incorporation of the minor component in the matrix of the major one (Shah et al. 2014). The co-precipitation became

known both for the production of compounds with small particle size and the improvement of the final properties of challenging crystalline APIs (I. Duarte, 2016; Pouretedal, 2014; Thorat and Dalvi, 2011). Nowadays, this technology has been emerging to improve the drug solubility (I. Duarte, 2016) and also for taste masking applications. In this way, Sharma et al. (2012) compared the results obtained for several sumatriptan succinate formulations produced by different taste masking technologies, and concluded that the precipitation method was one of the best techniques for this particular drug. All the volunteers that made part of the human panel considered the formulation as being completely taste masked. In the same way, Limmatvapirat et al. (2012) showed that the taste masking of dextromethorphan (DEX) can be easily accomplished by the co-precipitation technique, using a shellac (SHL) based matrix. The major evidence was an *in-vitro* study in artificial saliva at DEX-SHL weight ratios of 5:10 or less, that revealed a drug release lesser than 1 %.

2.4.1. Phase Equilibrium and General Considerations

The solubility is defined as the capacity of a solute to dissolve in a solvent originating a homogeneous solution, i.e., the maximum concentration of solute that can exist in a certain volume of solvent in equilibrium with the solid form of the solute precipitated. The equilibrium of solubility is dynamic, and in certain conditions the concentration of solute may exceed the solubility value to originate a suspension (Savjani et al., 2012).

The equilibrium phase diagram of solubility showed in figure 2.3, is an important tool to understand the causes of the precipitation phenomena, and also which is the more adequate process for the production of a given drug substance.
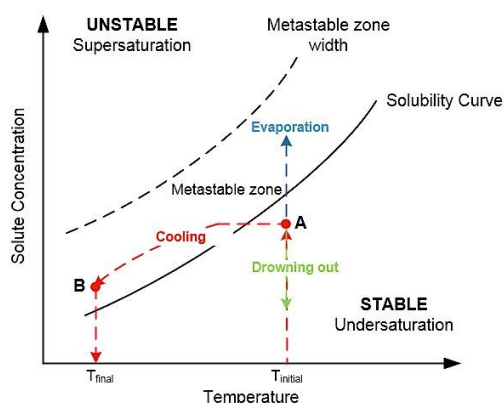
Figure 2.3 Phase equilibrium diagram with the different zones, where it is represented the trajectory to the cooling precipitation (red line), evaporative precipitation (blue line) and antisolvent precipitation or drowning out (green line) adapted from (Cogoni, 2012; Smith, 2005).

There are three distinct zones figuring out in the diagram: **undersaturated region** - crystals will dissolve, it is also called stable zone -, **metastable region** - supersaturated region, in which crystals grow through heterogeneous nucleation – and, **supersaturated region** – in which occurs spontaneous nucleation and crystal growth (Cogoni, 2012; Paiva Lacerda, 2013).

According to Mansour et al. (2013), the process of precipitation involves the creation of supersaturation, that induce nucleation and simultaneously growth by coagulation or condensation. However, the agglomeration can become more evident if the growth occurs uncontrolled. As known and as highlighted

by Panagiotou and Fisher (2011), in order to generate solids from a liquid phase, the thermodynamics aspects are important. Therefore, firstly it is necessary to change the thermodynamic state of the solution to reduce the solubility of the compound, by temperature, pH and concentration changes or altering the solubility coefficients (Agrawal, 2010).

In the unstable region, it is not necessary to have heterogeneous nucleation sites to initiate the formation of the solid phase. In this zone, as the supersaturated liquid isn't stable neither is in equilibrium, take place a spontaneous homogeneous nucleation and rapid growth of the solids. Panagiotou and Fisher (2008) look at this zone as the desired initial operational region, since leads to the creation of a large number of nucleation sites, minimizing the ultimate size of the individual particles and making possible the control of particle's morphology.

Thorat and Dalvi (2011) realized that the high and rapid supersaturation is the main driving force of the process and Cogoni (2012) has proposed a way to calculate it through the change in chemical potential between standing and equilibrium states.

Nucleation is a result of the molecules combination of a particular element, in a process called molecular assembly. Nucleation may be heterogeneous, as previously said, or homogeneous, depending on whether it uses foreign substances or not, respectively. After the process of nucleation, the crystal growth dominates, allowing to obtain a crystal form with defined size and shape (Sriamornsak and Burapapadh, 2015).

2.4.2. Precipitation Techniques

There are several precipitation methods that have been used in pharmaceutical industry, such as: melt, evaporative and cooling precipitation (Sriamornsak and Burapapadh, 2015), supercritical antisolvent precipitation (SAS) and antisolvent precipitation (Danish et al., 2013).

2.4.2.1. Cooling Precipitation

This process is based on the fact that temperature affects the solubility of the majority of the compounds (Holañ et al., 2015) and is the most widely used technique to create supersaturation (Wey and Karpinski, 2002).

This technique is applied when the solubility of a substance decreases significantly with temperature (Baliga, 1970). In figure 2.3 a trajectory from a cooling process from point A to point B is illustrated. Point A is located in the unsaturated zone; by cooling, the process can be directed towards the metastable zone. Then, a specific cooling and controlled profile is designed until the final temperature, which allows us to obtain the desirable properties of the crystals (Smith, 2005).

In this process, the tank is fed with the unsaturated solution that is cooled inside the tank or via an external jacket. In order to keep supersaturation practically constant during the cooling period the cooling rate should be set (Mersmann 2001).

Raghavan et al. (2003) prepared a pediatric formulation of taste masked gatifloxacin using a cooling precipitation method, resulting in a crystalline co-precipitate of gatifloxacin with a stearic acid and/or palmitic acid. They reported the efficiency of taste masking in mouth and in aqueous suspension through a full dosage cycle of about fourteen days.

Similarly, Bellinghausen et al. (2009) invented a new taste-masked powder, for oral administration with the formation of a coated solid, by a cooling precipitation method. The authors proved that, the bitter taste of praziquantel with Wax C80 wasn't perceived, even after a period of 10 minutes after the tablet application, into the tongue. In fact, even if the formulation had been chewed for a few minutes, it did not release the bitter taste.

2.4.2.2. Evaporative Precipitation

As the name implies, the creation of supersaturation in this method is a result of the solvent evaporation, leading to the formation of a solid phase (Lewis et al. 2015).

This technique can be applied for compounds that have an "inverse" dependence of the solubility with temperature (e.g. Na_2SO_4) or that the solubility depends weakly on temperature (e.g. NaCl) (GEA Process Engineering, 2012; Giulietti et al., 2001). The equipment used for this process operates at reduced pressure (GEA Process Engineering, 2012) and constant temperature (Wey and Karpinski, 2002).

In this process, the tank is fed with an undersaturated solution, which is heated until the boiling point of the solution to promote a faster evaporation of the solvent. Once again, in order to keep the supersaturation practically constant it is favorable to set the rate of evaporation so that an optimum value for crystal size distribution may be obtained (Mersmann, 2001).

Shishu et al. (2010) developed taste masked ordinazole microspheres by solvent evaporation technique, and the taste assessment was done by panelist. All the voluntary humans reported microspheres as tasteless, however when microspheres were compressed into Fast Disintegrating Tablets (FDTs) the majority of people classified it as a good taste and only one person as tasteless. Thus, the final dosage form is a factor to have in account, since it impacts the taste masking properties.

2.4.2.3. Antisolvent Controlled Precipitation (ACP)

The ACP is also known as a bottom up approach, based on the arrangement of atoms, molecules or macromolecules, making possible a better control of particle size and a more homogeneous particle size distribution (De et al., 2014). The concept of antisolvent controlled precipitation (ACP) is the mix of a solution, composed by API and excipient dissolved in a certain solvent, with an antisolvent, in which the API must be insoluble. The mix of the solution with the antisolvent is responsible for an increasing of supersaturation, leading to the precipitation, as a result of a reduction of drug solubility (Matsumoto et al. 2013; Viçosa et al. 2012). In figure 2.4, the process aforementioned explained is shown.
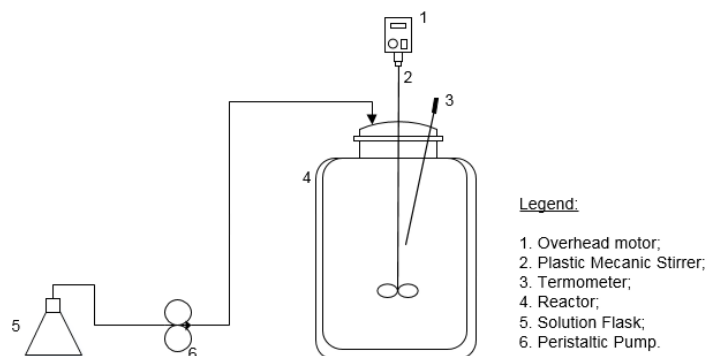
Figure 2.4 Schematic representation of a batch antisolvent precipitation process (adapted from (Yu et al., 2005)).

The antisolvent precipitation has been used to produce co-crystals (Wang et al., 2013), single drug particles (Dong et al., 2009; Viçosa et al., 2012) and amorphous solid dispersions (Í. Duarte et al., 2015; Porfírio et al., 2015; N. Shah et al., 2013). The process can operate at two modes: batch and continuous confined flow. In a batch process, the solution with the API and polymer is injected into the vessel by a small orifice, promoting the rapid mix of the resulting suspension. The main drawback is the poor mixing when compared to the continuous confined geometries, thus the control of the particle size could be compromised, conducting to the production of larger size particles (D'Addio and Prud'homme, 2011).

An alternative is the simultaneously injection of solvent and antisolvent streams into a cavity called "confined impinging jet" (CIJ) mixers. There are other geometries like static mixers, Y-mixer and "multiple inlet vortex mixers" (MIVM). Thakur et al. (2003) indicated the following as main pros when compared to the traditional continuous stirred-tank reactor (CSTR): the small space required, short residence times, good mixing at low shear rates, low equipment cost and no power required except pumps. However, scale-up may be difficult since there is a tendency to clog easily (Alvarez and Myerson, 2010).

This technique has been employed to produce several drugs, with a specific particle size according to the operational conditions, as indicated in table 2.1. Regarding the information collected in the table, the most commonly used solvents are ethanol (Kakran et al., 2013; S. Kim et al., 2012) and methanol (H. X. Zhang et al., 2009; Z. Zhang et al., 2012). However, in some cases may be required the use of other type of solvents like dimethylsulfoxide (DMSO) (Panagiotou et al., 2009) or dimethylacetamide (DMA) (Li et al., 2011). Distillated water is typically used as antisolvent (Park and Yeo, 2012; Sriamornsak and Burapapadh, 2015; Wang et al., 2013; Yu et al., 2005). The value of stirring speed widely used in the studies presented in the table is 1000 rpm. Nevertheless, some authors study higher speed agitations. Although the size of the particles depended on a panoply of factors, the stirring speed is clearly important. Thus, Yu et al. (2005) studied the effect of agitation speed (200-600 rpm) in the agglomeration and particle size and concluded that a lower agitation speed, result in an excessive nucleation and highly agglomerated products. Also noted, that when the stirring speed was increased smaller particles were produced due to the disruption of the agglomerates. Other authors, namely Kakran et al. 2013; C. Li et al. 2011; Nyvlt and Zacek 1986, reached to similar conclusion.

Table 2.1 Previous work done in the production of APIs using ACP process (T-temperature (ºC), S-solvent, SA Ratio-solvent/antisolvent ratio, SS - stirring speed (rpm), PS – particle size (μm), n.s.- not specified).

Drug	Aim of the sudy	Operational Conditions		Ref.
artemisinin	Enhanced dissolution rates	T: 10-20 S: Ethanol SA Ratio: 1:10-1:20	SS: 200-1000 DC: 5-15 PS: Diameter-1,5; Length-3,8	(Kakran et al., 2013)
atorvastacin	Prepare ultrafine powder	T: n.s. S: Methanol SA Ratio: 1:10	SS: 1000 DC: 20-80 PS: 1-3	(H. X. Zhang et al., 2009)
bicalutamide	Enhanced dissolution rate	T: 3-30 S: N,N-dimethyl acetamide SA Ratio: 1:20	SS: 1000-15000 DC: n.s. PS: 0,326-0,334	(C. Li et al., 2011)
carbamazepine	Study the effects of the process parameters	T: 25-45 S: Ethanol SA Ratio: n.s.	SS: n.s. DC: 10-40 PS: 13,9-112,3	(Park and Yeo, 2012)
curcumin	Improved dissolution properties	T: 5-25 S: Ethanol SA Ratio: 1:10-1:20	SS: 200-1000 DC: 5-15 PS: Diameter: 0,155-0,30; Length: 0,920-1,68	(Kakran et al., 2012)
irbesartan	Enhanced dissolution rate	T: n.s. S: Methanol SA Ratio: n.s.	SS: 2500 DC: 1 %wt. PS: 0,055	(Z. Zhang et al., 2012)
nitrendipine	Enhanced dissolution and oral bioavailability	T: 3 S: Mixture of PEG 200 and acetone (1:1) SA Ratio: n.s.	SS: 400 DC: 30 PS: 0,2-0,218	(Xia et al., 2010)
norfloxacin	Produce nanosuspensions	T: n.s. S: Dimethylsulfoxide SA Ratio: 1:3-1:10	SS: n.s. DC: 5-20 PS: 0,17-0,35	(Panagiotou et al., 2009)
quercetin	Enhanced dissolution	T: n.s. S: Ethanol SA Ratio: 1:10-1:25	SS: 300-1000 DC: 5-15 PS: 0,17$\pm$0,03-0,56$\pm$0,02	(M. Kakran et al. 2012)
rifaximin	Taste Masking and enhanced solubility	T: <3 S: Mixture of PEG 200 and acetone (1:1) SA Ratio: 1:10	SS: 400 DC: 200 PS: 0,129	(Danish et al., 2013)
trans-resveratrol	Enhanced oral bioavailability	T: 5-25 S: Ethanol SA Ratio: n.s.	SS: 1000 DC: 60 PS: 0,232-0,560	(S. Kim et al., 2012)

As the previous table shows, the majority of the recent studies performed, using an antisolvent precipitation process, had the aim of enhancing dissolution rates, only existing a reference pointing out the study of taste masking effects.

Danish et al. (2013) based on *in-vitro* studies, suggested that by reducing the particle size of formulations of rifaximin, through the preparation of nanosuspensions by antisolvent precipitation, the efficiency of taste masking can be improved.

Kulkarni et al. (2005) developed a taste masked pharmaceutical composition of cefuroxime axetil (an extremely bitter taste drug) comprising a pH sensitive polymer through antisolvent precipitation, using acetone as solvent and water as antisolvent. According to the authors, X-ray Diffraction (XRD) and

Differential Scanning Calorimetry (DSC) data support that the use of higher molecular weight polymers is efficient in taste masking. Also, it was shown that even at very low drug polymer ratio there was an inhibition of drug's crystallization in the amorphous matrix.

Table 2.2 contains a summary of the main advantages and disadvantages of taste masking technologies aforementioned. Despite some limitations of the ACP process, the benefits of this technique towards other methods are notorious. Firstly, only ACP and SD methods are suitable for processing heat sensitive molecules, since they are low temperature processes. Secondly, ACP is also appropriate for compounds that are difficult to formulate, called "brick dust" compounds, since they can't be processed by melt-based techniques, as long as they have low solubility in volatile organic solvents and high melting points (Sandhu et al. 2014). Thus, they are dissolved, without affecting their chemical stability, in polar solvents with high boiling points, such as dimethylformamide (DMF) or DMA, which isn´t possible with an SD technique (I. Duarte, 2016). An example of a successful commercial product, recently developed through ACP to try to solve this problem, was Zelboraf®. The production of this commercial product was based in vemurafenib ASD, which is the API for the treatment of melanoma (N. Shah et al., 2013).

Finally, a huge advantage of ACP is the fact that the particle's size and morphology can be controlled by adjusting the parameters of the process such as flow rates, agitation speed, temperature, etc. However, the properties of the final product depend not only on the operational conditions aforementioned (Holañ et al., 2015; Lonare and Patel, 2013) but also on formulation variables, such as properties of the drug, polymer, drug load and solvent/antisolvent (SAS) volume ratio (Lonare and Patel, 2013). As an example, and according to Miller et al., (2007) the intimately mixing of the drug and hydrophilic excipients reduce the mean crystal size, resulting in an increased surface area with improved wetting properties, that will lead to an enhanced dissolution rate. Regarding the formulation variables, Zu et al. (2014) observed that by increasing the SAS volume ratio from 1:2.5 to 1:10 the average particle size of taxifolin decreased from 40 nm to 20 nm. This suggests that the amount of ultrafine particles generated per unit volume of liquid, was reduced by increasing the SAS volume ratio, i.e. a lower population density, that leads to a reduction of the collision and agglomeration phenomena between the particles (Thorat and Dalvi, 2011), contributing for a smaller particles formation.

Table 2.2 Advantages and limitations of taste masking technologies.

Methods	Advantages	Limitations	References
SD	- Continuous Process (allows change operating conditions without interruption); - Fast process; - Flexible particles sizes; - Thermosensitive products can be processed under low temperature and pressures due to the short contact time with the heat source;	- Large equipment required; - High initial cost of the units; - Droplet/particle deposition on the chamber walls; - Difficulty in cleaning; - Use of solvents; - Low throughput; - Generally, production of irregular geometry and porous surface due to the evaporation solvent.	(Mujumdar et al., 2010); (Oliveira and Petrovick, 2010); (Qiyun, 2008); (Oliveira W.P et al. 2010); (K. Kolter et al. 2012)
SC	- Free process solvent; - Fast cooling process (formation of droplets/particles in few seconds); - Production of spherical and dense particles suitable for tableting, capsule filling or injection; - Don't require post processing, like secondary drying, milling or pelletization; - Less energy consumption and time when compared with SD.	- Not suitable for heat labile molecules;	(Cordeiro et al. 2013); (Matos and Duarte, 2016); (Okuro et al. 2013); (Duarte et al. 2016)
HME	- Fast, simple, economic, continuous process and easy to scale-up; - Processing in absence of solvents; - Possible to shape the drug-matrix mixture into implants or oral dosage forms; - Suitable to moisture sensitive actives.	- Limited number of available polymers; -Flow properties of polymers are essential to the process; - Thermal process (drug/polymer stability); -Not suitable for relatively high heat sensitive molecules (like proteins, microbial species); - High energy input; - Downstream process (milling or pelletization of extruded).	(Jagtap et al. 2012); (Maniruzzaman et al. 2014); (Dixit AK et al. 2012); (Patil et al. 2016); (R.V. Tiwari et al. 2016); (K. Kolter et al. 2012); (M.M. Crowley et al. 2007)
ACP	- Rapid, easy to perform and easily scalable; - Adaptable from batch to continuous processing; - Low temperature process (suitable for heat-sensitive substances); - Particle size and morphology controlled by adjusting the parameters (flow rates, temperature, etc.); - Not necessary the dissolution of API and excipient in the same solvent (the excipient may be dissolved in the antisolvent); - Suitable for "brick dust" compounds; - Particles with high surface area; - Reproducibility; - Require less consumption energy than evaporation process.	- Utilization of solvents; - Difficult to remove completely the solvents used (leading to physical and chemical instabilities of formulation); - Difficulty in maintaining the size of the particles produced after precipitation (with a rapid growth rate that leads to a broad PSD); - Not applicable to drugs that are poorly soluble in aqueous and nonaqueous media; - Tendency for the agglomeration of organic compounds as fine particles into amorphous structures.	(Viçosa et al., 2012); (Kurup et al. 2016); (Lonare and Patel, 2013); (Krishna et al. 2015); (Sandhu et al. 2014); (Peltonen et al. 2016); (Savjani et al., 2012);

3. Overview of Taste Masking Assessment Technologies

In case of APIs incorporated in solid oral dosage forms, it is extremely important to mask their bitter taste, since the drug can be released in the oral cavity (Pein et al. 2014).

The formulations can be evaluated in regard to taste masking using *in vivo* or *in vitro* techniques. In the first category, the humans or animals are subject to stimuli that are applied in their tongues. These studies include human taste panel studies, electrophysiological methods and animal preference tests (Uchida and Yoshida, 2013). The other approach is based in indirect methods for assessing the taste of the product, measuring some parameters of the final product that are in some way related to taste. These methods include drug release studies, surface characterization techniques and also taste sensors, like for example, the electronic tongue (Anandet al., 2007).

A brief description, main advantages and limitations of each approach for the evaluation of taste masking formulations, are evidenced in table 3.1.

Table 3.1 *In vitro* and *in vivo* approaches for taste masking assessment (Anand et al., 2007; Hughes, 2010; Rachid et al., 2010).

Method	Description	Pros	Limitations
Taste panel studies	Taste evaluation in healthy human volunteers	Well-established method; Applies to all taste masking techniques;	Subjectivity; Time Consuming; Human ethical considerations; Representative subjects; Low throughput; Lack of analytical standardization; Expensive.
Electrophysiological methods	Response measurement to nerve stimulation of an anesthetized animal	Evaluation of taste difference; Screening of new chemical entities (NCEs).	Require surgery; Investment on equipments; Difficult interpretation and analysis; Low throughput; Animal Ethical considerations.
Animal taste preference tests	Analysis of animal behavioral when subject to bottle preference and conditioned taste aversion tests	Screening of NCEs by evaluation through animal preference.	Qualitative test; Low throughput; Animal Ethical considerations; Expensive.
***In vitro* drug release studies**	Measurement of the quantity of API released in a specific period of time	No subjectivity; Low cost; Quality control; Applied for novel/special dosage forms (such as: semi-solid dosage forms and transdermal).	Restricted to methods that reduce the buccal exposure of the drug (coating, IERs and cyclodextrins (CD's)); Can't be applied in liquid formulations.
Surface characterization techniques	Elemental chemical mapping/ quantification of a specific element	No subjectivity; Determination of the EE.	Some techniques-drug dependent; Expensive; Difficult analysis and interpretation; Can't be applied in liquid formulations.
Electronic sensor Methods	Measurement of an electrical potential across different membranes	No subjectivity; Assess the bitterness of NCEs; Applied to any taste masking technology.	Difficult interpretation and analysis; Require the development of a model; Equipment needed more expensive.

3.1. Taste Panel Studies

The work done in panelist tests assessment, reported by several authors, used different taste masking strategies with different APIs formulations and dosage forms (table 3.2). As far as the information presented in the table is concerned, the ages of the small group (6-20 people) of healthy human volunteers vary between 18 and 29 years (Maniruzzaman et al. 2012; Sadrieh et al. 2005). It is also important to take into account their nationality and eating habits for the significance of the results i.e., to ensure a highly representation of the target population as discussed by Hughes (2010).

The taste quality and intensity of the tastants are evaluated by the attribution of different adjective scales or scores. The majority of the scales uses numeric systems (Liew et al., 2012; Lorenz et al., 2009), but there are some scales that use other scoring systems: for example, Singh et al. 2012 uses the signals – and + that represent no taste masking and completely taste masking formulation. Thus, a certain subjectivity is inherent to this method, since the results are dependent on the appreciation of people that made part of the panel test, as well as safety, economical and human ethical concerns.

Before determining taste masking properties, it is necessary to fulfill the train of the panelists (Albertini et al. 2004; F.M. Mady et al. 2010) and determine the threshold concentration of the API (Albertini et al. 2004; Bora et al. 2008) to ensure the panel results and their reliability.

A huge advantage of this assessment technique comparing to others, is the fact that it can evaluate dosage forms produced through several taste masking strategies, for example, double emulsion evaporation solvent (Chiappetta et al., 2009), granulation processes (Albertini et al., 2004), coating (Shahzad et al., 2011) and coacervation method (Shrotriya et al., 2013).

Among the different studies shown in the table, it can be seen that the administration of the oral dosage form is very distinct as a solution, dispersion or a tablet placed on the tongue depending on the final purpose of the medication. Beyond that, the time points of evaluation are very distinct from study to study, but generally the dosage form is held in the mouth for given periods of time.

Table 3.2 Previous work done in taste panelist evaluation (RDT – Rapidly-Disintegrating Tablets, ODT – Orally Disintegrating Tablets, DRC – Drug Resin Complex, DPC – Drug Polymer Complex, N – number of panelists, n.s. – not specified).

API	Dosage Form	Taste-masking strategy	Panelists	Perception threshold (mg/ml)	Panelist Training	Dose of the sample (mg)	Administration of the solid oral dosage form	Time point of evaluation	Taste-masking assessment procedure	Ref.
acetaminophen	Granules	Use of different granulation processes	N: 6 Age: n.s. Sex: n.s.	1,08	Yes	22,5	As solution (granules are dissolved over 3 min)	After the solution was held in the mouth for 5 s	Scoring of pure API solution against solution of the formulation	(Albertini et al., 2004)
dextromethorph an hydrobromide	Granules	Formation of DRC with Ionex QM 1011, Ionex WC 23 and Kyron T-114	N: 6 Age: n.s. Sex: n.s.	0,04	n.s.	15	One granule placed onto the tongue	After the granule was held in mouth for 2, 10 and 60 s	Bitterness score using a numerical scale	(Sana et al., 2012)
diclofenac sodium	ODT	Addition of Mannitol, saccharine, MCC, croscarmellose sodium and magnesium sterate	N: 12 Age: n.s. Sex: n.s.	n.s.	n.s.	500	One tablet placed onto the tongue	Immediately after administratio n and at several intervals for 10 min	"Time intensity method" followed by bitterness scores	(Sona et al., 2011)
dihydroartemisin in	Granules	Use of different coating materials	N: 6 Age: n.s. Sex: n.s.	0,8	Yes	35	As solution (granules are dissolved over 2 min)	After the solution was held in the mouth for 5 s	Scoring of pure API solution against solution of the formulation	(Shahzad et al., 2011)
doxycycline	Tablets	Addition of mixing agents	N: 20 Age: 20-29 Sex: m/f	n.s.	n.s.	100	As crushed tablet, mixed with masking agents	After administratio n (10 s) and after swallowing (1 min)	Palatability scores	(Sadrieh et al., 2005)

indivanir	Microparticles	Prepared by w/o/o double emulsion solvent evaporation	N: 10 Age: n.s. Sex: n.s.	0,02-0,045	n.s.	100	As solution	Held in the center of the tongue by 1 and 5 min for 20 s	Bitterness score using a numerical scale	(Chiappetta et al., 2009)
promethazine hydrochloride	FDT	Addition of Camphor (sublimating agent) and Mannitol (diluent)	N: 6 Age: n.s. Sex: n.s.	n.s.	n.s.	150	One tablet placed onto the tongue	Immediately after administration and at several intervals for 15 min	"Time intensity method" followed by bitterness scores	(Kolhe et al., 2013)
rizatriptan benzoate (RZBT)	Dispersible tablet	Formation of RZBT-CD Binary Systems of inclusion complexes	N: 6 Age: 22-27 Sex: 3f/3m	0,35	n.s.	10	As dispersion (one tablet dispersed in 10 ml water)	Held 1 ml of the dispersion in the mouth for 30 s	Bitterness score using a numerical scale	(Birhade et al., 2010)
sitagliptin phosphate monohydrate	RDT	Formation of DRC with addition of Indion 414, crospovidone, croscarmellose sodium, sodium starch glycolate	N: 11 Age: n.s. Sex: n.s.	n.s.	n.s.	100	One tablet placed onto the tongue	Immediately after administration and at several intervals for 15 min	"Time intensity method" followed by bitterness scores	(Surinder et al., 2013)
sumatriptan succinate	Granules	Addition of Eudragit E-100, β–CD and sweetener	N: 12 Age: n.s. Sex: n.s.	n.s.	n.s.	Depend on TM strategy	Granules placed "on posterior lobe of tongue"	After administration (4-6 s)	Taste-masking and grittiness evaluation	(Singh et al. 2012)
tramadol	RDT	Formation of DPC by coacervation method with addition of Eudragit EPO and sodium hydroxide	N: 20 Age: 20-25 Sex: n.s.	0,02	n.s.	50	As dispersion (1 g Tramadol dispersed in 50 ml water)	Held 1 ml of the dispersion in the mouth for 30 s	Bitterness score using a numerical scale	(Shrotriya et al., 2013)

3.2. Electrophysiological Methods

Katsuragi et al. (1997) focused their attention in a method for inhibit the human taste sensation to bitter tastants and suggested, through the use of Bullfrogs (*Rana catesbeiana*), that a lipoprotein called PA-LG (composed by PA and β-LG) suppressed selectively the taste responses, as a result of a complex formation, with certain type of bitter tastants in the medium.

Other interesting study, led by Sato et al. (2010), was the response to cold and warm stimuli measured by a receptor potential of frog taste cells, which showed that this type of cells are sensible to thermal stimuli of 5-35 ºC, leading to depolarizing and hyperpolarizing of the receptor's potentials. The authors found that during a warm stimulation of the frogs' tongue, they can perceive thermal sweet responses, due to a correlation between depolarizations by warm stimuli of 30 ºC and depolarizations induced by 1 M sucrose of 20 ºC.

3.3. Animal Preference Tests

Tiwari et al. (2015) investigated the palatability of caffeine citrate formulation produced by HME technology using 21 rats. They were submitted to privation of water for 22 h to stimulate the response to thirst, then they had free access to water (or formulations with different concentrations of the API) for a period of 30 min, followed by the removal of the bottles. The volume consumed from the bottle was recorded, as well as the taste aversion behaviors of rats, resulting of responses to the bitter-taste stimuli such as retreating, jaw smacking, nose wrinkle, head shake, paw shakes and oral grooming.

The rats' behavior and the volume consumed of the solutions suggested that they didn't appreciate the taste of the solution with the pure API and all the taste masked formulations tested, showed effective taste masked effect.

Also Noorjahan et al. (2014) performed a similar study and even a taste assessment by human volunteers, obtaining a good correlation between the behaviors that were verified in rats and humans.

3.4. *In vitro* Drug Release Studies

During taste masking assessment by in vitro drug release studies, it is critical to assure that the dissolution method is able to mimic the oral cavity in terms of composition of the dissolution medium, pH, temperature, volume and agitation (Gittings et al., 2014). Attending to the International Pharmaceutical Federation/American Association of Pharmaceutical Scientists (FIP/AAPS) guidelines, the selection of the suitable apparatus is also important since it simulates the hydrodynamics of human body, although it is also necessary to take into consideration the type of dosage form and its physical and chemical properties (Santos, 2012). Thus, for oral dosage forms, the apparatus of first choice is the Apparatus 2 (paddles).

In figure 3.1, an illustration of a paddle apparatus is shown, as well as a schematic representation of the dimensions/distances related to the vessels, that are stipulated in the International Pharmacopeia 3rd Edition.
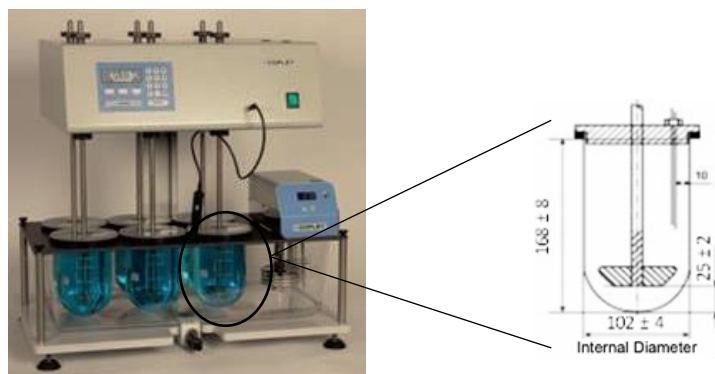
Figure 3.1 Illustration of a paddle apparatus (a) and schematic representation of the recommended dimensions and distances (in mm) related to the vessels (b) (adapted from (Paleshnuik, 2009)).

As illustrated in the previous figure, the vessel must have specific dimensions, which should be invariable from vessel to vessel to assure the reliability and reproducibility of the dissolution tests. To start the dissolution study, the sample should be introduced and deposited in the vessel´s bottom before stirring, usually between 50-75 rpm. If the oral dosage form has the tendency to float, it is convenient the use of an appropriate dispositive called sinker, that will be able to fix the oral dosage form (Stippler, 2011).

The sample collection is performed in the middle of the vessel to assure that only the dissolved solution is collected and not the drug that will dissolve over time, in the vessel's bottom. Furthermore, the sample´s volume removed can be reestablished by adding the same volume of dissolution medium. If the replacement of the dissolution medium is not performed, it is necessary to take into consideration the volume variation that occurred in the calculations of the dissolution velocity (Santos, 2012).

In terms of the dissolution media, typically research groups used a single one (Albertini et al. (2004) ; Mady et al. (2010)), namely: phosphate buffer solution (PBS) at different pH values 6.8, 7.4 (F. Q. Li et al., 2010), and 7.5 (Vaassen et al., 2012) and also simulated saliva fluid (SSF) at pH 6.2 (Yan et al. 2010) and 7.4 (Guhmann et al., 2012). Other common dissolution medium is water (Shirai et al. 1994) once it is the most abundant and economic solvent. Frequently a surfactant, such as Tween 80 (Mizumoto et al., 2008) and polysorbate 80 (Hamashita et al., 2007), is added to improve the wettability of the taste masked particles.

According to the studies shown in table 3.3, the volume used for the dissolution tests, ranges from 50 to 900 mL, nevertheless the volume of saliva in the mouth is typically less than 1.5 mL (Lagerlof and Dawes, 1984); so the use of such larger volumes, may not be representative when it comes to estimate the quantity of drug released. Despite that, it may be reasonable to use volumes of 200-300 mL when the dosage form requires the ingestion with a glass of water (Gittings et al. 2014).

The FIP/AAPS guidelines established general criteria, consisting in the use of a neutral medium where the API dissolves usually less or equal to 10 % in 5 min to achieve taste masking. As far as it depends on the intensity of the bitter taste of API, a multi-point profile with early time-points of analysis (e.g. < 5 min) (Siewert et al., 2003) is recommended. For this purpose, Anand et al. (2007) argued that taste masking is achieved when, until the first 5 minutes, the API is not detected or its quantification is below the threshold limit. As presented in table 3.3, the authors that follow this criteria are a minority.

The dissolution methods have been evolved over time, SHIRAI et al. (1996) used a simplified dissolution method that consists in mixing fine granules of sparfloxacin (SPFX) in 10 mL of distillated water in a 10 mL syringe, agitating it by revolving the syringe end to end five times within 30 s. More recently, Kondo et al. (2011) used an equivalent method for coated paracetamol granules, but in this case the agitation was given by 10 repeat syringe inversions over 30 s.

For the evaluation of the taste masking efficiency of clarithromycin, Yajima et al. (2002) suggested a more sophisticated dissolution method, that operates in a continuous flow system. The system is described as a mini column (that contains the powder) in which the dissolution medium (phosphate buffer at pH of 6.5) is injected at different flow rates using a syringe pump, and the final sample collected in a small vessel. The authors concluded that better results were obtained by using this method, in terms of correlations between sensory analysis and *in vitro* studies, when compared with shaking, inversion or paddle methods.

The quantification of API in the dissolution medium at each time point is performed by HPLC (high performance liquid chromatography) or UV (ultraviolet) spectroscopy. The first is usually preferred in the presence of UV-absorbing components (for example, sweeteners) and since UV estimation can be difficult sometimes in terms of distinguishing the signal from the background, especially when the ratio excipient-drug is high. (Anand et al., 2007).

Table 3.3 Previous work done *in vitro* assessment of taste masking (RDT – Rapid Disintegrating Tablet, ODT – Orally Disintegrating Tablets; SSF- Simulated Salivary Fluid, T – temperature, V-volume, AS – Agitation Speed; n.s. –not specified).

API	Dosage Form	Taste Masking Strategy	In vitro assessment tool	Taste Masking criteria	Dissolution settings	Drug dose (mg)	Sample (pre)treatment	Sampling timepoint	Ref.
acetaminophen	Granules	Preparation by different granulation techniques	UV spectroscopy (243 nm)	Drug release of pure API> release of taste masked formulations	V: 900 mL M: phosphate buffer pH: 6.8 T: 37 ± 0.1 ºC AS: 50 rpm Apparatus: paddle	22,5	Dissolution in paddle apparatus according to USP24 (12,5 ml/min)	3 min	(Albertini et al., 2004)
brompheniramine maleate	Capsules	Formation of complexes with tannic acid, prepared by the solvent evaporation method	HPLC	Drug release of pure API> release of taste masked formulations	V: 500 mL M: phosphate buffer (0.2 M) and HCl buffer (0.1 N) pH: 6.8 T: 37 ºC AS: 50 rpm Apparatus: paddle	12	Dissolution in paddle apparatus according to USP II	n.s.	(Rahman et al., 2012)
cetirizine dihydrochloride	Microparticles	Entrapment of microparticles within chitosan nanoparticles followed by microencapsulation using SD	HPLC	Drug release of pure API> release of taste masked formulations	V: 100 mL M: phosphate-buffered saline (PBS) pH: 7.4 T: 37 ± 0.5 ºC AS: 50 rpm	20	Microparticles placed into a membrane dialysis bag	15 min	(F. Q. Li et al., 2010)
diclofenac (acid form, sodium and potassium salt)	Granules	Coating with Eudragit EPO through fluidized bed followed by wet granulation	HPLC	Drug release of pure API> release of taste masked formulations	V: 50 mL M: SSF pH: 7.4 T: 37 ± 0.5 ºC AS: 50 rpm	232,5	n.s.	0,5;1;1,5;2; 2,5 and 3 min	(Guhmann et al., 2012)
famotidine	RDTs	Preparation of binary (drug-β-CDs) and ternary systems	UV spectroscopy (269 nm)	Drug release of pure API> release of taste masked formulations	V: 900 mL M: phosphate buffer pH: 6.8 T: 37 ± 0.5 ºC	20	n.s.	5 min	(Mady et al. 2010)

		(drug-β-CDs-Povidone K30) through kneading and freeze-drying methods		Comparison of drug release between binary and ternary systems	AS: 50 rpm Apparatus: rotating paddle			
ibuprofen	ODT's	Coating with different polymers, addition of sweetener and superdisintegrants	UV spectroscopy (220 nm)	Drug release of pure API> release of taste masked formulations	V: 500 mL M: phosphate buffer pH: 6.8 T: 37 ± 0.1 ºC AS: 100 rpm Apparatus: paddle	700	Sample filtration (5 ml) before off-line detection.	10 min	(Fini et al., 2008)
mefloquine hydrochloride	Microparticles	Prepared by coacervation method using Eudragit EE and sodium hydroxide as precipitant	UV spectroscopy (284 nm)	Drug release of pure API> release of taste masked formulations	V: 900 mL M: phosphate and HCl buffer pH: 6.8 and 1.2 T: 37 ± 0.5 ºC AS: 75 rpm Apparatus: paddle	250	Dissolution in paddle apparatus according to USP XXIV	1, 5 min until 60 min	(Shah et al., 2008)
NPX 1210	Lipid based pellets	Lipid formulation (lipids function as taste masking agents)	UV spectroscopy (295 nm)	< 5% drug release within 2 min	V: 900 mL M: potassium dihydrogenphosphate buffer pH: 7.5 T: 37 ± 0.5 ºC AS: 75 rpm Apparatus: paddle	50 % drug load	Dissolution in paddle apparatus according to USP33 Method 2	Drug release after 2 min	(Vaassen et al., 2012)
sparfloxacin	Granules	Coated fine granules with low-substituted hydroxypropylcellulose	UV spectroscopy (291 nm)	Drug release of pure API> release of taste masked formulations	V: 900 mL M: water pH: 7.5 T: 37 ºC AS: 50 rpm	50	Dissolution in paddle apparatus according to the JP XII	15 min	(SHIRAI et al., 1994)

3.5. Electronic Sensor Methods

The concept of electronic tongue was proposed to mimic the functions of humans gustatory receptors by Hayashi et al. 1990 and K. Toko et al. 1994 in the 90's.

Murray et al. (2004) used a consensus classification to check the three different phases of biological taste recognition by an e-tongue: the receptors (in humans are called taste buds, in the e-tongue are probe membranes), the circuit (in humans is performed by neural transmission, in the e-tongue by a transducer) and the perceptual phase (in humans is performed by a cognition in the thalamus, in the e-tongue by a computer and a statistical analysis).

The concept of this technique is based on interaction of the sensors with the tastants at the surface, resulting in alterations that can be measured, for example potentials and voltages if used potentiometric or voltammetric sensors, respectively (Zou et al., 2015). These signals are compared and evaluated on the data basis of the sensor responses that are recorded in the computer (Latha and Lakshmi 2012).

Therefore, an e-tongue is constituted by an automatic sample, an array of chemical sensors with different selectivity, instrumentation to capture the signal and a software with a developed algorithm able to process the signal and generate results (Escuder-Gilabert and Peris, 2010).

Rachid et al. (2010) demonstrated that the electronic tongue can be an important tool in taste masking evaluation for an intensely bitter substance. In their study, they had shown that the e-tongue can identify the agent that best masks the bitter taste of the epinephrine bitartrate. They developed and validated a bitterness standard model, obtaining correlation coefficients above 80 %. They also determined the threshold concentration of the e-tongue sensors and concluded that the formulation with 9 mM of EB and 0.5 mM of citric acid was the best formulation in terms of taste masking effects, since it cannot be detected by the sensors of the e-tongue.

The taste masking effects of formulations of doxycycline mixed with different masking agents were evaluated by Sadrieh et al. (2005) through an electronic tongue using seven sensors. The criteria used for taste masking was based on group distances calculated by the electronic tongue between placebo samples (matrix only) and drug formulations. Accordingly, the best masking agent is identified through the smallest group distance, which suggests that the two tastes aforementioned (placebo and drug formulations) are more similar. Therefore, they have concluded that the low-fat chocolate milk was the best food matrix for doxycycline, with better taste masking efficiency.

3.6. Surface Characterization Techniques

Surface characterization has been widely studied in several areas such as metallurgy, corrosion, among others. The use of these techniques had a huge increment since the researchers realized that the future of the materials is composite, i.e. a mix of different materials, and for that reason is important to understand the properties of the material surfaces that will be in contact with each other. Hence, there are an innumerous number of techniques that are used with the purpose of characterize the surface of the materials, such as SEM-EDS, XPS, High Resolution Electron Energy Loss Spectroscopy (HREELS) and Auger Electron Spectroscopy (AES) (Rego, 1993).

3.6.1. Scanning Electron Microscopy – Energy Dispersive Spectroscopy (SEM-EDS)

SEM is a technique based on the creation of micro-imaging of an innumerous surface's materials, making possible to study the texture of that surface and determine the particle size. The interaction of the electrons, from the electron beam that is focused on the sample, with the different atoms presented in the sample produce several types of signals (secondary electrons, x-rays, auger electrons). These signals are then collected by the detectors, amplified and used to modulate the intensity of a select X-ray line, and finally, the scanning of the beam is synchronized and electron images are originated (Zunbul, 2005).

Energy Dispersive X-ray Spectroscopy is a powerful tool when associated with SEM, allowing not only to determinate the elemental composition of surfaces but also its elemental quantification. The principle of the technique is grounded on the emission of x-rays by the sample as a response of the electron beam, generating peaks at specific energies, according to the elements that the sample contains since, each element has a unique atomic "digital impression"; the concentration of the elements are determined through the integration of the peak are (Canli, 2010; Peterson, 2011).

In this work, EDS was used to study the elemental composition on the particles surface and to quantify the elements that were present, in particular nitrogen, in order to determine the EE.

3.6.2. X-Ray Photoelectron Spectroscopy (XPS)

The XPS technique provides information about the atomic composition of the surface, nature and connection of atoms, and is considered the main technique used in surface characterization (Gonçalves, 1999).

The concept of this technique is similar to the EDS, however in this case the photoelectrons that contribute for the resulting peaks in XPS are the ones that are produced near the surface and without loss of energy, i.e. the identification of the elements is performed from the kinetic energies of ejected photoelectrons (Barros, 2009).

The output of XPS are spectra as a function of the binding energy of the electrons from the inner layers of the atoms (Ferraria, 2002).

4. Materials and Methods

4.1. Materials

The model drug used in this work is an API produced by Hovione Farmaciência SA. A commercially available polymer, Methacrylic Acid and Methyl Methacrylate Copolymer (1:2) (Eudragit® S100, Evonik Röhm GmbH, Darmstadt, Germany) was selected as an excipient. The selection of the polymer was based on an enteric polymer that dissolves at pH>7, to assure that when in contact with the salivary fluid within the oral cavity it doesn't dissolve protecting the core material, since the salivary pH varies between 6.7-7.4 (Hans et al., 2016). The antisolvent and solvent used were deionized water and DMF, respectively, both of an analytical grade. To acidify, a 37 wt. % hydrochloric acid solution (Sigma-Aldrich, Missouri, USA) was used, in order to force the polymer to precipitate (antisolvent effect).

4.2. Methods

The production process was divided into two steps, followed by powder characterization: production of co-precipitated suspensions and isolation of the suspensions by spray drying and analytical characterization of the co-precipitated spray-dried powders. The first stage of the process started with the planning of the DoE, described in subchapter 4.2.1., which was conducted to produce the co-precipitated suspensions through several technologies: conventional approach (stirred reactor), Covaris technology and PureNano. The operational conditions used for each technology are described in detail in subchapters 4.2.2/3/4. The second step of the process is designated as an isolation step of the co-precipitated suspensions, based on the drying of the suspensions through SD in order to obtain co-precipitated spray-dried powders. The operational conditions are described in subchapter 4.2.5. Finally, after obtaining the final powder it was necessary to evaluate the CQAs, in this case API solid state form, particle size and morphology and *in vitro* dissolution. The powders were characterized by diverse analytical techniques, such as: SEM-EDS, XPS, XRPD (X-Ray Powder Diffraction), DSC, TGA (Thermogravimetric Analysis), UPLC (Ultra-Performance Liquid Chromatography) and *in vitro* dissolution. The methods used for each technique are described in subchapters 4.2.6 until 4.2.15.

4.2.1. Design of Experiments

A 2^3 full factorial design of experiments was designed with the aim of studying the effect of formulation variables on CQAs of powders produced by co-precipitation. The formulation variables studied were: the SAS volume ratio (1:6, 1:8 and 1:10), the drug load (30, 45 and 60 % w/w) and the feed solids concentration (8, 10 and 12 % w/w), as described in table 4.1. and figure 4.1(a).

Preliminary studies performed with the stirred reactor indicated that for drug loadings lower than 45 % occurs the formation of polymer filaments; for that reason, only one face of the cub was considered corresponding to a constant drug load of 60 %, as shown in figure 4.1(b).
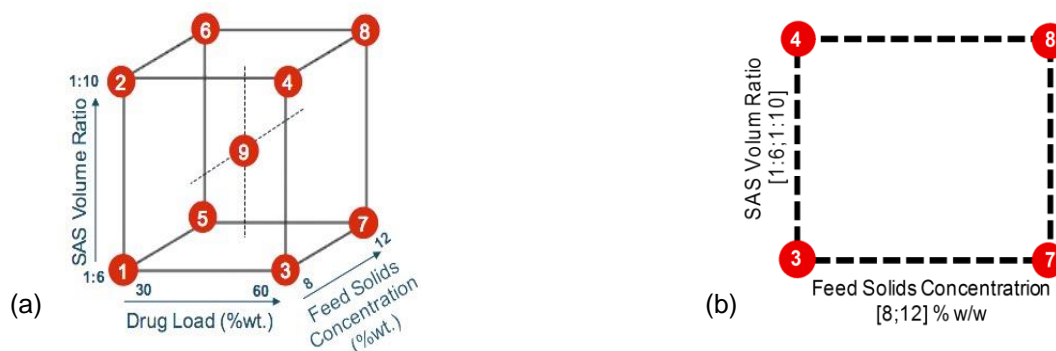
Figure 4.1 Schematic illustration of the (a) DoE initially designed and (b) DoE adopted for the co-precipitation stirred reactor process study.

Table 4.1 Experimental design for the co-precipitation stirred reactor process study.

Experience Number	SAS Volume Ratio	Drug load (%w/w)	Feed solids concentration (% w/w)
1	1:6	30	8
2	1:10	30	8
3	1:6	60	8
4	1:10	60	8
5	1:6	30	12
6	1:10	30	12
7	1:6	60	12
8	1:10	60	12
9	1:8	45	10

4.2.2. Batch Stirred Reactor

For the application of the DoE 4 solutions were prepared, corresponding to trials #3, #4, #7 and #8, whose SAS volume ratio and feed solids concentration ranged accordingly as described in table 4.1. The antisolvent (water) was acidified to ensure that pH ranges from 3 to 4 to enhance the antisolvent conditions for the polymer, using a 37 wt. % hydrochloric acid solution. The process took place at a room temperature of 25 ± 2 ºC. The co-precipitation occurred in a jacketed stirred lab reactor of 1000 mL (Radley, United Kingdom) whose setup is schematic illustrated in figure 2.4. The antisolvent was inside the reactor, the solution was added using a peristaltic pump (Watson Marlow 323, Falmouth, United Kingdom) at a controlled rate, according to the ratio antisolvent/solvent used and so that the solution was added for 10 min. The agitation was provided during 120 minutes by a mechanic stirrer (IKA® RW 20 Digital, Staufen, Germany) with an agitation speed of 181 rpm. Four suspensions were obtained and for that reason, the particles were then subjected to an isolation step, being dried in a lab-scale spray dryer.

4.2.3. Adaptive Focused Acoustics Technology

A Covaris S120X 1,062 MHz and 42,5 Ω (LGC-KBioscience UK Ltd., Teddington, United Kingdom) was used to produce 4 suspensions, corresponding to trials #3, #4, #7 and #8. This approach uses a

commercially available ultrasonicator. The flow cell was fed with two streams: the antisolvent and the solution of API and polymer, by two peristaltic pumps for each stream. The peristaltic pumps were calibrated so that the antisolvent flow rate was 6 or 10 times higher when compared with the solvent flow rate, according to the SAS volume ratio used for each trial. The streams connect to each other in the focal zone, where acoustic waves are conveyed through the water and focused in that specific zone. The process described is illustrated in figure 4.2. A preliminary screening study was performed in order to fit the values for given parameters. The values that were considered more adequate for the process were: 1 000 cycles per burst (CPB), a duty factor (DF) of 50 %, a peak incident power (PIP) of 300 and a temperature of 35 ± 5 ºC. In the end, 4 suspensions were obtained, isolated through a lab-scale spray dryer and subjected to a post-dry process in a tray dryer oven under vacuum at 20 ºC for 18 hours.
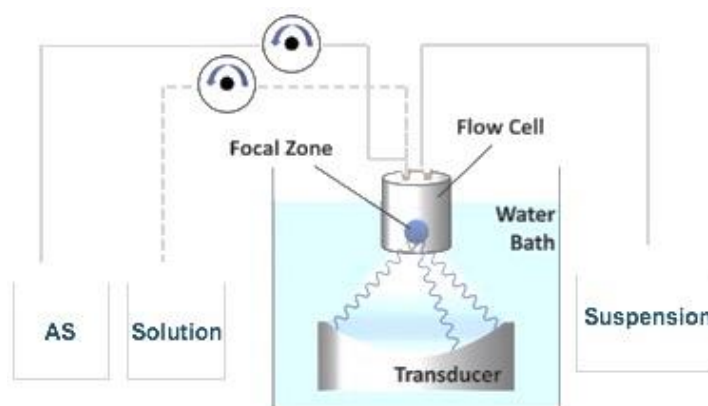
Figure 4.2 Schematic representation of experimental setup with Adaptive Focused Acoustics (adapted from (Hanefeld et al., 2015)).

4.2.4. Microfluidization Process

Four solutions of model drug and polymer were prepared in DMF, corresponding to trials #3, #4, #7 and #8 whose SAS volume ratio, feed solids concentrations and drug loadings are established in table 4.1. The water was acidified with a hydrochloric acid solution in order to obtain a H^+ concentration between 10^{-3} M and 10^{-4} M, which correspond to pH 3 and 4, respectively.

The solvent/antisolvent controlled precipitation experiments were performed using PureNano™ Microfluidics Reaction Technology (MRT, CR5 Reactor model) with the setup that is illustrated in figure 4.3. Two streams, one with solvent and another with antisolvent are fed into an intensifier pump at individually controlled flow rates. The intensifier pump was set at the maximum processing pressure which corresponds to 20 kPsi, approximately 1379 bar. The solvent flow rate was calibrated in order to maintain the SAS volume ratio, while the antisolvent flow rate was imposed by the pressure of the system.

At the intensifier pump the two streams were pressurized in a combined stream and directed to an interaction chamber, which comprises of two mixing chambers: the first, with diameter reaction channels of 75 μm (F20Y), followed by another chamber with 200 μm (H30Z). The first chamber had the purpose of promoting and intensifying the mixing rate, while the second stabilizes the solution. After the interaction chambers, the suspension was delivered to a heat exchanger, to control the temperature increase of the resulting suspension. For the 4 trials, only one single passage through the processor

was performed. After this, the suspensions were isolated and collected through a lab-scale spray dryer and subjected to a post-dry process in a tray dryer oven under vacuum at 20 ºC for 18 hours.
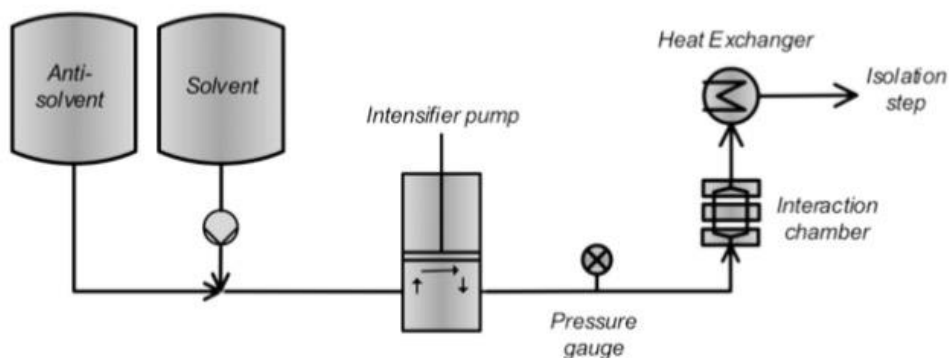
Figure 4.3 Schematic representation of a Microfluidization process, in which results the production of suspensions, that are isolated by spray drying.

4.2.5. Spray Drying

To dry the suspensions corresponding to trials #3, #4, #7 and #8 produced by (1) the conventional approach; (2) the Covaris technology; (3) the Microfluidics Reactor Technology and (4) an amorphous powder of the model drug, a laboratory scale spray dryer (BÜCHI Mini Spray Drier B-290, Switzerland) was used, equipped with a two fluid nozzle with a 1.4 mm cap and 0.7 mm tip. The process took place in an open cycle mode characterized by the inexistence of a gas recycle unit, as mentioned in chapter 2.1. The spray dryer was stabilized with gas (nitrogen) and also with stabilization solvent (DMF and water, in the same proportion present in the suspension) so that the inlet and outlet temperatures were stable. The inlet temperature was adjusted, altering the inlet temperature set point, until achieving an outlet temperature of 100 ºC. After this process, the suspensions were permanently mixed, using a magnetic stirring system, and simultaneously fed into the nozzle by a peristaltic pump at a flow rate of 0.29 kg/h, being atomized in the nozzle with a flow rate of 0.96 kg/h. In the spray drying chamber, the droplets were dried through a co-current nitrogen stream at a flow rate of 32.5 kg/h. The resulting dried particles were directed to a cyclone, being collected at the bottom. The final powder was subjected at a post-drying process in a tray dryer oven under vacuum at 20 ºC for 18 hours.

For the production of the amorphous powder (4), a solution of model drug in DMF with 9 % of feed solids concentrations was prepared and the powder was dried according to the following conditions: flow rate of drying gas equal to 35 kg/h, atomization feed of 0.925 kg/h, flow rate of 0.28 kg/h and an outlet temperature of 100 ºC.

4.2.6. Scanning Electron Microscopy - Energy Dispersive Spectroscopy (SEM-EDS)

The collected samples were examined to study their morphology by SEM; moreover, in order to have insights in what concerns the EE, EDS was applied. The particles were fixed to adhesive carbon tapes, which are attached to an aluminum plate, and sprayed with pressurized air to remove the excess powder. After this process, the aluminum plate, already containing the samples for analysis, was coated with gold/palladium (South Bay Technologies, model E5100, San Clement, CA) and introduced in the

microscope under vacuum conditions. The micrographs were obtained at several magnifications, ranging from 250x to 20 000x, by a JEOL JSM-7001F/Oxford INCA Energy 250/HKL scanning electron microscope (JEOL, Tokyo, Japan) that operates at an accelerating voltage of 15 kV.

The EDS mode allows an elementary characterization and quantification of the periodic elements identified in the sample by the microscope. For this purpose, a given area of the sample was selected, typically at a magnification of 1000x, to assure that no agglomeration was verified nor that the particles were too far apart.

4.2.7. Particle Size

The particle size of the spray dried co-precipitated powders was estimated as the mean circular equivalent diameter, through an image analysis software called ImageJ (National Institute of Health, Bethesda, MD, USA). 300 particles were randomly selected from each sample, in order to assure a normal distribution of the particle sizes. The mean circular equivalent diameter is defined as the diameter of a circle that have the same area of the particle manually selected in the micrographs of SEM (Olson, 2011).

Using the image analysis software, the area of the particle was measured and then, the mean circular equivalent diameter was estimated using the following equation:

$$d = \frac{\sqrt{4\,A}}{\pi}$$

Equation 4.1

4.2.8. X-ray Photoelectron Spectroscopy (XPS)

The encapsulation efficiency was also studied through a XPS spectrometer, in particular in a XSAM800 designed by KRATOS (Manchester, United Kingdom). Samples of trials #7R, #8C and #7P were fixed to a double sheet glue, attached on a small aluminum plate. These were then placed in the entry chamber, it was necessary to wait until it reached a pressure vacuum in the order of magnitude of 10^{-7} Pa. Subsequently, the samples were placed in the analysis chamber with a 45º take-off angle (TOA), where the ultra-high vacuum is achieved (pressures of about $10^{-10}\,Pa$). The spectrometer operated in the Fixed Analyzer Transmission (FAT) mode, with pass energy of 20 eV. The samples were subject to a non-monochromatized Mg Kα X-radiation (hv= 1253.6 eV), produced using a voltage of 12 kV and a current of 10 mA. The acquisition of the spectrums was performed through a software called VISION version 1.0 designed by KRATOS (Manchester, United Kingdom) and the data files in ASCI format were analyzed and processed through a software called XPS peak version 4.1 (Raymond Kwok, Hong Kong, China).

4.2.9. X-Ray Powder Diffraction (XRPD)

To evaluate the crystallinity of the powders, XRPD experiments were conducted in a X'Pert Pro PANalytical X-ray Diffractometer (Almelo, The Netherlands) using a source of cooper radiation (Cu kα=1.5406 A) at a current of 40 mA and a voltage of 40 kV. A Beta-Filter Nickel was used with a thickness of 0.020 mm. The preparation of the samples involved pressing the powder in the sample

holder, in order to obtain a smooth surface. The samples were subject to the aforementioned radiation, over a 2θ interval from 3 to 40 º with a step time of 26 seconds and a step size of 0.0167 º. The resulting diffractograms were collected through a software designated Data Collector version 4.1 and analyzed through a software called Data Viewer version 4.1.

4.2.10. Differential Scanning Calorimetry (DSC)

The thermal behavior of all powders produced was analyzed through differential scanning calorimetry (DSC Q200 V24.4 Build 116, TA Instruments Thermal Analysis, New Castle, USA). About 2-8 mg of sample were loaded into an aluminum pan (pinhole hermetic type); the same type of pan was used as reference. Continuous dry nitrogen gas at a flow rate of 50 mL/min was employed, and the samples were heated from 20 to 300 ºC at a constant heating rate of 10 ºC/min. The DSC thermograms were processed and analyzed through a software called Universal V4.5A TA Instruments.

4.2.11. Thermogravimetric Analysis (TGA)

The weight loss related with water and residual solvents that occurred in all the formulations produced was determined by thermogravimetric analysis (TGA Q500 V20.10 Build 36, TA Instruments Thermal Analysis, New Castle, USA). Some mg of sample were loaded into a platinum pan that was then subjected to a heating ramp inside a furnace. The weight loss is determined using as reference an empty platinum crucible. Continuous nitrogen gas was employed in the balance and in the sample, at a flow rate of 40 and 60 mL/min, respectively. The method used consisted in heating the samples until 350 ºC at a heating rate of 10 ºC/min. The TGA thermograms were processed and analyzed through a software called Universal V4.5A TA Instruments.

4.2.12. Ultra-Performance Liquid Chromatography (UPLC)

For the quantification of the model drug, a Waters UPLC system (model Acquity UPLC H-Class) was used with a dual wavelength absorbance detector (model PDA Detector) (Waters, Milford, USA). The column used was an Acquity CSHC18 (100 mm x 2.1 mm, 1.7 μm). The mobile phase consisted of 50:50 % v/v of Methanol:Dipotassium hydrogen phosphate, the pH being adjusted to 8 with phosphoric acid and degassed for 10 minutes in a sonicator bath (VWR Ultrasonic Cleaner USC-THD) before use. The injection volume was 1.0 μL and the flow rate was constant at 0.3 mL/min, at a column temperature of 40 ºC and an autosampler temperature of 5 ºC. The quantification of the model drug was performed at a wavelength of 280 nm, the chromatographs were processed using the software Empower Version 3.0 (Waters, Milford, USA).

4.2.13. Determination of Encapsulation Efficiency

As previously mentioned, the evaluation of the EE was performed using both SEM-EDS and XPS techniques. Based on the data collected in both cases, it was possible to quantify the nitrogen present in a given point of the sample and consequently to estimate the EE. Besides the specific samples that

were analyzed through these techniques, also some standard samples (pure API and a physical mixture of drug/polymer at a ratio 60:40 % wt.) were analyzed in order to compare the intensity of the elementary peaks identified by the microscope. Finally, the EE was estimated as indicated in the following equation.

$$\% \ EE = \frac{\% \ of \ detected \ N \ in \ the \ standard - \% \ of \ detected \ N \ in \ the \ sample}{\% \ of \ detected \ N \ in \ the \ standard} \times 100$$

Equation 4.2

Note that the standard sample used in this equation was the pure model drug, for both EDS and XPS analysis.

4.2.14. Drug Content in the formulations

The drug content present in all the formulations was assayed through the UPLC method described in section 4.2.12. For all the formulations, solutions with a model drug concentration of 200 μg/mL were prepared, weighing about 33.34 mg of each formulation and dissolved in 100 mL of methanol (MeOH) in a volumetric flask. The solutions were agitated at 800 rpm in a multi shaker for 5 minutes until they were completely dissolved. The quantification of the model drug in the formulations was performed against a calibration curve with pure model drug dissolved in MeOH, with concentrations that varied from 20 to 200 μg/mL. The drug content of each sample was determined in duplicate, and D-check was calculated to assure the reliability of the results.

4.2.15. *In-vitro* Dissolution Studies

Two approaches were used for these studies: conventional dissolution in 6-well plate and pH shift dissolution methods. The purpose of the first approach was to verify the drug release of the formulations in the oral cavity, and the second one to understand if the enhanced taste masking properties that are expected in the samples didn't impact its dissolution profile.

The experiments that correspond to the first approach were conducted in a 6-well plate in an ES – 20/60, Orbital Shaker – Incubator (Biosan, Riga, Latvia) at a temperature of 37 ºC and an agitation of 70 rpm. In the 6-well plate 10 mL of simulated salivary fluid (SSF) at a pH of 6.75 were placed, being degassed for 10 minutes at a sonicator and preheated to 37 ºC before use. The composition of the aforementioned medium is described in table 4.2. As the concentration of the model drug was 10 times higher when compared to the pH shift approach, these dissolution experiments occurred under non sink conditions. Samples of 2 mL were taken at two time points, 5 and 10 min, with dissolution medium replacement. The samples were filtered using Acrodisc® 0.45 μm syringue filter with a hydrophilic polypropylene (GHP) membrane (PALL Corporation, New York, USA) without discarding the first mL and were diluted so that the final concentration stayed within the range of values of the calibration curve.

In the second approach a Paddle Apparatus (Copley Dissolution Tester DIS 6000, Nottingham, UK) was used in a 37 $\pm$ 0,5 ºC temperature water bath. The dissolution media consisted of 30 mL of HCl 0,1 N and 70 mL of FeSSIF (Fed State Simulated Intestinal Fluid) biorelevant medium 1.3 times more concentrated (pH=5) (Biorelevant.com, Croydon, Surrey, UK). The dissolution media were degassed in

a sonicator for 10 minutes and preheated to 37 ºC before use. The sink conditions were assured when the FeSSIF medium, 1.3 times more concentrated, was added and the quantity weight of the formulations was estimated taken into account the drug loading of each formulation. Samples of 3 mL were taken at different time points (5, 15, 30, 45, 60, 90, 120, 150 and 180 min) with dissolution medium replacement, in the first 30 min using HCl 0.1 N and then normal FeSSIF. The samples were filtered using Acrodisc® 0.45 μm syringue filter with GHP membrane (PALL Corporation, New York, USA) discarding the first mL and were diluted until the final concentration fell within the range of values of the calibration curve. In the beginning, HCl 0.1 N was used as the dissolution media, the pHs of the taken samples were adjusted to 8, with ammonium hydroxide, since at this pH the majority of the molecules are in the free form, not affecting the residence time in the chromatograms. The pH shift occurred at 30 min-time point, by adding FeSSIF medium 1.3 times more concentrated.

The drug released from all formulations at different time intervals was determined by UPLC according to the method reported in Section 4.2.12.

Table 4.2 Composition of the SSF media (Koland et al., 2011; Peh and Wong, 1999).

Components	Quantity Weight
Disodium hydrogen phosphate	2,38 g
Potassium dihydrogen phosphate	0,19 g
Sodium Chloride	8,00 g
Milli-Q water	1 L
Phosphoric Acid	Enough to adjust pH to 6,75

5. Results and Discussion

To produce co-precipitated suspensions, three different co-precipitation processes (Stirred Reactor, Covaris and PureNano) were used. Spray drying was applied in order to isolate the suspensions produced, obtaining spray-dried co-precipitated powders.

After the powders production, different analytical characterization techniques (SEM-EDS, XPS, XRPD, DSC, TGA, UPLC, Dissolution) were employed to evaluate the CQAs (morphology and particle size, solid state and in vitro dissolution performance) and for benchmarking purposes of the co-precipitation processes, regarding taste masking properties of the different spray-dried co-precipitated powders.

5.1. Morphology of the Spray-Dried Co-Precipitated Powders

SEM micrographs for the spray-dried co-precipitated powders corresponding to trials #3, #4, #7 and #8 of the DoE (in figure 4.1) performed using three different technologies are presented in figure 5.1.

As the micrographs show, in general, for all the formulations tested spherical particles were obtained, independent of the technology used for the co-precipitation process. This type of morphology is characteristic of the isolation process selected for all the suspensions produced - spray drying (Passos and Birchal, 2010; Vehring, 2008). This type of morphology is frequently encountered for taste masking purposes, due to the low cost of SD production; furthermore, a high level of protection and controlled release is provided to the core material entrapped within the microsphere (Oxley, 2016).
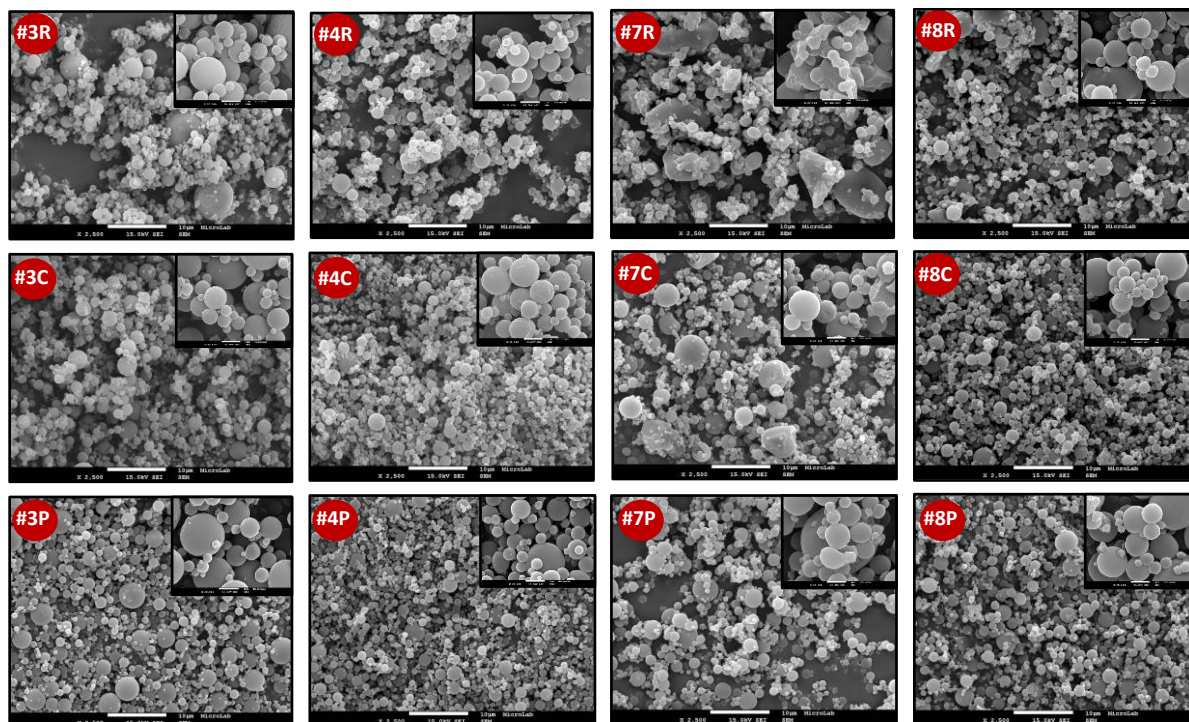
Figure 5.1 SEM micrographs corresponding to trials #3, #4, #7 and #8 of the DoE performed in the stirred reactor approach (#R), Covaris technology (#C) and PureNano technology (#P). Note that the bigger micrographs were taken at a magnification of 2 500x, while the smallest micrographs were taken at a magnification of 20 000x.

At higher magnifications it is possible to see the surface of the particles, revealing in the majority of the trials, a smooth surface and inflated particles. According to Vicente and Ferreira 2015 and Dobry et al.

2009, if starting from a solution, this type of structure suggests that a fast drying possibly occurred as a result of a high T_out that is near or above the boiling point of the DMF, when the droplet skin is formed. Thus, when the particle dries, the vapor pressure keeps it "inflated" leading to a hollow-sphere morphology. Typically, this type of morphology is characterized as having a low bulk density and a low percentage of residual solvent.

However, in this particular case the starting point of SD was a suspension, so it's necessary to be careful with the conclusions drawn. Starting from a suspension in SD, there will always exist a residual solubility that will act as a glue between the particles, as the solvent is evaporated in SD process, forming agglomerate structures. These agglomerate structures can be seen in some micrographs, and are specially noted in micrograph of the trial #7R. In some micrographs, namely #3C, #3R, #3P, #4P, #7P, #7C and #8C it is possible to distinguish some particles that present a rough surface as a result of a possible slower and/or deficit drying.

The micrograph corresponding to trial #4C reveals a warning that probably the EE and consequently taste masking effect could have been compromised, since it detects, in a representative form in the sample, the presence of API particles at a crystalline form on the surface of the spherical microparticles. Also, trial #7C seems to present crystalline pure drug on the surface of the spherical particles. Nevertheless, for this case, it is not representative of the sample.

If we look more carefully at the micrographs at a magnification of 20 000x, e.g. for #3C, #4R, #8R, #7P, #8P, #8C, but specially for trial #7R, it can be concluded that the surface of the particles is a result of the aggregation of multiple single primary particles. Most of these particles have a mean diameter that ranges in the nanoscale. Therefore, it is possible to conclude that in the co-precipitation process used, the suspensions can be classified as nanosuspensions, nevertheless when SD is applied as an isolation step, the particles aggregated as submicronparticles followed by the encapsulation of a polymer layer, hopefully, forming an almost perfect sphere. This type of structures is probably a result of the formation of crystalline solid dispersions, crystalline drug within an amorphous polymeric matrix. Therefore, the type of particulate structure obtained may not be hollow, typically as a result of SD, but probably inside will present a certain level of compaction.

With regard to the aggregation of the particles and considering the micrographs #3R and #7R, #3C and #7C, #4C and #8C, #4P and #8P that are distinguished by the increase of the feed solids concentration from 8 to 12 % wt., it perceives a higher degree of particles aggregation. These results can be explained by an increase in population density, i.e., number of particles in solution, leading to an increase in the agglomeration rate, according to Thorat and Dalvi, 2011. For trials #3P and #7P, #4R and #8R no significant differences were detected.

In terms of SAS volume ratio, the degree of aggregation does not appear to be significantly impacted, since when it compares with the micrographs #3C and #4C, #3R and #4R, #3P and #4P, #7C and #8C, #7P and 8P no significant differences are detected. The exception is micrographs #7R and #8R, in which a higher degree of aggregation in the first micrograph mentioned was verified. This can be related with a low agitation speed resulting in an insufficient mixing capacity that leads to an excessive nucleation and, consequently, formation of highly agglomerated products (Yu et al., 2005).

Nevertheless, it is important to note that a great number of scientific publications claim that the amount of polymer stabilizer in the formulation is the main cause for the particles aggregation phenomena, and that the addition of polymer stabilizers inhibits the excessive crystal growth and subsequently facilitates particle aggregation (Ali et al., 2011; Ghosh et al., 2011; Meer et al., 2011). Also, the SD isolation step is referred in literature as a possible factor of increasing the particles aggregation, thus several research groups have been studying different approaches to prevent secondary aggregation during SD (Kumar et al. 2014; Lu 2014).

5.2. Particle Size of the Spray-Dried Co-Precipitated Powders

The mean circular equivalent diameter (MCED) of the powders produced was roughly estimated as indicated in subchapter 4.7, and are represented in μm in figure 5.2.

In general, among all the technologies used, the MCED varies from 0.84 μm to 1.57 μm and it seems to be homogeneous independent on the technology used, with similar particles size being observed. According to the high standard deviations observed in figure 5.2, it is not possible to distinguish the different technologies used regarding the MCED. The use of other techniques based on laser light diffraction would allow more accurate determinations of the particle size.

In figure 5.2, it can be observed that when comparing trials 3 to 7 and trials 4 to 8, i.e., increasing the feed solids concentration, the MCED remain practically constant.

According to Park and Yeo, 2012, a decrease on the PS with the increase of the drug concentration in solution was expected - as a result of higher supersaturation levels, increasing the nucleation rate that leads to the formation of a large number of smaller nuclei and consequently, smaller crystal size

However, in this case, the result obtained can be explained by the fact that not only the drug concentration was increased but also polymer concentration, and both were increased similarly. Moreover, it was not possible to increase the initial feed solids concentration more in order to keep the solubility of the model drug below its limit and to maintain the SAS volume ratio. It should also be noted that the only exception for the trend aforementioned was trials #4P to #8P, where a significant increase in the MCED value was observed.

Though is not possible to draw particular conclusions, regarding to the state of the art, it would be expected to obtain a smaller PS and a narrow PSD for Covaris technology (Dhumal et al. 2009; Narducci et al. 2011; Patel and Murthy 2011), and Microfluidization.

For both technologies, the elevated mixing capacity is responsible for the disruption of the agglomerates, reducing the PS and PSD (Yu et al., 2005). In the first case, the high shear mixing promoted by the Ultrasound treatment is increased about 10 times in comparison with the mechanical stirrer (Kim et al., 2002). Thus, enabling a further reduction of the powders PS, since a rapid mixing will allow to achieve a higher supersaturation degree in a short period of time, which is a key issue in nanoparticles (NPs) formation (Thorat and Dalvi, 2011). In case of the microfluidizer, the process pressure determines the energy dissipation, additionally impacting the PS of the formulations, generally through its reduction (Panagiotou et al. 2009; Peltonen et al. 2016). This even may occur since the liquid streams are forced to form turbulent and opposite jets with high velocities, forcing the liquids to mix in the nanometer scale (Panagiotou et al., 2007).
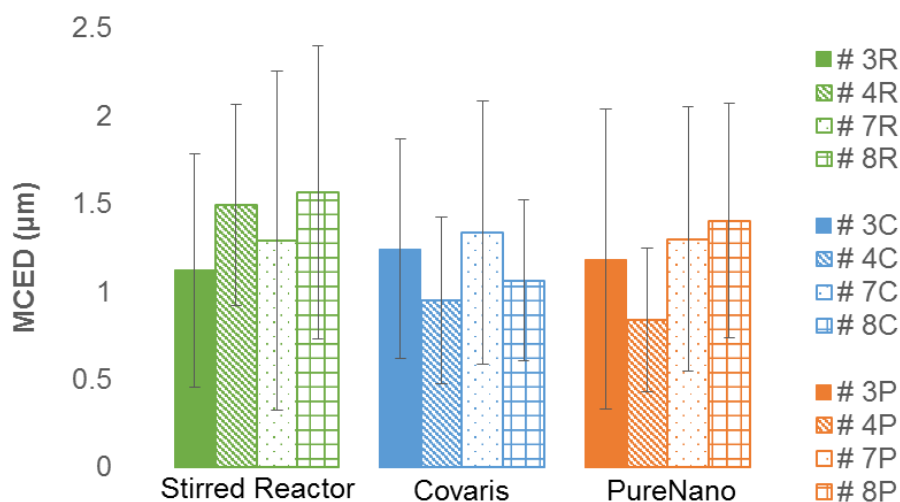
Figure 5.2 Mean Circular Equivalent Diameter, in μm, obtained through image analysis for all the formulations (Blue - Covaris Formulations, Green – Reactor Formulations, Orange – PureNano formulations). Note that the bars represent the standard deviation between the 300 particles that were measured.

5.3. Drug's Solid State in the Spray-Dried Co-Precipitated Powders

In figure 5.3 the powder diffractograms corresponding to the raw materials (polymer and pure model drug) are presented as well as trials #3, #4, #7 and #8 performed for each technology and amorphous powder of the model drug produced by SD.

The XRPD analysis was performed to evaluate the presence of crystalline drug material in the formulations produced. Thus, regarding the drug's solid state of the formulations, there were differences in the spray dried co-precipitated powders produced using different technologies. When overlapping the drug substance and formulations (7 and 8) diffractograms, a single polymorphic form of the model drug was observed (coincidence peaks' characteristics from pure model drug in all trials). So, no polymorphic changes occurred during the co-precipitation and SD processes.

The first conclusion is that trials #3C, #4C, #3R, #4R and #4P are in the amorphous form, as no characteristic crystalline diffraction peaks of the model drug appear, it can only be found a hallow characteristic of the amorphous form. Secondly, it can be concluded that all powders generated in trials #7 and #8 contain crystalline API, meaning that crystalline solid dispersions were formed in these cases. Regardless of the technology applied, these are the trials with the higher feed solids concentration (12%). This can be justified by the fact that the initial solution is nearest the supersaturated state for the trials that present higher feed solids concentration when compared to the lower ones (#3 and #4). This would increase the level of supersaturation, and as this parameter is the driving force of the precipitation process, result in a major amount of crystalline material that precipitates, or in other words, less material delays in solution to precipitate, probably in SD process under amorphous form.

It is worth mentioning that for trial #3P crystalline API was also detected in the corresponding XRPD diffractogram: nevertheless, the amount present, if one considers the intensity of the characteristic peak of the API (localized at about 10.3º 2θ) as reference, is much smaller than the one of #7 and #8 trials.

The diffractograms of formulations #7 and #8 show a significant lower peaks intensity when compared to the pure drug substance or even to the blend drug:polymer, meaning that the integrity of the raw materials was not maintained. Nevertheless, it is important to highlight that for formulations #7C and

#8C, the peak is smaller than for #7R and 8R, meaning that more amorphous drug is present on the first ones (data below will prove this). Thus, and as already mentioned, the formation of amorphous drug material was promoted, possibly when subject to SD, as a result of the amount of dissolved material that remains in solution (Pietilainen, 2013). This event may be due to the fact that the antisolvent flow rate was higher than the solution flow rate for all the technologies, may provide a sporadic uptake of saturated solution (Brown et al., 2015).
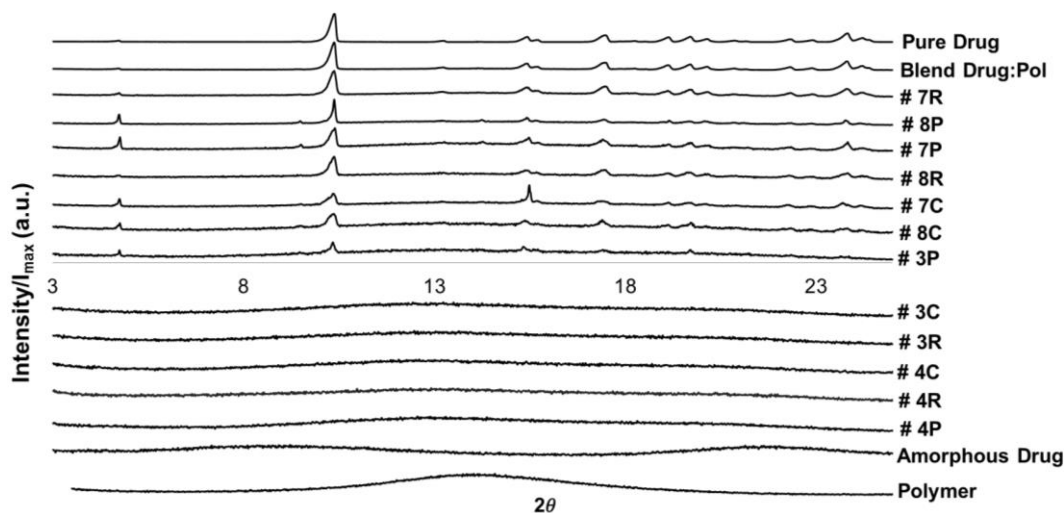
Figure 5.3 Powder diffractograms correspondent to trials #3, #4 #7 and #8 produced by the three technologies used and also the raw materials and amorphous drug. Note that all the diffractograms were normalized, dividing the intensity in all the points by the maximum intensity verified in each sample. Besides that, a constant was added at each diffractogram in order to separate them, so the units are arbitrary.

In order to quantify the percentage of crystalline material present in each formulation produced, and to conclude which sample presents a higher percentage of crystallinity, it was thought to use the DSC technique. This technique not only is important to evaluate endothermic and exothermic events and to determine the temperatures at which those occur, as mentioned in 4.2.10, but also, according to Gill et al. 2010, allows the estimation of the percentage of crystallinity, without being mandatory the preparation of a calibration curve, by using the following equation:

$$\% \, Crystallinity = \Delta H_f - \frac{\Delta H_c}{\Delta H_f^{Pure}} \times m$$

Equation 5.1

where ΔH_f refers to the heat of fusion of the sample, ΔH_c the heat of crystallization of the sample, ΔH_f^{Pure} the heat of fusion of pure crystalline sample and m is the weight of the sample.

As the equation shows, to determine the percentage of crystallinity it is necessary to use the DSC thermograms with a well-defined peaks corresponding to recrystallization and fusion. However, the DSC thermograms present in figure 5.4 do not reveal the crystallization peak and the melting attributed to the API is not resolved from the endothermic transition assigned to water release from the API crystalline structure. Based on this, the approach proposed to estimate crystallinity cannot be applied in this case. The DSC curves (Figure 5.4 (a) and (b)) show that at 50-90 ºC there is a broad endothermic peak that can be attributed to bulk water release. At higher temperatures (110-140ºC), another large endothermic

transition is clearly visible both on the API on the physical mixture and on formulations #7R and #8R (Figure 5.4 (a)). This is due to the release of the water from the crystalline structure of the API; at this stage, the anhydrous form of the model drug is obtained. With increasing temperature, this will melt which is given by a small endothermic transition observed at above 150ºC. For the amorphous formulations (#3 and #4) and for the ones with lower crystallinity (e.g. #7C, #8C) a step change in the baseline is verified at about 130ºC (Figure 5.4 (b)); this is most probably attributed to the glass transition temperature of the amorphous material. In fact, the amorphous API has a glass transition temperature, as determined by mDSC, of about 134ºC (figure 5.5). In all cases, at higher temperatures, above 200 ºC, the degradation of the drug occurs which is characterized by an exothermic event.
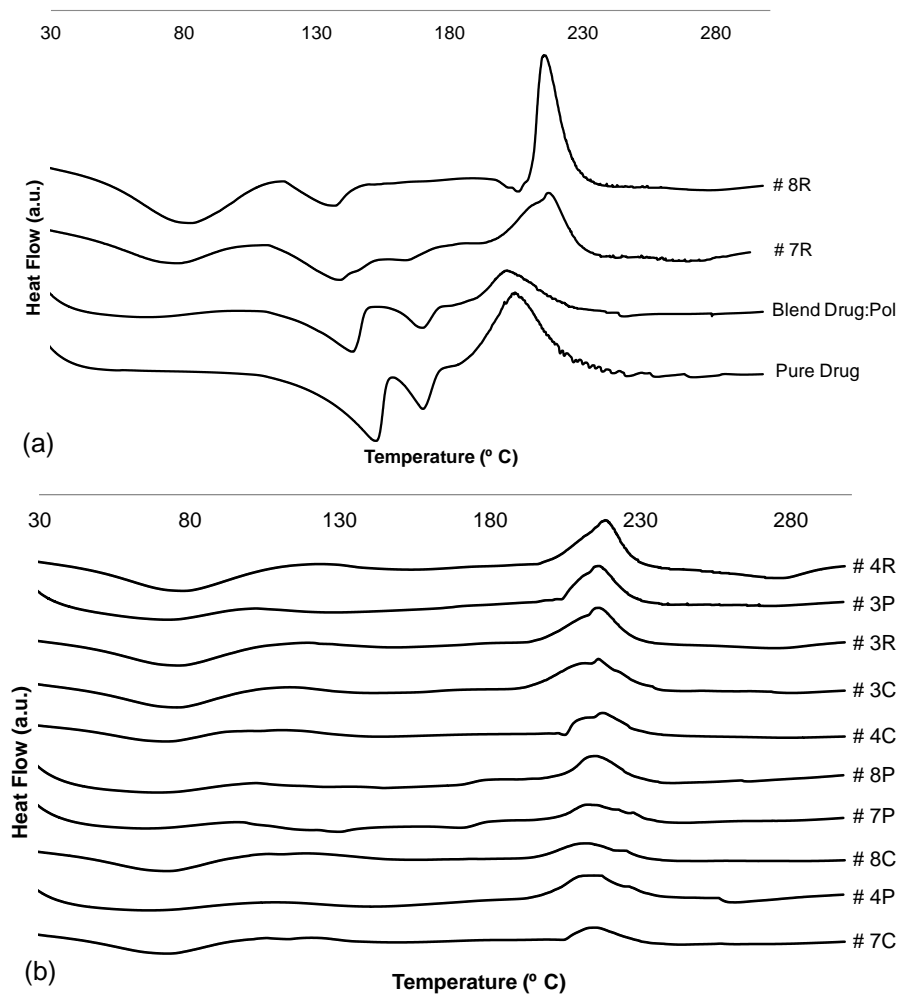
Figure 5.4 DSC thermograms corresponding to (a) crystalline trials #7R, #8, pure drug substance and physical mixture and (b) amorphous trials #3, #4 for all technologies and #7 and #8 for Covaris and PureNano technologies.
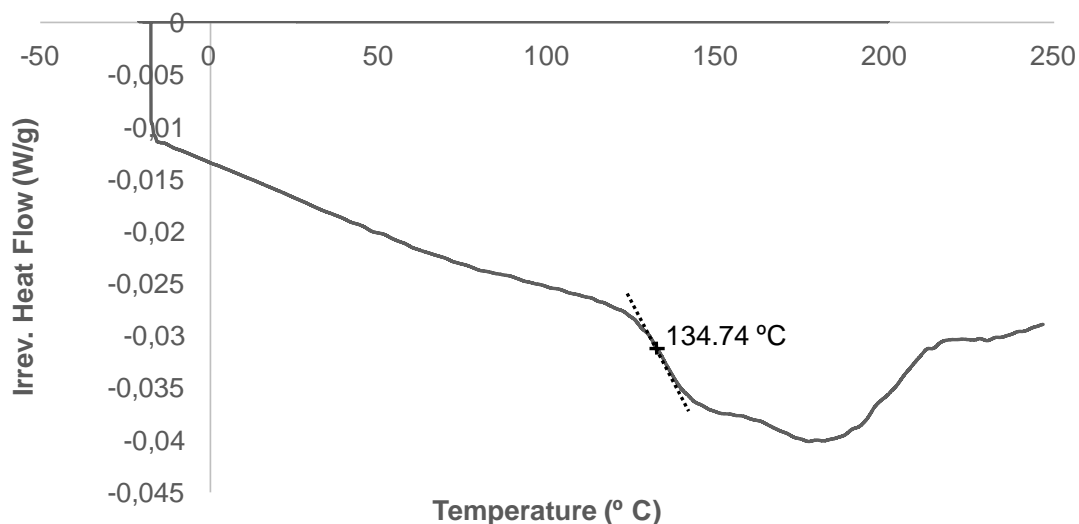
Figure 5.5 Reversible heat flow curve of mDSC thermogram corresponding to pure drug substance in the amorphous state.

After reaching the conclusion that it is not possible to obtain an estimative of the amount of crystalline material present in the samples by the DSC technique, an alternative approach was used by XRPD. This approach was based on the comparisons between the net height of the characteristic API peak localized at $2\theta = 10,3°$ of the physical mixture and of the formulations which reveal some content in crystalline material in XRPD analyses, i.e., #7 and #8 trials. In table 5.1., it is shown the net heights of the different formulations measured by Data Viewer software and the respective percentage of crystallinity, using the physical blend as the standard sample.

Table 5.1 Net heights of the different formulations measured by Data Viewer software and the respective percentage of crystallinity.

	Net Height	% of Crystallinity
#7R	5985.4	41.6
#8R	2798.2	19.4
#7C	1827.5	12.7
#8C	1276.4	8.9
#7P	2566.9	17.8
#8P	6061.3	42.1
Physical Mixture	14395.5	100

Although this approach only provides a rough estimation of the crystallinity percentage in each sample, an ascending ranking order related with the amount of crystalline material could be established: 8C < 7C < 7P < 8R < 7R < 8P. Analyzing these results, no valid explanation can be proposed as according to the differences in the formulations and production processes used no correlation or logic trend can be drawn.

5.4. Determination of Drug Content in the Formulations

Figure 5.6 presents the drug content for all the formulations corresponding to trials #3, #4, #7 and #8 of the DoE performed using the three different technologies. The final values of the drug content were corrected according to the TGA analysis, whose purpose was to determine the weight loss related with residual solvents and water.

As far as the information presented in the figure is concerned, it is possible to conclude that, in all cases, the drug content of the formulations produced is lower than the theoretical value (60 % wt.). Considering the conventional and the Covaris technologies, identical values are obtained within each group, being the only exception in Covaris technology for trial #7C, that presents even a lower drug content, i.e approximately 10 % less when compared to the other trials produced by the same technology. PureNano technology presents large fluctuations of drug contents, particularly noted in trials 7 and 8.

In order to understand if the cause for this low drug content could be related with the UPLC method used, in particular with the correspondent sample preparation, pure drug samples diluted in MeOH were injected with certain known concentrations using the UPLC, and the values acquired were in accordance with the expectation (i.e. 98%), moreover, good agreement was obtained for different sample preparations (D-checks between 95-105 %). So the only possible explanation for the lower drug content (about 10 % less than the theoretical value), could be related with some problems verified in SD process, namely the clogging of the nozzle, resulting in the loss of some material, that deposits in the chamber walls as a result of pulse actions to try to unclog the nozzle. This is also confirmed by the low yield rates obtained in SD, especially in formulations 7 and 8. A suggestion to address this problem is the use of an orifice with a wider diameter (2.2 mm), avoiding or minimizing the clogging of the nozzle. Nevertheless, this change would have an influence on the final particle size of the spray-dried co-precipitated powders.

When comparing the drug content of the formulations produced with the conventional approach and Covaris Technology, it is possible to conclude that a higher drug content is obtained when the latter technology is used. Although the yield of the Covaris process cannot be calculated since it is followed by an isolation step (SD), the fact that the process elapsed at continuous controlled temperature may provide higher recovery yields and make possible to preserve the fidelity of the sample (Covaris, 2016).
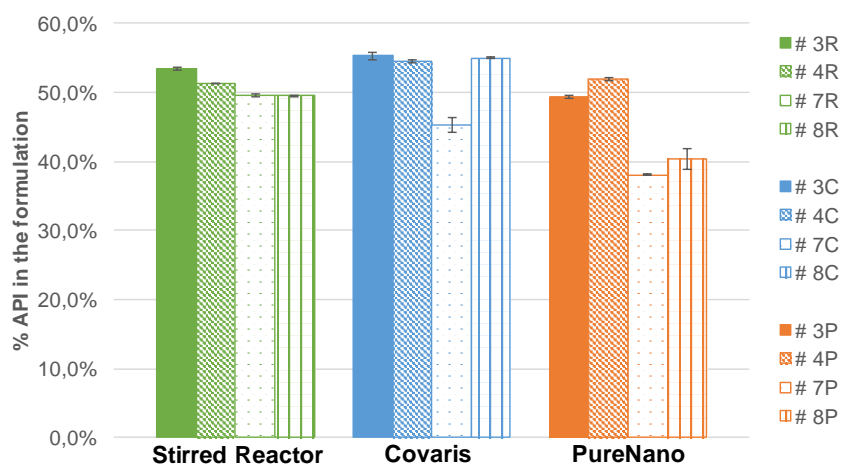
Figure 5.6 Drug Content present in the formulations produced through the different technologies used (Blue – Covaris Formulations, Green – Reactor Formulations, Orange – PureNano formulations). Note that the bars represent the standard deviation from the drug content studies performed in duplicate.

Figure 5.7, presents the TGA analysis performed for all the formulations produced through the three technologies used in this thesis. TGA analysis was performed with the main purpose of studying the weight loss attributed to water and residual solvents, revealing consistent results, in what concerns thermal sample behavior, with the DSC analysis.

In the beginning of the weight loss curve (%) there isn't a well-established and defined plateau, in comparison to the pure model drug curve. Indeed, the formulations soon begin to lose weight when subjected to temperatures slightly higher than the room temperature (first down ramp in the curve), which means that the formulation contains, as expected, bulk water that is coming out with increasing temperature. Then, a small-weight loss occurs possibly because of the presence of residual solvents used in the process (DMF and water); this is represented by the second down ramp observed in the formulations TGA curves. Lastly, the down ramp that follows at about 140-170 ºC, corresponds to the water from the API crystalline structure (monohydrate). In fact, this weight loss is occurring at the same temperature as for the pure API for which the % weigh loss is of 4.13 %, which is in agreement with the theoretical value for the monohydrate (3.6 - 4.6 %). At higher temperatures (>200 ºC), and in agreement with the DSC, melting, followed by decomposition, occurs.
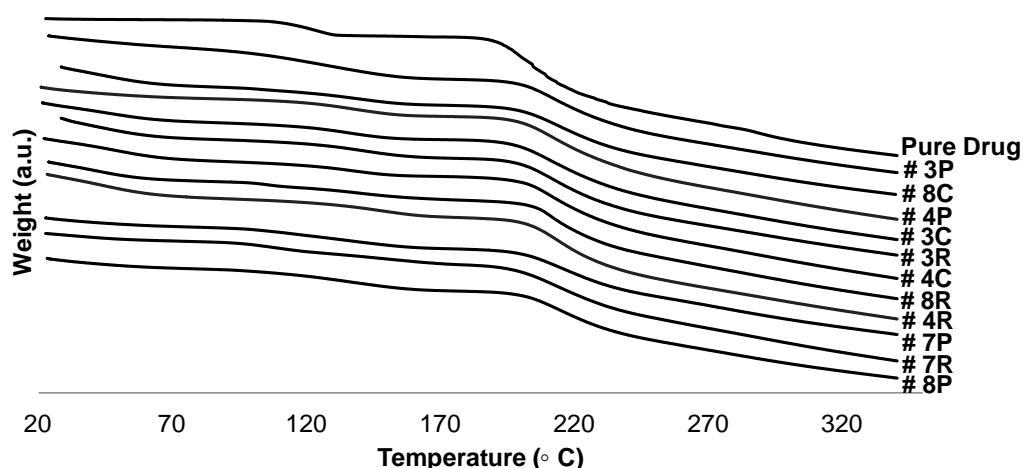
Figure 5.7 TGA thermograms corresponding to all the formulations produced using different technologies, as well as the pure model drug thermogram.

In table 5.2., the total weight loss of water obtained for all the formulations is presented. The values listed in the table are very similar among the different technologies used, however the aforementioned values are extremely high when compared to the theoretic value of water content that the model drug should present, 3.6 to 4.6 % wt. defined by the European Pharmacopeia 5.0. The value of water content in pure model drug, as determined by the TGA experiment, is 4.13 % wt., which is in the range already mentioned. As the formulations were produced using water as the antisolvent and contained also a polymeric matrix, with the ability to swell incorporating water molecules, the values discrepancy between the theoretical total weight loss and the values obtained was predictable. Like this, the drying conditions in the isolation step are fundamental, so an optimization of the conditions can improve the mentioned difference in the values of weight loss.

43

Table 5.2 Total weight loss (% wt.) obtained for all the formulations produced, through TGA analysis.

	Stirred Reactor (#R)	Covaris (#C)	PureNano (#P)
#3	11.18	9.33	11.08
#4	10.91	9.51	7.68
#7	7.91	17.55	7.81
#8	9.63	9.71	8.30

As previously stated, these values were used to calculate the drug content of the formulations presented in figure 5.6.

5.5. *In vitro* Dissolution Studies

In figure 5.8 the results for all the formulations produced using three different technologies are shown, within the first 10 min of the first approach of *in vitro* dissolution studies in simulated salivary fluid medium. The time-points were selected considering the residence time of drugs in the oral cavity, which is about 5-10 min (Bartlett and van der Voort Maarschalk, 2012).

A result expected is the fact that the amorphous API dissolves more than the crystalline API, since the first polymorphic form represents the best solubility case, which according to Noyes-Whitney equation (Noyes and Whitney, 1897) translates in a higher dissolution rate and consequently better bioavailability. Nevertheless, the difference in the amount of drug release between amorphous and crystalline API was not so significant as expected, since it combines the amorphous form (promoting better dissolution rates) with smaller size particles (produced by SD), supposedly further increasing the dissolution rate. However, investigations with pure nanocrystals, i.e. 100 % API with no use of stabilizer or polymers, that aims to study the effect that the particle size can have in dissolution rate haven't been reported with the desired frequency (Deng et al., 2012). For that reason, for many drugs there is a gap of the true impact that the particle size can have on the dissolution rate. In the situation mentioned above, we should keep in mind that the amorphous drug was produced by spray drying technology starting from a solution and according to what was mentioned in subchapter 5.1, the spray dried powder would be inflated, most likely resulting in a lower bulk density (when compared to the raw material, pure API), occasioning subsequently an increasing in the dissolution rate.

The API by itself present a higher drug release when compared with some of the formulations, which was expected since the polymer coating plays an important role in what concerns the reduction of the drug release, as reported by Hoang Thi et al., 2012. Additionally, considering that the pure drug is 100 % crystalline and in some cases the formulations are fully amorphous, and according to the reasons stated previously, some formulations may present a higher dissolution rate than would be expected if the polymorphic form was the intended.

Thus and concluding, the polymorphic form (amorphous or crystalline) seems not to have a significant impact on the dissolution profiles of the formulations. Hence, it was not possible to establish a correlation between the dissolution profiles and the amount of crystalline material roughly estimated in XRPD analysis, in subchapter 5.1.

According to the general criteria announced before, in subchapter 3.4, the FIP/AAPS guidelines suggest that in order to achieve taste masking, the API has to dissolve usually less or equal to 10 % in the first 5 min of dissolution. Regarding the results displayed in the following figure, this condition was verified for the commercial product and trials #7R, #8R, #4C, #3P, #4P, #7P and #8C. Nevertheless, it is important to note that the dosage form of the commercial product is not powder but a dispersible tablet, that suffers compression, and beyond that, the tablet is coated with enteric excipients. As mentioned in literature, the dissolution profile can be clearly affected by the oral dosage form, excipients used (Habib et al., 2000), compression forces (Ghadiyali et al., 2013), as well as the particle size of the result powder (Habib et al., 2000), making it necessary to be careful when comparing with the formulations produced. The formulation with the lower drug release in the first 5 minutes was trial #7P, releasing about 3.97 % of the drug. There are other promising formulations, namely #4C, #3P, #4P, however, the API in these formulations is in the amorphous form, which is not the target polymorphic form.
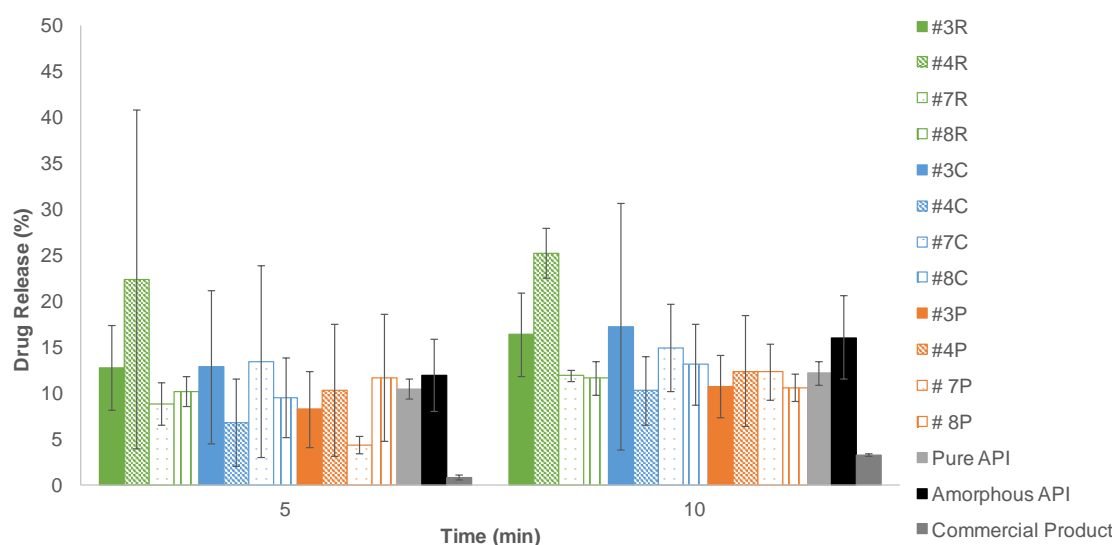
Figure 5.8 Dissolution profiles corresponding to all the formulations produced (Blue – Covaris Formulations, Green – Reactor Formulations, Orange – PureNano formulations) and also the amorphous powder produced through SD, raw material (crystalline model drug) and a commercial product. Note that the bars represent the standard deviation from the performed dissolution profiles performed in duplicate.

As previously described, a second approach, the pH shift one, was also applied to evaluate the dissolution profile of the formulations.

The drug release profiles, using the pH shift approach as a function of dissolution time of the trials #7R, #8C and #7P in comparison to the commercial triturated and not triturated product, i.e., as a dispersible and coated tablet, are shown in figure 5.9. Considering that the model drug is partially absorbed in the stomach and upper gastrointestinal tract (O'Connor, 2004), two dissolutions medium were selected to mimic these conditions. The first dissolution medium selected, HCl 0.1 N, intended to mimic the stomach content. To mimic the gastrointestinal tract, FeSSIF was selected, attending that the absorption of the model drug is improved with food, i.e., after the ingestion of food (O'Connor, 2004).
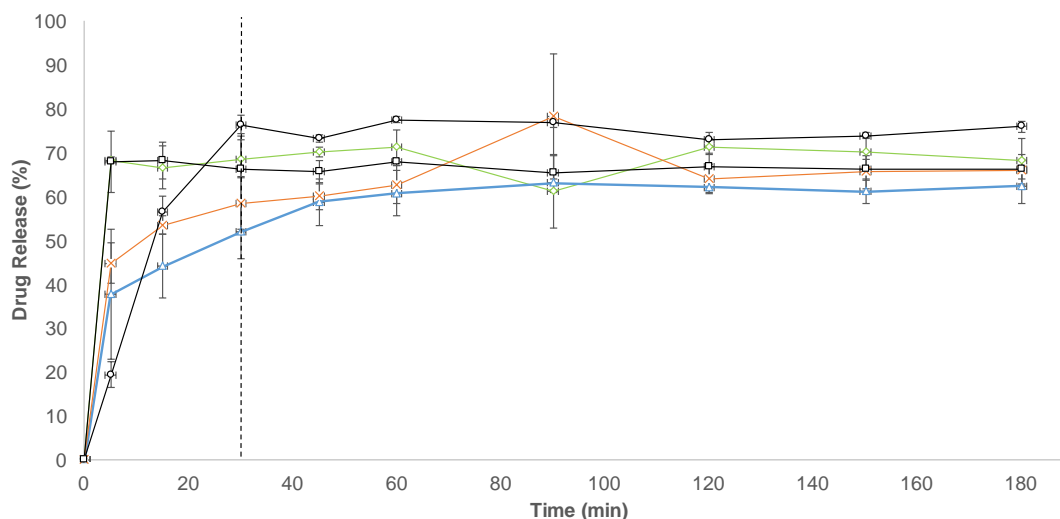
Figure 5.9 Dissolution profiles corresponding to the pH shift approach tested in the formulations #7R (green line, lozenges), #8C (blue line, triangles), #7P (orange line, cross) and commercial triturated (black line, quadrates) and not triturated (black line, circle) product. The vertical dashed line at the 30 min time point corresponds to the pH-shift. The bars correspond to the standard deviation from duplicates experiments.

The pH change performed at 30 minutes for all the formulations tested, does not impact the solubility of the drug, or in other words, the solubility is independent of pH.

These dissolution profiles seem to indicate that once the drug reaches the stomach, it dissolves very well and maintains its solubility when directed towards the intestine. This is a good sign since the drug is absorbed in the final stage of the stomach and in the upper intestine.

Generally, a drug release of between 60 to 80 % was obtained for all the formulations tested. For benchmarking purposes, the dissolution profiles of the promising formulations were compared with the one acquired for the commercial product triturated and not triturated, showing similar dissolution profiles, in the stomach and the intestine. Thus, the pH shift dissolution method allows to conclude that the formulations do not seem to have been impacted by any of the co-precipitation processes used.

In this approach, the commercial product was tested as a coated and dispersible tablet (not triturated) but also as a powder (triturated), in order to study the differences in the dissolution profile. The results show that the burst release in the first 15 minutes was significantly higher as a powder rather than as a tablet. This result was expected since the enteric polymer coating film was destroyed with the triturate process, for that reason the drug is faster released in the dissolution medium and, subsequently a higher burst release was obtained in this case.

Throughout the experiments conducted, it was observed that apparatus 2 is not the most suitable dissolution apparatus to use, when the dosage form is powder. The powders fluctuate, and when the samples are taken, material is removed from the medium, generating experimental errors. Thus, the utilization of apparatus 4, a Flow-Through Cell Apparatus, would be important to minimize and avoid the propagation of errors.

In order to study all the trajectory of the drug release in the human body, beginning in the mouth, stomach and finally the intestine, it would be very interesting to develop new methods that can mimic these pH changes, volumes and dissolution media in a continuous mode (Fotaki, 2011). In the future, the utilization of apparatus 4 for this effect should be studied and evaluated.

5.6. Determination of Encapsulation Efficiency

5.6.1. SEM-EDS Analysis

The purpose of EDS analysis was to assess the encapsulation, relating it with the taste masking properties. According to the molecular structure of API and polymer, the only differentiator element between both is nitrogen and thus, this element was used in this analysis. The concept used is very simple: if the nitrogen is detected by an EDS microscope in lower percentage when compared with the standard sample (pure drug substance), it is possible to conclude that the encapsulation is efficient and probably good taste masking properties will be obtained.

Figure 5.10 shows the encapsulation efficiency determined through EDS analysis for the trials #7 and #8 of each one of the technologies used (crystalline samples). In table 5.3 the detected values of nitrogen by EDS microscope are shown, as well as the associated error to this detection.

A first indication that something wasn't right in this technique, was the nitrogen weight percentage detected by EDS microscope for a pure API sample, 13.8 % (table 5.3). This value is very inflated, since the theoretical value of percentage by weight of nitrogen is about 6.4 %. As the EDS microscope does not detect hydrogen, this calculated theoretical value of percentage by weight of nitrogen was corrected, becoming 5.8 %.

The results were consistent regarding the detected values of nitrogen between the pure API sample and the first point analyzed through EDS microscope in the physical mixture (blend 60:40 % wt. of API:Polymer), confirming the presence of API in this mixture.

In the second point of the physical mixture analyzed by EDS microscope, the negative nitrogen detected value of -11 % has no physical meaning. Thus, the interpretation of these results should be considered carefully and cannot be taken literally. Accordingly, the only conclusion possible to draw is that no nitrogen could be detected at this point of the sample, which combined with the SEM micrographs, i.e., analysis of particles morphology, allows to infer that only the polymer is present.

Another indication of the variability and error of this technique is the fact that, in the majority of the analysis, the standard deviation of the nitrogen element was much higher when compared to the detected value by SEM-EDS microscope. Thus, it is not possible to conclude if there is nitrogen or not.

As figure 5.10 and table 5.3 shows, for the trials where the value of nitrogen detected was higher than the nitrogen detected in the pure API sample (#8R, #7P and #8P), the EE was negative. As mentioned before this does not make any physical sense, indeed, the only conclusion that can be made in this case is that the entrapment of the drug within the polymer was not accomplished for those trials.

Knowing the information that EDS has a limitation in the detection of light elements with atomic weight inferior than 11 (Australian Microscopy and Microanalysis Research Facility, 2014)), everything points to the fact that this technique is not suitable to provide information about the encapsulation efficiency, and consequently taste making properties, for this particular drug substance.
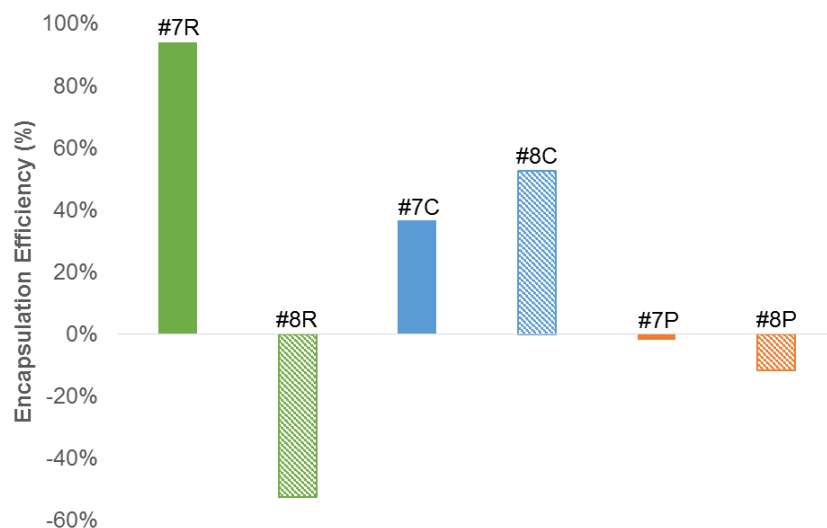
Figure 5.10 Encapsulation Efficiency corresponding to trials #7R, #8R and #7C, #8C determined through the nitrogen detected values by EDS microscope.

Table 5.3 Values detected of nitrogen by EDS microscope and associated error to this detection, both in weight percentage.

	N Detected (weight %)	σ (weight %)
#7R	0.9	19.7
#8R	21.9	8.4
#7C	9.2	14.6
#8C	6.8	19.4
#7P	14.6	7.0
#8P	16.1	5.7
Physical Mixture	14.4	5.75
	-11.96	23.24
Pure API	13.8	6.93

It is important to note that the duration of the electron beam in the samples was not always the same, as well as the number of counts in all the trials, this can impact the precision of the measurement of nitrogen value present in the samples.

The large depth analysis characteristic from EDS, that can reach to a few μm (Ferraria, 2002; van der Heide, 2012), is a huge limitation. And, due to the small particle size of the samples, the electron beam may penetrate the entire particle, giving information of the overall composition of the particle instead of its surface composition. For that reason, an alternative that would allow the evaluation of the encapsulation efficiency had to be found, and this was to perform XPS analysis.

5.6.2. XPS Analysis

This technique allows to obtain a detailed chemistry composition of the surface with a depth analysis that can reach up to 10 nm-outermost layer composition of particles, in certain cases giving the possibility of characterizing the first 10 to 20 atomic layers of the irradiated surface (Ferraria, 2002).

Besides that, this technique also consents the study of the oxidation numbers of the elements identified in the sample.

In table 5.4, the experimental atomic concentrations (%) and atomic ratios for the formulations as well as for pure drug and physical mixture can be seen and, for comparison purposes, the nominal atomic concentrations and ratios are also included.

Table 5.4 Experimental and theoretical atomic concentrations (%) and atomic ratios of the formulations #7R, #7P, #8C and standards of pure drug and physical mixture.

	Experimental Values					Theoretical Values	
	Pure Drug	Physical Mixture	# 7R	#8C	#7P	Pure Drug	Physical Mixture
C	66.0	65.0	65.8	64.7	65.9	66.7	68.0
O	27.3	31.9	31.2	31.2	31.2	27.3	28.4
N	6.7	3.1	3.0	4.2	3.0	6.1	3.7
Ratio O/C	0.41	0.49	0.47	0.48	0.47	0.41	0.42
Ratio N/C	0.10	0.05	0.05	0.06	0.04	0.09	0.05
Ratio N/C$_{carboxyl}$	-	0.42	0.37	0.67	0.34	-	0.62
EE (%)	-	-	55	37	55	-	-

The value of nitrogen for the pure drug standard sample (6.7 %) is comparable with the theoretical value (6.1 %). This is also confirmed by the match between the experimental ratio (0.10) between nitrogen and carbon and the theoretical value (0.09). Nevertheless, this ratio quantifies all the carbon atoms that exist in the system, including the carbons from aliphatic contamination (from the double sheet glue). Thus, this quantification might lead to inconclusive comparisons.

The value of nitrogen detected in the physical mixture (a blend of polymer-drug in the proportion used to produce the different formulations), is only slightly smaller (3.1 %) when compared to the theoretical value considering a homogeneous mixture, without stratification (3.7 %).

The O/C ratio does not provide considerable information on the system analyzed, since similar values were obtained and no substantial differences were noted in the atomic concentrations of oxygen and carbon.

The ratio that allows us to extract more information is the ratio between nitrogen and carboxyl groups. In fact, this ratio can provide insights to the distribution profile of the model drug and polymer in the sample, since the nitrogen atom only exists in the model drug and carboxyl and ester groups only exist in the polymer.

The experimental value of the physical mixture is lower than the theoretical value (a homogeneous mixture, with no stratification). So apparently, this result is compatible with some microencapsulation of the model drug by the polymer, in the physical mixture. However, it is important not to forget that the particle sizes of polymer and drug are significantly different and this blend was not processed. Thus, it is not about a microencapsulation process, but a stratification phenomenon of the polymer at the surface of the model drug molecules. The occurrence of this phenomena can be confirmed comparing the SEM micrographs for the physical mixture and pure drug (figure B.1 and B.2, Supplementary Information). For this reason, less nitrogen was found (from the pure drug) and more carboxyl groups were detected

(from the polymer). Thus, this experimental result shouldn't be used for comparison purpose and to determine the EE, since it's a source of errors propagation.

The samples #7R and #7P are the ones that apparently present a more efficient encapsulation, since the ratios N/C$_{carboxyl}$, 0.37 and 0.34 respectively, are lower than the theoretical value (0.62). On the other hand, the sample #8C appears to be segregated at the surface of the polymer, since the ratio N/C$_{carboxyl}$ is higher (0.67) when compared with the theoretical value (0.62). However, the EE was determined using the same formula applied in EDS analysis, i.e., in which the standard sample was the pure drug. If stablishing an ascending ranking order for the formulations in terms of EE, it would be: 8C < 7R ≈ 7P. But undoubtedly, #7P is the best formulation since when the ratios between nitrogen and carboxyl groups are compared with trial #7R, the first one is slightly lower.

The results of EE are well correlated with the dissolution studies, and thus dissolution studies data can be a good indication of EE. Nevertheless, as clearly shown, if the aim is to determine or quantify the drug entrapped on the polymeric matrix, the use of XPS analysis is preferred instead of EDS analysis. Furthermore, this technique can be an important and useful tool for the systems that don't have any distinct element in their molecular structures, but only differ in functional groups, as explained by Hoang Thi et al., 2012.

Figure 5.11, shows XPS region (a) C 1s and (b) N 1s for the different formulations tested. N 1s was fitted using two peaks with different binding energies. The peak that is centered at the lower binding energy ($\sim$ 399.6 $\pm$ 0.1 eV) corresponds to the presence of pure model drug amide ((C=O)-NH$_2$) and amine groups (N-CH$_3$), the other peak at the higher binding energy ($\sim$402.1 eV) is assigned to protonated nitrogen (N$^+$). The C 1s region includes the aliphatic C-C and C-H (peak at 285 eV, which also includes aromatic carbons), C-N at 286 eV from tertiary amines, C-O and C=O which, on average, are 1.4 eV apart from each other, included in a single peak centered at 287 eV. At 289.4 eV is assigned the contributions from O-C=O and COOH.

Comparing the spectrums of C 1s regions among the different formulations, it seems that only the model drug exhibits peaks at 290.8$\pm$ 0.2 eV, assigned to the $\pi - \pi^*$ transitions typical from systems with delocalized electrons, as the benzene rings of the model drug. So, apparently, no model drug is present at the surface of the spray-dried particles. Nevertheless, these electronic transitions may be present in the formulations but covered by other interactions, since for values near that binding energy, there is peak at 289.4 eV, that appears in all the formulations, assigned to –O–C=O and –COOH, characteristic from polymer.

Contemplating the N 1s regions of the produced formulations and also the ratio between protonated nitrogen and total nitrogen, in table 5.5, the formulation that apparently present a higher relative amount in protonated nitrogen is #7R, followed by #8C and finally #7P. The expected result would be formulation #8C presenting a higher relative amount in N$^+$, since this formulation was produced with a higher SAS volume ratio (1:10) when compared to the other formulations produced with 1:6 of SAS volume ratio. So, in the case of the #8C trial, there is more quantity of acidic medium, and since the model drug is a weak base it would be expected that protonation is favored and therefore a higher amount of N$^+$ should be predictable when compared to the other formulations. However, these relative amounts don't represent the absolute value in protonated nitrogen and although the #7R trial was produced with less

amount of antisolvent, the use of a stronger acid (lower pH value) may result in a higher level of protonation, leading to a higher relative amount in N^+. Therefore, the use of high SAS volume ratio and strong acids seem to compromise the EE provided. Moreover, attending the standard deviation in dissolution profiles in SSF and that the SAS volume ratio can impact the relative amount in N^+, if trial #7C was evaluated, it should demonstrate a high EE when compared to trial #8C.

If the spectra of formulation #7P is compared with the other formulations and even with the standard samples (pure model drug and physical mixture), it can be seen that the two peaks, which comprise the spectra, seem to be less distinguishable or in other words, the peak assigned to amide and tertiary amines in N 1s of sample 7P is slightly shifted to higher binding energies, as can be seen in table 5.6. So, a modification on the nitrogen structure occurred as a consequence or an effect of an efficient encapsulation, and thus, there are more nitrogen atoms available to stablish hydrogen bonds, acting like a donor of its isolated par.

Table 5.5 Ratio between protonated nitrogen and total nitrogen calculated for all the formulations.

	Ratio N^+/N_{total}
Pure Drug	0.37
Physical Mixture	0.40
# 7R	0.42
# 8C	0.32
# 7P	0.29

Table 5.6 Binding energies, in eV, of N 1s fitted peaks.

	Assignments	Pure Drug	Physical Mixture	#7R	#7P	#8C
N1	-(C=O)-NH$_2$; N-CH$_3$	399.6	399.5	399.5	399.9	399.7
N2	N^+	402.3	402.1	402.1	402.1	402.3
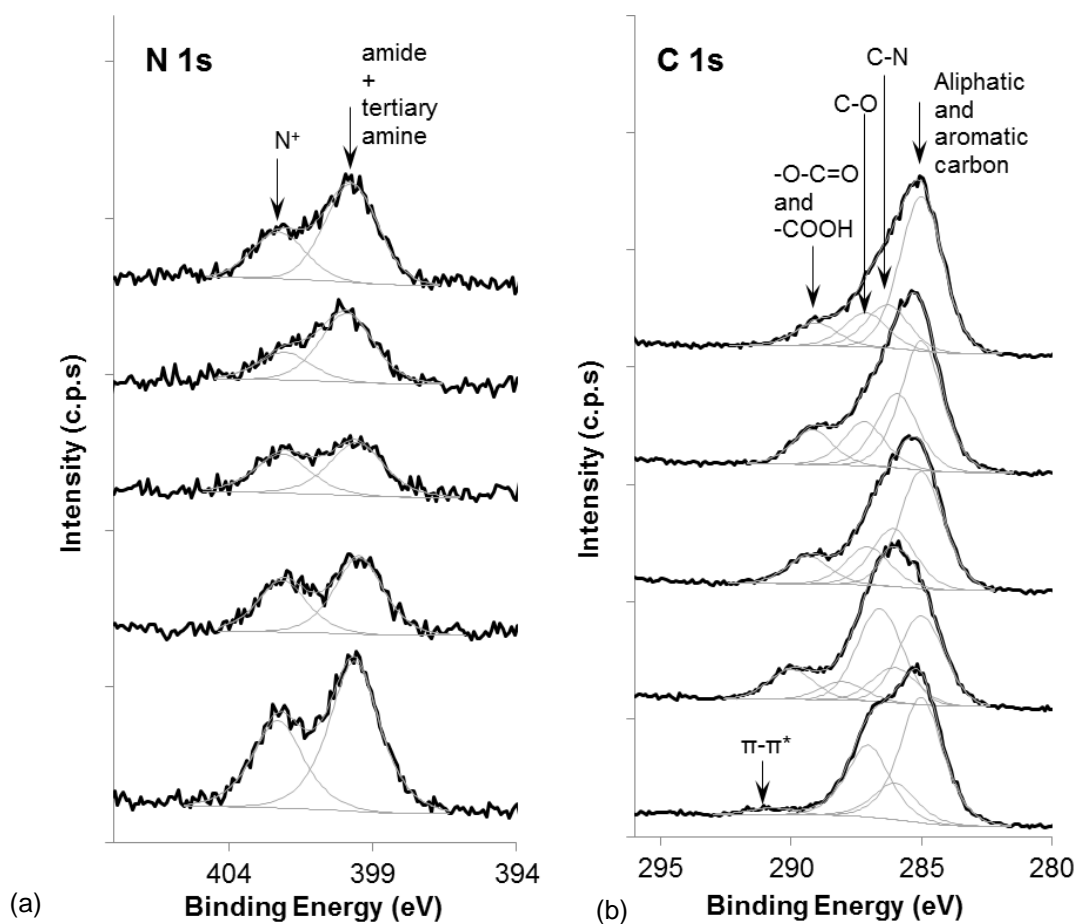
Figure 5.11 XPS (a) C 1s regions and (b) N 1s regions of the different formulations tested: pure drug, physical mixture, #7R, #7P and #8C (from the bottom to the top). Note that a constant was added to separate the spectrums.

6. Conclusions and Future Work

Taste masking is critical in the development of solid oral dosage forms since it is related to patient compliance, especially for pediatric populations. For that reason, the development of new processes that can assure the achievement of taste masking is important. For this effect, and considering the several approaches that already exist, microencapsulation was selected, using different co-precipitation processes to produce a suspension followed by an isolation step by spray drying.

Considering the particles morphology, similar micrographs were obtained among the different technologies used to produce the formulations. Particles obtained were spherical, which was expected due to the isolation step selected. The SEM images reveals no API particles at the surface of the spherical ones, with the exception of trial #4C, where probably the EE and taste masking properties could have been compromised. The presence of agglomerate structures was verified in some of the micrographs, due to the residual solubility that will always exist in the suspension, used as a starting point on SD process.

The particle size indicates a narrow PSD and smaller particles for Covaris, followed by Purenano and finally the conventional approach, mainly because of the elevated mixing capacity promoted by the first two technologies.

The results suggest that the formulations were taste masked using any of the processes disclosed in this work. Nevertheless, the encapsulation of the model drug by PureNano technology was the best approach when compared to Covaris technology as welll as the conventional approach. Thus, the best formulation was #7P, presenting a slower drug release in SSF medium, which is in accordance with the high particle size when compared to other formulations, and also the best results in terms of EE by XPS analysis.

The fact that PureNano seems to be the best technologies in order to achieve taste masking when compared to the conventional approach, can be related with a high mixing rate, resulting in a comparable time between NPs assembly and solvent diffusion, and consequently, a major amount of drug can be encapsulated within the carrier (Sarghini, 2015).

Higher values of EE were expected, namely in MRT, since several studies reported encapsulation efficiency values in order of 95 % or greater, due to the generation of single droplets during microparticles formation, where no drug is lost in the droplets (Sarghini, 2015). Nonetheless, it is important to highlight that following the co-precipitation process, an isolation step was performed and the problems already identified in the process, namely the clogging of the nozzle, can have an impact on EE. For that reason, the orifice of the nozzle should be altered for the bigger size. So, an optimization on the SD process and a compromise between several parameters is necessary.

In this work, the formulation variables studied were the drug load, SAS volume ratio and feed solids concentration. However, there are other variables that can impact the CQAs of the final product. In future studies, other formulation variables should be considered, as for example the type of polymer used and the addition of surfactants, as well as other process variables, such as flow rate and mixing capacity.

Considering that in this work only an intermediate product was obtained, it would be important to produce a final product (e.g. capsule or tablet) and re-evaluate the characteristics related with taste masking, in order to analyze if the process mentioned has any impact in taste masking properties.

Regarding EE results, it was concluded that EDS analysis had many limitations and was not appropriate for this particular model drug, contrary to XPS analysis. It was also possible to conclude that the dissolution studies provide good indications of EE, that are well correlated with XPS analysis, being the best formulations in terms of taste masking properties: 7P > 7R > 8C. Further works should be conducted to study and develop new methods/apparatus that are able to mimic the oral cavity, in terms of volumes, medium and time-points (tighter time-points in the first 5 minutes of dissolution).

The criteria established by FIP/AAPS regarding the accomplishment of taste masking is very generalized and does not take into consideration the model drug and its bitterness threshold concentration. And although the bitterness threshold concentration of the model drug used is not reported in literature, further works should be performed in order to determine this value and have the possibility of comparing the drug's release in the formulations in the first minutes with the bitterness threshold concentration, so that it is possible to conclude about the success of taste masking the bitter taste of the drug.

It would be also very interesting to develop new dissolution methods for this particular drug that can mimic its complete trajectory in the human body, from the oral cavity, passing through the stomach to the intestine tract, where the drug is absorbed, in order to study the success of encapsulation but also the drug's release in the human body. For this purpose, as mentioned before, apparatus 4 should be used.

Concerning the *in-vitro* data obtained, it would be very interesting to correlate it with *in-vivo* studies, namely in panel human tests or animal preference tests. But attending the ethical concerns of the experiments mentioned, it would certainly be more appropriate to test other types of approaches, for example electronic sensor methods, in particular an electronic tongue.

In conclusion, all the objectives proposed for this work were successfully achieved, namely concerning the benchmarking of the different co-precipitation techniques used, and their impact in the CQAs and mainly, in EE and subsequently taste masking properties.

Bibliographic References

Agrawal, S. (2010). *Investigation and Optimization of a Solvent / Anti- Solvent Crystallization Process for the Production of Inhalation Particles*. PhD Dissertation, Virginia Commonwealth University.

Al-Omran, M. F., Al-Suwayeh, S. A., El-Helw, A. M. and Saleh, S. I. (2002). Taste masking of diclofenac sodium using microencapsulation. *Journal of Microencapsulation*, *19*(1), 45–52.

Albertini, B., Cavallari, C., Passerini, N., Voinovich, D., González-Rodríguez, M. L., Magarotto, L. and Rodriguez, L. (2004). Characterization and taste-masking evaluation of acetaminophen granules: Comparison between different preparation methods in a high-shear mixer. *European Journal of Pharmaceutical Sciences*, *21*(2-3), 295–303.

Ali, H. S., York, P., Ali, A. M. and Blagden, N. (2011). Hydrocortisone nanosuspensions for ophthalmic delivery: A comparative study between microfluidic nanoprecipitation and wet milling. *Journal of Controlled Release*, *149*(2), 175–181.

Alvarez, A. J. and Myerson, A. S. (2010). Continuous Plug Flow Crystallization of Pharmaceutical Compounds. *Crystal Growth & Design*, *10*(5), 2219–2228.

Anand, V., Kataria, M., Kukkar, V., Saharan, V. and Choudhury, P. K. (2007). The latest trends in the taste assessment of pharmaceuticals. *Drug Discovery Today*, *12*(5-6), 257–265.

Australian Microscopy & Microanalysis Research Facility. *Training for advanced research with MyScope™: Quantitative EDS X-ray microanalysis using SEM.* Available from: "http://www.ammrf.org.au/myscope/analysis/eds/quantitative/" (Accessed 12 September 2016)

Ayenew, Z., Puri, V., Kumar, L. and Bansal, A. K. (2009). Trends in pharmaceutical taste masking technologies: a patent review. *Recent Patents on Drug Delivery & Formulation*, *3*(1), 26–39.

Baliga, J. B. (1970). *Crystal nucleation and growth kinetics in batch evaporative crystallization*. PhD Dissertation, Iowa State University.

Barros, R. (2009). *Desenvolvimento de óxidos semicondutores tipo-p para aplicação em transístores de filme fino*. Master Dissertation, Faculdade de Ciências e Tecnologia.

Bartlett, J. A. and van der Voort Maarschalk, K. (2012). Understanding the Oral Mucosal Absorption and Resulting Clinical Pharmacokinetics of Asenapine. *AAPS PharmSciTech*, *13*(4), 1110–1115.

Bellinghausen, R., Rudhardt, D., Ridder, F., Steinbeck, M., Zank, J., Weiss, M., Behrend, O. and Stiphout, U. V. (2009). Masking the taste of powders. Patent Number US20090269411A1

BETE Fog Nozzle. (2005). Spray Dry Manual. Available from: http://www.bete.com/pdfs/BETE_SprayDryManual.pdf (Accessed 3 July 2016)

Bhalekar, M. R., Madgulkar, A. R., Padalkar, R. R. and Manwar, D. B. (2014). Comparative Evaluation of Taste Masking Methods of Ondansetron HCl. *World Journal of Pharmacy and Pharmaceutical Sciences*, *3*(8), 982–995.

Birhade, S. T., Bankar, V. H., Gaikwad, P. D. and Pawar, S. P. (2010). Preparation and evaluation of cyclodextrin based binary systems for taste masking. *International Journal of Pharmaceutical Sciences and Drug Research*, *2*(3), 199–203.

Bora, D., Borude, P. and Bhise, K. (2008). Taste masking by spray-drying technique. *American Association of Pharmaceutical Scientists*, *9*(4), 1159–64.

Brown, C. J., Adelakun, J. A. and Ni, X. (2015). Characterization and modelling of antisolvent crystallization of salicylic acid in a continuous oscillatory baffled crystallizer. *Chemical Engineering and Processing: Process Intensification*, *97*, 180–186.

Canli, S. (2010). *Thickness analysis of thin films by energy dispersive x-ray spectroscopy*. Master Dissertation, Middle East Technical University.

Chiappetta, D. A., Carcaboso, A. M., Bregni, C., Rubio, M., Bramuglia, G. and Sosnik, A. (2009). Indinavir-loaded pH-sensitive microparticles for taste masking: toward extemporaneous pediatric anti-HIV/AIDS liquid formulations with improved patient compliance. *AAPS PharmSciTech*, *10*(1), 1–6.

Chirag, P., Tyagi, S., Dhruv, M., Ishita, M., Gupta, A. K., Usman, M. R. M., Mallik, J., Shree, N. and Paswan, S. K. (2013). Pharmaceutical Taste Masking Technologies of Bitter Drugs: a Concise Review. *Journal of Drug Discovery and Therapeutics*, *1*(5), 39–46.

Cogoni, G. (2012). *Stochastic Modeling of Nonisothermal Antisolvent Crystallization Processes*. PhD Dissertation, Università Degli Studi Di Cagliari.

Cordeiro, P., Temtem, M. and Winters, C. (2013). Spray congealing: applications in the Pharmaceutical Industry. *Chimica Oggi-Chemistry Today*, *31*(5), 69–73.

Cordeiro, P., Temtem, M. and Winters, C. (2014). Comparison of Spray Congealing and Hot Melt Extrusion for the taste masking of bitter drugs.Poster presented at: The 14th AIChE Annual Meeting, 2014 November 16-21, Atlanta, USA.

Covaris. (2016). S-220 Focused-ultrasonicators with AFA Technology. Available from: http://covarisin.com/products/afa-ultrasonication/s-series/ (Accessed 9 August 2016)

O'Connor, R.P. (2004). Tetracyclines, Chloramphenicol, Macrolides and Lincosamides. In *Modern Pharmacology with Clinical Applications*, (eds. Craig, C. R. and Stitzel, R. E.), 6th Edition, p. 544–5, Lippincott Williams & Wilkins.

Crowley, M. M., Zhang, F., Repka, M.A., Thumma, S., Upadhyde, S.B., Battu, S.K., McGinity, J.W. and Martin C. (2007). Pharmaceutical Applications of Hot-Melt Extrusion: Part I Review Article. *Drug Development and Industrial Pharmacy*, *33*, 909–926.

Cuña, M., Lorenzo-lamosa, M. L., Vila-Jato, J. L., Torres, D. and Alonso, M. J. (1997). pH-Dependent Cellulosic Microspheres Containing Cefuroxime Axetil: Stability and In Vitro Release Behavior. *Drug Development and Industrial Pharmacy*, *23*(3), 259–265.

D'Addio, S. M. and Prud'homme, R. K. (2011). Controlling drug nanoparticle formation by rapid precipitation ☆. *Advanced Drug Delivery Reviews*, *63*(6), 417–426.

Danish, M. A. M., Shetsandi, A., and Bhise, K. S. (2013). Formulation Development and Taste Masking of Rifaximin Nanosuspension. *Inventi Rapid: Pharm Tech*, *2013*(4), 1–5.

De, A., Mishra, S. and Mozumdar, S. (2014). Synthesis of Nanovehicles. In *Advanced Healthcare Materials* (ed. Tiwari A.), John Wiley & Sons, Inc., Hoboken, NJ, USA.

Dhumal, R. S., Biradar, S. V., Paradkar, A. R., and York, P. (2009). Particle engineering using sonocrystallization: Salbutamol sulphate for pulmonary delivery. *International Journal of Pharmaceutics*, *368*(1-2), 129–37.

Dixit, A. K., Singh, R. P., and Stuti, S. (2012). Solid Dispersion - A Strategy for Improving the Solubility of Poorly Soluble Drugs. *International Journal of Research in Pharmaceutical and Biomedical Sciences*, *3*(2), 960–966.

Dobry, D. E., Settell, D. M., Baumann, J. M., Ray, R. J., Graham, L. J., and Beyerinck, R. A. (2009). A model-based methodology for spray-drying process development. *Journal of Pharmaceutical Innovation*, *4*(3), 133–142.

Dong, Y., Ng, W. K., Shen, S., Kim, S., and Tan, R. B. (2009). Preparation and characterization of spironolactone nanoparticles by antisolvent precipitation. *International Journal of Pharmaceutics*,

375(1-2), 84–88.

Duarte, I. (2016). *Development of new screening methodologies and preparation methods with application in amorphous solid dispersions and pharmaceutical cocrystals*. PhD Dissertation, Universidade de Lisboa.

Duarte, Í., Andrade, R., Pinto, J. F. and Temtem, M. (2016). Green production of cocrystals using a new solvent-free approach by spray congealing. *International Journal of Pharmaceutics*, *506*(1-2), 68–78.

Duarte, Í., Porfírio, T., Serôdio, P., Corvo, M. L., Vicente, J., Pinto, J. F. and Temtem, M. (2015). Production of Amorphous Nano-Solid Dispersions using a Solvent Controlled Precipitation. Poster presented at: The 15th AIChE Annual Meeting, 2015 November 8-13, Salt Lake City, Utah, USA.

Escuder-Gilabert, L. and Peris, M. (2010). Review: Highlights in recent applications of electronic tongues in food analysis. *Analytica Chimica Acta*, *665*(1), 15–25.

European Pharmacopeia (2005), Volume 5, 5th Edition, Council of Europe. Available from: http://library.njucm.edu.cn/yaodian/ep/EP501E/16_monographs/17_monographs_d-k/doxycycline_monohydrate/0820e.pdf (Accessed: 29 March 2016)

Ferraria, A. M. da C. (2002). *Estudos de Fluoração de Superfícies Poliméricas*. Master Dissertation, Faculdade de Ciências da Universidade de Lisboa.

Fini, A., Bergamante, V., Ceschel, G. C., Ronchi, C. and de Moraes, C. A. F. (2008). Fast dispersible/slow releasing ibuprofen tablets. *European Journal of Pharmaceutics and Biopharmaceutics*, *69*(1), 335–341.

Fotaki, N. (2011). Flow-Through Cell Apparatus (USP Apparatus 4): Operation and Features. *Dissolution Technologies*, *18*(4), 46–49.

GEA Process Engineering. Mass Crystallization from Solutions. Available from: http://www.gea.com/en/binaries/2012-05_Solution%20Crystallization_sm2_tcm11-21921.pdf (Accessed 3 May 2016)

Ghadiyali, S. N., Vyas, J. R., Upadhyay, U. M. and Patel, A. A. (2013). Study of processing parameters affecting dissolution profile of highly water soluble drug. *Der Pharmacia Lettre*, *5*(3), 211–222.

Ghosh, I., Bose, S., Vippagunta, R. and Harmon, F. (2011). Nanosuspension for improving the bioavailability of a poorly soluble drug and screening of stabilizing agents to inhibit crystal growth. *International Journal of Pharmaceutics*, *409*(1-2), 260–268.

Gil, M., Vicente, J. and Gaspar, F. (2010). Scale-up methodology for pharmaceutical spray drying. *Chimica Oggi*, *28*(4), 18–22.

Gill, P., Moghadam, T. T. and Ranjbar, B. (2010). Differential Scanning Calorimetry Techniques: Applications in Biology and Nanoscience. *Journal of Biomolecular Techniques*, *21*(4), 167–193.

Gittings, S., Turnbull, N., Roberts, C. J. and Gershkovich, P. (2014). Dissolution methodology for taste masked oral dosage forms. *Journal of Controlled Release*, *173*(1), 32–42.

Giulietti, M., Seckler, M. M., Derenzo, S., Ré, M. I. and Cekinski, E. (2001). Industrial Crystallization and Precipitation from Solutions: State of the Technique. *Brazilian Journal of Chemical Engineering*, *18*(4), Online version.

Gonçalves, J. E. (1999). O uso simultâneo das técnicas "XPS" e "EXAFS" no estudo de superfícies. *Akrópolis - Revista de Ciências Humanas Da UNIPAR*, *7*(27), 34–48.

Guhmann, M., Preis, M., Gerber, F., Pöllinger, N., Breitkreutz, J. and Weitschies, W. (2012). Development of oral taste masked diclofenac formulations using a taste sensing system.

International Journal of Pharmaceutics, *438*(1-2), 81–90.

Guyton, A. (1977). *Tratado de Fisiologia Médica*, 5th Edition, Interamericana, Rio de Janeiro.

Habib, M. J., Venkataram, S. and Hussain, M. D. (2000). Fundamentals of Solid Dispersions. In *Pharmaceutical Solid Dispersion Technology (ed.* Habib, M.J.), p. 12–6, CRC Press, Boca Raton, Florida, USA.

Hamashita, T., Nakagawa, Y., Aketo, T. and Watano, S. (2007). Granulation of core particles suitable for film coating by agitation fluidized bed I. Optimum formulation for core particles and development of a novel friability test method. *Chemical & Pharmaceutical Bulletin*, *55*(8), 1169–1174.

Hans, R., Thomas, S., Garla, B., Dagli, R. J. and Hans, M. K. (2016). Effect of Various Sugary Beverages on Salivary pH, Flow Rate, and Oral Clearance Rate amongst Adults. *Scientifica, 2016*, 1–6.

Hayashi, K., Yamanaka, M., Toko, K. and Yamafuji, K. (1990). Multichannel taste sensor using lipid membranes. *Sensors and Actuators B: Chemical*, *2*(3), 205–213.

Hoang Thi, T. H., Morel, S., Ayouni, F. and Flament, M. P. (2012). Development and evaluation of taste-masked drug for paediatric medicines - Application to acetaminophen. *International Journal of Pharmaceutics*, *434*(1-2), 235–242.

Holañ, J., Ridvan, L., Billot, P. and Štěpánek, F. (2015). Design of co-crystallization processes with regard to particle size distribution. *Chemical Engineering Science*, *128*, 36–43.

Hughes, L. (2010). In Good Taste. *Pharmaceutical Manufacturing and Packing Sourcer*, 94–97.

International Pharmacopeia (2003), Volume 5, 3th Edition, World Health Organization, Geneva. Available from: https://pharmafed.files.wordpress.com/2013/04/international-pharmacopia.pdf (Accessed 3 April 2016)

Jagtap, P. S., Jain, S. S., Dand, N., Jadhav, K. R. and Kadam, V. J. (2012). Hot melt extrusion technology, approach of solubility enhancement: A brief review. *Der Pharmacia Lettre*, *4*(1), 42–53.

Kakran, M., Sahoo, N. G., Li, L. and Judeh, Z. (2012). Fabrication of quercetin nanoparticles by anti-solvent precipitation method for enhanced dissolution. *Powder Technology*, *223*, 59–64.

Kakran, M., Sahoo, N. G., Tan, IL. and Li, L. (2012). Preparation of nanoparticles of poorly water-soluble antioxidant curcumin by antisolvent precipitation methods. *Journal of Nanoparticle Research*, *14*(3), 757.

Kakran, M., Sahoo, N. G., Li, L. and Judeh, Z. (2013). Particle size reduction of poorly water soluble artemisinin via antisolvent precipitation with a syringe pump. *Powder Technology*, *237*, 468–476.

Karaman, R. (2012). Computationally Designed Prodrugs for Masking the Bitter Taste of Drugs. *Drug Designing*, *2*:e106.

Karaman, R. (2014). Prodrugs for Masking the Bitter Taste of Drugs, *Application of Nanotechnology in Drug Delivery*, PhD. Ali Demir Sezer (Ed.), InTech. Available from: http://www.intechopen.com/books/application-of-nanotechnology-in-drug-delivery/prodrugs-for-masking-the-bitter-taste-of-drugs

Karaman, R. (2015). From Conventional Prodrugs to Prodrugs Designed by Molecular Orbital Methods. In *Frontiers in Computational Chemistry - Computer Applications for Drug Design and Biomolecular Systems,* Volume 2 *(*eds. Ul-Haq, Z. and Madura, J. D.*)*, p.209-10. Bentham Science Publishers Ltd.

Katsuragi, Y., Kashiwayanagi, M. and Kurihara, K. (1997). Specific inhibitor for bitter taste: inhibition of frog taste nerve responses and human taste sensation to bitter stimuli. *Brain Research Protocols*,

1(3), 292–298.

Kaushik, D. and Dureja, H. (2015). Taste masking of bitter pharmaceuticals by spray drying technique. *Journal of Chemical and Pharmaceutical Research*, *7*(4), 950–956.

Kim, S., Ng, W. K., Dong, Y., Das, S. and Tan, R. B. H. (2012). Preparation and physicochemical characterization of trans-resveratrol nanoparticles by temperature-controlled antisolvent precipitation. *Journal of Food Engineering*, *108*(1), 37–42.

Kim, Y. H., Lee, K., Koo, K. K., Shul, Y. G. and Haam, S. (2002). Comparison Study of Mixing Effect on Batch Cooling Crystallization of 3-Nitro-1,2,4-triazol-5-one (NTO) Using Mechanical Stirrer and Ultrasound Irradiation. *Crystal Research and Technology*, *37*(9), 928–944.

Koland, M., Charyulu, R.N., Vijayanarayana, K. and Prabhu, P. (2011). In vitro and in vivo evaluation of chitosan buccal films of ondansetron hydrochloride. *International Journal of Pharmaceutical Investigation*, *1*(3), 164-171.

Kolhe, S., Ghadge, T. and Dhole, S. N. (2013). Formulation and Evaluation of Taste Masked Fast Disintegrating Tablet of Promethazine Hydrochloride. *IOSR Journal of Pharmacy*, *3*(11), 1–11.

Kolter, K., Karl, M. and Gryczke, A. (2012). Introduction to Solid Dispersions. In *Hot-Melt Extrusion with BASF Pharma Polymers*, 2nd Revised and Enlarged Edition, p. 1–201, BASF - The Chemical Company, Ludwigshafen, Germany.

Kondo, K., Niwa, T., Ozeki, Y., Ando, M. and Danjo, K. (2011). Preparation and Evaluation of Orally Rapidly Disintegrating Tablets Containing Taste-Masked Particles Using One-Step Dry-Coated Tablets Technology. *Chemical & Pharmaceutical Bulletin*, *59*(10), 1214–1220.

Krishna, K., Koradia, H., Navin, S. and Mahesh, D. and (2015). The impact of critical variables on properties of nanosuspension: a review. *International Journal of Drug Development & Research* *7*(1), 150–161.

Kulkarni, M.G. and Menjoge, A. R. (2005). Taste masked pharmaceutical composition comprising ph sensitive polymer. Patent Number WO2005055986 A1

Kumar, P. (2015). Taste masking potential of bitter drugs : a review. *International Journal Of Pharma Professional's Research*, *6*(1), 1200–1206.

Kumar, S., Gokhale, R. and Burgess, D. J. (2014). Sugars as bulking agents to prevent nano-crystal aggregation during spray or freeze-drying. *International Journal of Pharmaceutics*, *471*(1-2), 303–311.

Kurup, M. and Raj R., A. (2016). Antisolvent Crystallization: A novel approach to bioavailability enhancement. *European Journal of Biomedical and Pharmaceutical Sciences*, *3*(3), 230–234.

Lagerlof, F. and Dawes, C. (1984). The Volume of Saliva in the Mouth Before and After Swallowing. *Journal of Dental Research*, *63*(5), 618–621.

Latha, R. S. and Lakshmi, P. K. (2012). Electronic tongue: an analytical gustatory tool. *Journal of Advanced Pharmaceutical Technology&Research*, *3*(1), 3–8.

Lewis, A.; Seckler, M.; Kramer, H. and Rosmalen, G. V. (2015). Thermodynamics, crystallization methods and supersaturation. In *Industrial Crystallization: Fundamentals and Applications*, p. 1–10, Cambridge University Press, UK.

Li, C., Li, C., Le, Y. and Chen, J. F. (2011). Formation of bicalutamide nanodispersion for dissolution rate enhancement. *International Journal of Pharmaceutics*, *404*(1-2), 257–263.

Li, F.Q., Ji, R.R., Chen, X., You, B.M., Pan, Y.H. and Su, J.C. (2010). Cetirizine dihydrochloride loaded microparticles design using ionotropic cross-linked chitosan nanoparticles by spray-drying method.

Archives of Pharmacal Research, *33*(12), 1967–1973

Liew, K. B., Tan, Y. T. F. and Peh, K. K. (2012). Characterization of Oral Disintegrating Film Containing Donepezil for Alzheimer Disease. *AAPS PharmSciTech*, *13*(1), 134–142.

Limmatvapirat, S., Piyawatakarn, P., Tabtimsri, S., Sriamornsak, P., Nunthanid, J. and Limmatvapirat, C. (2012). Design of Taste Masked Dextromethorphan Through Incorporation Into Shellac-Based Matrix. *Advanced Science Letters*, *14*(1), 409–412.

Lonare, A. A. and Patel, S. R. (2013). Antisolvent Crystallization of Poorly Water Soluble Drugs. *International Journal of Chemical Engineering and Applications*, *4*(5), 337–341.

Lorenz, J. K., Reo, J. P., Hendl, O., Worthington, J. H. and Petrossian, V. D. (2009). Evaluation of a taste sensor instrument (electronic tongue) for use in formulation development. *International Journal of Pharmaceutics*, *367*(1-2), 65–72.

Lu, H. (2014). *Spray Drying Functional Whey Protein Soluble Aggregates Made at Neutral pH*. PhD Dissertation, North Carolina State University.

Lukas, S., Evans, A.M., Dwyer, M. and Pitman, I. H. (1997). Taste masked paracetamol compositions. Patent Number WO1997039747A1

Maccari, M., Calanchi, M. and Kydonieus, A. (Eds.). (1980). *Controlled Release Technologies - Methods, Theory and Applications*, Volume 2, 1st Edition, CRC Press Inc., Boca Raton, Florida.

Mackaplow, M. B., Zarraga, I. E. and Morris, J. F. (2006). Rotary spray congealing of a suspension: Effect of disk speed and dispersed particle properties. *Journal of Microencapsulation*, *23*(7), 793–809.

Mady, F. M., Abou-Taleb, A. E., Khaled, A. K., Yamasaki, K., Iohara, D., Ishiguro, T., Hirayma, F., Uekama, K. and Otagiri, M. (2010). Enhancement of the aqueous solubility and masking the bitter taste of famotidine using drug/SBE-B-CyD/Povidone K30 complexation approach. *Journal of Pharmaceutical Sciences*, *99*(10), 4285–4294.

Mady, F. M., Abou-Taleb, A. E., Khaled, A. K., Yamasaki, K., Iohara, D., Taguchi, K., Anraku, M., Hirayma, F., Uekama, K. and Otagiri, M. (2010). Evaluation of carboxymethyl-β-cyclodextrin with acid function: Improvement of chemical stability, oral bioavailability and bitter taste of famotidine. *International Journal of Pharmaceutics*, *397*(1-2), 1–8.

Maniruzzaman, M., Boateng, J. S., Bonnefille, M., Aranyos, A., Mitchell, J. C. and Douroumis, D. (2012). Taste masking of paracetamol by hot-melt extrusion: An in vitro and in vivo evaluation. *European Journal of Pharmaceutics and Biopharmaceutics*, *80*(2), 433–442.

Maniruzzaman, M., Boateng, J. S., Chowdhry, B. Z., Snowden, M. J. and Douroumis, D. (2014). A review on the taste masking of bitter APIs: hot-melt extrusion (HME) evaluation. *Drug Development and Industrial Pharmacy*, *40*(2), 145–56.

Maniruzzaman, M., Boateng, J. S., Snowden, M. J. and Douroumis, D. (2012). A review of hot-melt extrusion: process technology to pharmaceutical products. *ISRN Pharmaceutics*, *2012*(2), 436763–436769.

Maniruzzaman, M., Douroumis, D., Boateng, J. S. and Snowden, M. J. (2012). Hot-Melt Extrusion (HME): From Process to Pharmaceutical Applications. In A. Demir (Ed.), *Recent Advances in Novel Drug Carrier Systems* (pp. 3–16). InTech.

Mansour, H., Park, C.W., Jr., D. H.(2013). Nanoparticle Lung Delivery and Inhalation Aerosols for Targeted Pulmonary Nanomedicine. In *Nanomedicine in Drug Delivery* (ed. Kumar, A.; Mansour, H. M.; Friedman, A. and Blough, E. B.), p. 57–8, CRC Press, Boca Raton, Florida, USA.

Maschke, A., Becker, C., Eyrich, D., Kiermaier, J., Blunk, T. and Göpferich, A. (2007). Development of

a spray congealing process for the preparation of insulin-loaded lipid microparticles and characterization thereof. *European Journal of Pharmaceutics and Biopharmaceutics*, *65*(2), 175–187.

Matos, I. and Duarte, Í. (2016). Spray Congealing - Applications in the Pharmaceutical Industry. Webinar presented at: Hovione Farmaciência SA, 2016 February 25, Sete Casas, Loures.

Matsui, D.M. (1997). Drug Compliance in pediatrics. Clinical and research issues. *Pediatric Clinics of North America*, *44*(1), 1–14.

Matsumoto, M., Wada, Y. and Onoe, K. (2013). Enhanced production of unstable polymorph by antisolvent crystallization supplying minute-bubbles. *MATEC Web of Conferences*, *01056*(3).

Meer, T.A., Sawant, K.P. and Amin, P.D. (2011). Liquid antisolvent precipitation process for solubility modulation of bicalutamide. *Acta Pharmaceutica*, *61*(4),435-45.

Mersmann, A. (2001). Design of Crystallizers. In *Crystallization Technology Handbook* (ed. Mersmann, A.), 2nd Edition, p. 334–42, CRC Press, Boca Raton, Florida, USA.

Miller, D., McConville, J. T. and Williams III, R. O. (2007). Solid Dispersion Technologies. In *Advanced Drug Formulation Design to Optimize Therapeutic Outcomes* (Williams, R.O, Taft, D.R., McConville, J.T. Eds.), p. 454–55, CRC Press, LCC, Boca Raton, Florida, USA.

Mizumoto, T., Tamura, T., Kawai, H., Kajiyama, A. and Itai, S. (2008). Formulation design of an oral, fast-disintegrating dosage form containing taste-masked particles of famotidine. *Chemical & Pharmaceutical Bulletin*, *56*(7), 946–950.

Mujumdar, A. S., Huang, L. and Chen, X. D. (2010). An overview of the recent advances in spray-drying. *Dairy Science &Technology*, *90(2)*, 211–224.

Murray, O. J., Dang, W. and Bergstrom, D. (2004). Using an electronic tongue to optimize taste-masking in a lyophilized orally disintegrating tablet formulation. *Pharmaceutical Technology*, 2004, 42–52.

Narducci, O., Jones, A. G. and Kougoulos, E. (2011). An Assessment of the Use of Ultrasound in the Particle Engineering of Micrometer-Scale Adipic Acid Crystals. *Crystal Growth & Design*, *11*(5), 1742–1749.

Noorjahan, A., Amrita, B. and Kavita, S. (2014). In vivo evaluation of taste masking for developed chewable and orodispersible tablets in humans and rats. *Pharmaceutical Development and Technology*, *19*(3), 290–295.

Noyes, A. A. and Whitney, W. R. (1897). The Rate of solution of solid substances in their own solutions. *Journal of the American Chemical Society*, *19*(12), 930–934.

Nyvlt, J. and Zacek, S. (1986). Effect of the rate of stirring on crystal size in precipitating or salting-out systems. *Collection of the Czechoslovak Chamical Communications*, *51*(8), 1609–1617.

Okuro, P. K., de Matos Junior, F. E. and Favaro-Trindade, C. S. (2013). Technological challenges for spray chilling encapsulation of functional food ingredients. *Food Technology and Biotechnology*, *51*(2), 171–182.

Oliveira, O. W. and Petrovick, P. R. (2010). Secagem por aspersão (spray drying) de extratos vegetais: Bases e aplicações. *Brazilian Journal of Pharmacognosy*, *20*(4), 641–650.

Oliveira, W.P, Souza, C.R.F., Kurozawa, L.E. and Park, K.J. (2010). Spray Drying of food and herbal products. In *Spray Drying Technology,* Volume 1 (eds. Woo, M.W., Mujumdar, A.S., Daud, W.R.W.), p. 113–36, Published in Singapore.

Olson, E. (2011). Particle Shape Factors and Their Use in Image Analysis - Part 1:Theory. *Journal of GXP Compliance*, *15*(3), 85–96.

Oxley, J. (2015). Process-Selection Criteria. In *Handbook of Encapsulation and Controlled Release* (ed. Mishra, M.), p. 25–7, CRC Press, Boca Raton, Florida, USA.

Ozer, A. Y. and Hincal, A. A. (1990). Studies on the masking of unpleasant taste of beclamide: microencapsulation and tabletting. *Journal of Microencapsulation*, *7*(3), 327–339.

Paiva Lacerda, S. de; (2013). *Improvement of dissolution rate of a new antiretroviral drug using an anti-solvent crystallization technology*. PhD Dissertation, Université de Toulouse.

Paleshnuik, L. (2009). Dissolution. In *Workshop on regulatory requirements for registration of Artemisinin based combined medicines and assessment of data submitted to regulatory authorities*, p. 1–64, World Health Organization, Kampala, Uganda.

Panagiotou, T., Mesite, S., Fisher, R. and Gruverman, I. (2007). Production of Stable Drug Nanosuspensions Using Microfluidics Reaction Technology. *NSTI-Nanotech*, *4*, 246–249.

Panagiotou, T. and Fisher, R. J. (2008). Form Nanoparticles via Controlled Crystallization. *Chemical Engineering Progress*, 104(10), 33–39.

Panagiotou, T., Mesite, S. V and Fisher, R. J. (2009). Production of Norfloxacin Nanosuspensions Using Microfluidics Reaction Technology through Solvent / Antisolvent Crystallization. *Industrial&Engineering Chemistry Research*, *48*(4), 1761–1771.

Panagiotou, T. and Fisher, R. J. (2011). Enhanced Transport Capabilities via Nanotechnologies: Impacting Bioefficacy, Controlled Release Strategies, and Novel Chaperones. *Journal of Drug Delivery*, *2011*, 1–14.

Pandey, S., Kumar, S., Prajapati, S.K. and Madhav, N. V. S. (2010). An overview on taste physiology and masking of bitter drugs. *International Journal of Pharma and Bio Sciences*, *1*(3), 1–11.

Park, M. W., and Yeo, S. Do. (2012). Antisolvent crystallization of carbamazepine from organic solutions. *Chemical Engineering Research and Design*, *90*(12), 2202–2208.

Particle Sciences Inc. (2011). *Hot Melt Extrusion. Technical Brief*, Volume 3, Bethlehem, USA. Available from: http://www.particlesciences.com/docs/technical_briefs/TB_2011_3.pdf (Accessed 5 April 2016)

Passos, M. L. and Birchal, V. S. (2010). Manipulating physical properties of powder. In *Spray Drying Technology,* Volume 1, (eds. Woo, M.W., Mujumdar, A.S., Daud, W.R.W.), p. 37–42, Published in Singapore.

Patel, A., Sahu, D., Dashora, A., Garg, R., Agraval, P., Patel, P., Patel, P. and Patel, G. (2013). A review of hot melt extrusion technique. *International Journal of Innovative Research in Science, Engineering and Technology*, *2*(6), 2194 – 2198.

Patel, R.P.; Patel, M.P. and Suthar, A. M. (2009). Spray drying technology : an overview. *Indian Journal of Science and Technology*, *2*(10), 44–47.

Patil, H., Tiwari, R. V. and Repka, M. A. (2016). Hot-Melt Extrusion: from Theory to Application in Pharmaceutical Formulation. *AAPS PharmSciTech*, *17*(1), 20–42.

Pawar, H. A. and Joshi, P. R. (2014). Development and Evaluation of Taste Masked Granular Formulation of Satranidazole by Melt Granulation Technique. *Journal of Pharmaceutics*, *2014*, 1–7.

Peh, K.K. and Wong, C.F. (1999). Polymeric films as vehicle for buccal delivery: swelling, mechanical and bioadhesive properties. *Journal of Pharmacy & Pharmaceutical Sciences*, *2*(2), 53–61.

Pein, M., Preis, M., Eckert, C. and Kiene, F. E. (2014). Taste-masking assessment of solid oral dosage

forms-A critical review. *International Journal of Pharmaceutics*, *465*(1-2), 239–254.

Peltonen, L., Tuomela, A. and Hirvonen, J. (2015). Polymeric Stabilizers for Drug Nanocrystals. In, *Handbook of Polymers for Pharmaceutical Technologies: Bioactive and Compatible Synthetic/Hybrid Polymers,* Volume 4 (eds. V. K. Thakur and M. K. Thakur), p. 67–71, John Wiley & Sons, Inc., Hoboken, NJ, USA.

Petereit, H.U., Meier, C. and Gryczke, A. (2014). Melt Extrusion of salts of active ingredients. Patent Number US8642089B2

Peterson, B. P. (2011). *Energy Dispersive Spectroscopy Characterization of Solute Segregation in Ti-6Al-4V*. Master Dissertation, The Ohio State University.

Pietiläinen, J. (2013). *Spray Drying Particles from Ethanol-Water Mixtures Intended for Inhalation*. Master Dissertation, University of Helsinki.

Pimparade, M. B., Morott, J. T., Park, J. B., Kulkarni, V. I., Majumdar, S., Murthy, S. N., Lian, Z., Pinto, E., Bi, V., Durig, T., Murthy, R., Shivakumar, H. N., Vanaja, K., Kumar, P.C. and Repka, M. A. (2015). Development of taste masked caffeine citrate formulations utilizing hot melt extrusion technology and in vitro-in vivo evaluations. *International Journal of Pharmaceutics*, *487*(1-2), 167–176.

Porfírio, T., Duarte, I., Vicente, J. and Temtem, M. (2015). Particle Engineering through continuous solvent precipitation. Poster presented at: The 15th AIChE Annual Meeting, 2015 November 8-13, Salt Lake City, Utah, USA.

Pouretedal, H. R. (2014). Preparation and characterization of azithromycin nanodrug using solvent / antisolvent method. *International Nano Letters*, *4(1)*,103-111

Purves, D., Augustine, G. J., Fitzpatrick, D., Katz, L. C., LaMantia, A.S., McNamara, J. O. and Williams, S. M. (2001). *Neuroscience*, 2nd Edition, Sinauer Associates, Inc. Available from: https://www.ncbi.nlm.nih.gov/books/NBK11148 (Acessed: 15 April 2016)

Qiyun, G. (2008). *A study of factors affecting spray-congealed micropellets for drug delivery, PhD Dissertation, National University of Singapore.*

Rachid, O., Simons, F. E. R., Rawas-Qalaji, M. and Simons, K. J. (2010). An electronic tongue: evaluation of the masking efficacy of sweetening and/or flavoring agents on the bitter taste of epinephrine. *AAPS PharmSciTech*, *11*(2), 550–557.

Raghavan, K.S., Ranadive, S.A., Bempenek, K.S., Benkerrour, L., Trognon, V., Corrao, R.G. and Esposito, L. (2003). Pediatric Formulation of gatifloxacin. Patent Number US6589955 B2

Rahman, Z., Zidan, A. S., Berendt, R. T. and Khan, M. A. (2012). Tannate complexes of antihistaminic drug: Sustained release and taste masking approaches. *International Journal of Pharmaceutics*, *422*(1-2), 91–100.

Rego, A. M. B. do. (1993). XPS e HREELS: Duas espectroscopias de caracterização de superfícies. *QUÍMICA*, *48*, 28–33.

Sadrieh, N., Brower, J., Yu, L., Doub, W., Straughn, A., Machado, S., Pelsor, F., Martins, E.S., Moore, T., Reepmeyer, J., Toler, D., Nguyenpho, A., Roberts, R., Schuirmann, D.J., Nasr, M. and Buhse, L. (2005). Stability, Dose Uniformity, and Palatability of Three Counterterrorism Drugs — Human Subject and Electronic Tongue Studies. *Pharmaceutical Research*, *22*(10), 1747–1756.

Sagar, T., Amol, G., Rahul, D., Prashant, P. and Yogesh, S. (2012). Review on: Taste masking approaches and evaluation of taste masking. *International Journal of Pharmaceutical Sciences*, *4*(2), 1895–1907.

Sana, S., Rajani, A., Sumedha, N. and Mahesh, B. (2012). Formulation and Evaluation of taste masked

oral suspension of Dextromethorphan Hydrobromide. *International Journal of Drug Development & Research*, *4*(2), 159–172.

Sandhu, H., Shah, N., Chokshi, H., Malick, A.W. (2014). Overview of Amorphous Solid Dispersion Technologies. In *Amorphous Solid Dispersions - Theory and Practice* (eds. Shah, N.; Sandhu, H.; Choi, D. S.; Chokshi, H.; and Malick, A. W.), p. 106–9, Springer Science and Business Media, LLC, USA.

Santos, G. J. L. (2012). *Ensaio de dissolução das formas farmacêuticas: aplicações na investigação científica e na indústria farmacêutica*. Master Dissertation, Universidade Fernando Pessoa.

Sarghini, F. (2015). Microfluidic Encapsulation Process. In *Handbook of Encapsulation and Controlled Release* (ed. Mishra, M.), p. 370–2, CRC Press, Boca Raton, Florida, USA.

Sato, T., Nishishita, K., Okada, Y. and Toda, K. (2010). The Receptor Potential of Frog Taste Cells in Response to Cold and Warm Stimuli. *Chemical Senses*, *35*(6), 491–499.

Savjani, K. T., Gajjar, A. K. and Savjani, J. K. (2012). Drug solubility: importance and enhancement techniques. *International Scholarly Research Network Pharmaceutics*, *2012*, 1–10.

Shah, N., Iyer, R. M., Mair, H.J., Choi, D.S., Tian, H., Diodone, R., Fähnrich, K., Pabst-Ravot, A., Tang, K., Sheubel, E., Grippo, J.F., Moreira, S.A., Go, Z., Mouskountakis, J., Louie, T., Ibrahim, P.N., Sandhu, H., Rubia, L., Choskshi, H., Singhal, D. and Malick, W. (2013). Improved Human Bioavailability of Vemurafenib, a Practically Insoluble Drug, Using an Amorphous Polymer-Stabilized Solid Dispersion Prepared by a Solvent-Controlled Coprecipitation Process. *Journal of Pharmaceutical Sciences*, *102*(3), 967–981.

Shah, P. P., Mashru, R. C., Rane, Y. M. and Thakkar, A. (2008). Design and Optimization of Mefloquine Hydrochloride Microparticles for Bitter Taste Masking. *AAPS PharmSciTech*, *9*(2), 377–389.

Shah, N., Sandhu, H., Choi, D.S., Chokshi, H., Iyer, R. and Malick, A.W. (2014). MBP Technology: Composition and Design Considerations. In *Amorphous Solid Dispersions - Theory and Practice* (eds. Shah, N.; Sandhu, H.; Choi, D. S.; Chokshi, H. and Malick, A. W.), p. 324–7, Springer Science and Business Media, LLC, USA.

Shahzad, Y., Shah, S. N. H., Atique, S., Ansari, M. T., Bashir, F. and Hussain, T. (2011). The evaluation of coated granules to mask the bitter taste of dihydroartemisinin. *Brazilian Journal of Pharmaceutical Sciences*, *47*(2), 323–330.

Shen, R.W.W. (1991). Taste masking of ibuprofen by fluid bed coating. Patent Number WO1991015194 A1

Shet, N. and Vaidya, I. (2013). Taste masking: A pathfinder for bitter drugs. *International Journal of Pharmaceutical Sciences Review and Research*, *18*(2), 1–12.

SHIRAI, Y., SOGO, K., FUJIOKA, H. and NAKAMURA, Y. (1994). Role of Low-Substituted Hydroxypropylcellulose in Dissolution and Bioavailability of Novel Fine Granule System for Masking Bitter Taste. *Biological & Pharmaceutical Bulletin*, *17*(3), 427–431.

SHIRAI, Y., SOGO, K., FUJIOKA, H. and NAKAMURA, Y. (1996). Influence of Heat Treatment on Dissolution and Masking Degree of Bitter Taste for a Novel Fine Granule System. *CHEMICAL & PHARMACEUTICAL BULLETIN*, *44*(2), 399–402.

Shishu, Kamalpreet and Kapoor, V.R. (2010). Development of Taste Masked Oral Formulation of Ornidazole. *Indian Journal of Pharmaceutical Sciences*, *72*(2), 211–215.

Shrotriya, S. N., Ranpise, N. S., Bade, S. T. and Chudiwal, P. D. (2013). Taste Masking of Tramadol Hydrochloride by Polymer Carrier System and Formulation of Rapidly Disintegrating Tablets using Factorial Design. *Indian Journal of Pharmaceutical Education and Research*, *47*(1), 34–40.

Siewert, M., Dressman, J., Brown, C. K. and Shah, V. P. (2003). FIP/AAPS guidelines for dissolution/in vitro release testing of novel/special dosage forms. *Dissolution Technologies*, *10*(1), 6-15.

Simonelli, A. P., Mehta, S. C. and Higuchi, W. I. (1969). Dissolution Rates of High Energy Polyvinylpyrrolidone (PVP)-Sulfathiazole Coprecipitates. *Journal of Pharmaceutical Sciences*, *58*(5), 538–549.

Singh, S. K., Sharma, V. and Pathak, K. (2012). Formulation and Evaluation of Taste Masked Rapid Release Tablets of Sumatriptan Succinate. *International Journal of Pharmacy and Pharmaceutical Sciences*, *4*(2), 168–174.

Smith, R. (2005). Reaction, Separation and Recycle Systems for Batch Processes. In *Chemical Process: Design and Integration*, pp. 301–303, John Wiley & Sons, Inc., Hoboken, NJ, USA.

Sollohub, K., Janczyk, M., Kutyla, A., Wosicka, H., Ciosek, P. and Cal, K. (2011). Taste masking of roxithromycin by spray drying technique. *Acta Poloniae Pharmaceutica - Drug Research*, *68*(4), 601–604.

Sona, P. S. and Muthulingam, C. (2011). Formulation and Evaluation of Taste Masked Orally Disitegrating Tablets of Diclofenac sodium. *International Journal of PharmTech Research*, *3*(2), 819–826.

Sriamornsak, P. and Burapapadh, K. (2015). Characterization of recrystallized itraconazole prepared by cooling and anti-solvent crystallization. *Asian Journal of Pharmaceutical Sciences*, *10*(3), 230–238.

Stippler, E. (2011). Compendial Dissolution: Theory and Practice. [Webinar] Available from: http://www2.aaps.org/uploadedFiles/Content/Sections_and_Groups/Focus_Groups/In_Vitro_Rel ease_and_Dissolution_Testing/Resources/IVRDTFGStippler2011.pdf (Accessed 3 April 2016)

Sugao, H., Yamazaki, S., Shiozawa, H. and Yano, K. (1998). Taste Masking of Bitter Drug Powder without Loss of Bioavailability by Heat Treatment of Wax-Coated Microparticles. *Journal of Pharmaceutical Sciences*, *87*(1), 96–100.

Surinder, K., Tusharkumar, S., Ezhilmuthu, R. and Senthilkumar, K. (2013). Taste Masking of Sitagliptin Phosphate Monohydrate By Ion Exchange Resin and Formulation of Rapidly-Disintegrating Tablets. *Research and Reviews: Journal of Pharmacy and Pharmaceutical Sciences*, *2*(4), 37–44.

Suthar, A. M. and Patel, M. M. (2010). Ion Exchange Resin As an Imposing Method for Taste Masking: a Review. *Pharma Science Monitor An International Journal of Pharmaceutical Sciences*, (2), 6–12.

Thakur, R.K., Vial, C., Nigam, K.D.P., Nauman, E.B. and Djelveh, G. (2003). Static Mixers in the Process Industries - A Review. *Chemical Engineering Research and Design*, *81*(7), 787–826.

Thorat, A. A. and Dalvi, S. V. (2011). Liquid antisolvent precipitation and stabilization of nanoparticles of poorly water soluble drugs in aqueous suspensions : Recent developments and future perspective. *Chemical Engineering Journal*, *181-182*(2012), 1–34.

Tiwari, R. V, Patil, H. and Repka, M. A. (2016). Contribution of hot-melt extrusion technology to advance drug delivery in the 21st century. *Expert Opinion on Drug Delivery*, *13*(3), 451–64.

Tiwari, R. V., Polk, A. N., Patil, H., Ye, X., Pimparade, M. B. and Repka, M. A. (2015). Rat Palatability Study for Taste Assessment of Caffeine Citrate Formulation Prepared via Hot-Melt Extrusion Technology. *AAPS PharmSciTech*.

Toko, K., Matsuno, T., Yamafuji, K., Hayashi, K., Ikezaki, H., Sato, K., Toukubo, R. and Kawarai, S. (1994). Multichannel taste sensor using electric potential changes in lipid membranes. *Biosensors and Bioelectronics*, *9*(4-5), 359–364.

Tripathi, A., Parmar, D., Patel, U., Patel, G., Daslaniya, D. and Bhimani, B. (2011). Taste Masking : A Novel Approach for Bitter and Obnoxious Drugs. *Journal of Pharmaceutical Science and Bioscientific Research*, *1*(3), 136–142.

Uchida, T. and Yoshida, M. (2013). Quantitative Evaluation of Bitterness of Medicines. In *Biochemical Sensors: Mimicking Gustatory and Olfactory Senses* (ed. Toko, I.), p. 145–156, CRC Press, Boca Raton, Florida, USA.

Vaassen, J., Bartscher, K. and Breitkreutz, J. (2012). Taste masked lipid pellets with enhanced release of hydrophobic active ingredient. *International Journal of Pharmaceutics*, *429*(1-2), 99–103.

van der Heide, P. (2012). Introduction. In *X-ray Photoelectron Spectroscopy: An introduction to Principles and Practices*, p. 1–12, John Wiley & Sons, Inc., Hoboken, NJ, USA.

Vehring, R. (2008). Pharmaceutical Particle Engineering via Spray Drying. *Pharmaceutical Research*, *25*(5), 999–1022.

Vicente, J. and Ferreira, R. (2015). Development by Design - Hovione's Approach to Spray Drying Process Development Webinar presented at: Hovione Farmaciência SA, 2015 October 6, Sete Casas, Loures.

Viçosa, A., Letourneau, J.J., Espitalier, F., and Ré, M. I. (2012). An innovative antisolvent precipitation process as a promising technique to prepare ultrafine rifampicin particles. *Journal of Crystal Growth*, *342*(1), 80–87.

Vummaneni, V. and Nagpal, D. (2012). Taste Masking Technologies: An Overview and Recent Updates. *International Journal of Research in Pharmaceutical and Biomedical Sciences*, *3*(2), 510-524.

Wang, I. C., Lee, M. J., Sim, S. J., Kim, W. S., Chun, N. H. and Choi, G. J. (2013). Anti-solvent co-crystallization of carbamazepine and saccharin. *International Journal of Pharmaceutics*, *450*(1-2), 311–322.

Wey, J.S. and Karpinski, P.H. (2002). Batch Crystallization. In *Handbook of Industrial Crystallization* (ed. Myerson, A), 2nd Edition, p. 244–7, Butterworth-Heinemann.

Winnick, S., Lucas, D. O., Hartman, A. L. and Toll, D. (2005). How Do You Improve Compliance? *Pediatrics*, *115*(6), e718–24.

Xia, D., Quan, P., Piao, H., Piao, H., Sun, S., Yin, Y. and Cui, F. (2010). Preparation of stable nitrendipine nanosuspensions using the precipitation-ultrasonication method for enhancement of dissolution and oral bioavailability. *European Journal of Pharmaceutical Sciences*, *40*(4), 325–34.

Yajima, T., Fukushima, Y., Itai, S. and Kawashima, Y. (2002). Method of evaluation of the bitterness of clarithromycin dry syrup. *Chemical & Pharmaceutical Bulletin*, *50*(2), 147–52.

Yajima, T., Nogata, A., Demachi, M., Umeki, N., Itai, S., Yunoki, N. and Nemoto, M. (1996). Particle Design for Taste-Masking Using a Spray-Congealing Technique. *Chemical & Pharmaceutical Bulletin*, *44(1)*, 187–91.

Yan, Y.D., Woo, J. S., Kang, J. H., Yong, C. S. and Choi, H.G. (2010). Preparation and evaluation of taste-masked donepezil hydrochloride orally disintegrating tablets. *Biological & Pharmaceutical Bulletin*, *33*(8), 1364–70.

Yu, Z.Q., Tan, R.B.H. and Chow, P.S. (2005). Effects of operating conditions on agglomeration and habit of paracetamol crystals in anti-solvent crystallization. *Journal of Crystal Growth*, *279*(3-4), 477–88.

Zhang, H. X., Wang, J. X., Zhang, Z. B., Le, Y., Shen, Z. G. and Chen, J. F. (2009). Micronization of atorvastatin calcium by antisolvent precipitation process. *International Journal of Pharmaceutics*, *374*(1-2), 106–13.

Zhang, Z., Le, Y., Wang, J., Zhao, H. and Chen, J. (2012). Irbesartan drug formulated as nanocomposite particles for the enhancement of the dissolution rate. *Particuology*, *10*(4), 462–67.

Zou, Y., Wan, H., Zhang, X., Ha, D. and Wang, P. (2015). Electronic Nose and Electronic Tongue. In *Bioinspired Smell and Taste Sensors (*eds. Wang, P., Liu, Q., Wu, C. and Hsia, K. J.), 1st ed., p.19-44, Springer Press, Beijing, China.

Zu, Y., Wu, W., Zhao, X., Li, Y., Wang, W., Zhong, C., Zhang, Y. and Zhao, X. (2014). Enhancement of solubility, antioxidant ability and bioavailability of taxifolin nanoparticles by liquid antisolvent precipitation technique. *International Journal of Pharmaceutics*, *471*(1-2), 366–76.

Zunbul, B. (2005). *AAS, XRPD, SEM/ED, and FTIR studies of the effect of calcite and magnesite on the uptake of Pb2+ and Zn2+ ions by natural kaolinite and clinoptilolite.* Master Dissertation, Izmir Institute of Tehcnology.

Supplementary Information

A. *In-vitro* Dissolution Studies

In figure A.1, the calibration curve performed in UPLC method is shown, in order to quantify the model drug in the formulations and to assure that the linearity conditions were verified.
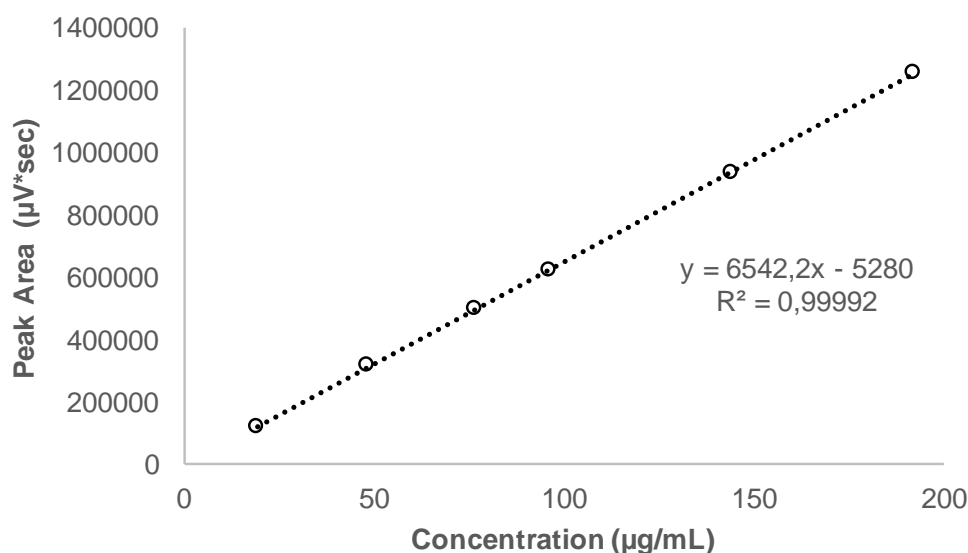
Figure A.1 Calibration curve of the model drug in methanol, with concentrations ranging from 20 to 200 μg/mL.

In order to obtain the final drug release in every time-point, the recovery area (quantified through the use of a single-point external standard of pure drug substance in MeOH - 80 μg/mL) was considered, the mass existing in the volume present in the vessel and also the replace of the medium.

Thus, the recovery area was calculated as the following formula suggest:

$$Recovery\ Area = \frac{Peak\ Area\ of\ the\ Standard\ Sample}{Concentration\ of\ the\ Standard\ Sample} \times \frac{Concentration\ of\ the\ Sample}{Peak\ Area\ of\ the\ Sample} \times 100$$

Equation A.1

where the concentration of the sample was corrected according to the dilution performed, through the use of the dilution factor, so that the concentration ranges between the values of the calibration curve.

The value obtained for each one of the time-points was multiplied by the volume present in the vessel and also by the replace volume medium, individually.

The final drug release was obtained by summing the mass present in the volume of the vessel in that time-point and the mass of the reposition volume media in the previous time-point.

The experiments were performed in duplicated, so in order to obtain the final drug release an average was done and the standard deviations were calculated.

From table A.1 to A.15, the obtained results for the first dissolution method applied are explicit, considering the calculations previously explained.

Table A.1 Final drug release and respective standard deviation (σ) correspondent to formulation #3R, in SSF dissolution media.

n=1	Recovery Area	Mass in 10 mL	Mass in 2 mL	Final Mass
0 min	0	0	0	0
5 min	1.60	15.97	3.19	15.97
10 min	1.64	16.39	3.28	19.58

n=2	Recovery Area	Mass in 10 mL	Mass in 2 mL	Final Mass
0 min	0	0	0	0
5 min	0.95	9.49	1.90	9.49
10 min	1.13	11.26	2.25	13.16

Time (min)	Average Mass	σ
0	0	0
5	12.73	4.58
10	16.37	4.54

Table A.2 Final drug release and respective standard deviation (σ) correspondent to formulation #4R, in SSF dissolution media.

n=1	Recovery Area	Mass in 10 mL	Mass in 2 mL	Final Mass
0 min	0	0	0	0
5 min	3.53	35.30	7.06	35.30
10 min	2.01	20.05	4.01	27.11

n=2	Recovery Area	Mass in 10 mL	Mass in 2 mL	Final Mass
0 min	0	0	0	0
5 min	0.92	9.18	1.84	9.18
10 min	2.10	21.04	4.21	22.87

Time (min)	Average Mass	σ
0	0	0
5	22.24	18.47
10	24.99	3.00

Table A.3 Final drug release and respective standard deviation (σ) correspondent to formulation #7R, in SSF dissolution media.

n=1	Recovery Area	Mass in 10 mL	Mass in 2 mL	Final Mass
0 min	0	0	0	0
5 min	1.01	10.05	2.01	10.05
10 min	0.99	9.90	1.98	11.91

n=2	Recovery Area	Mass in 10 mL	Mass in 2 mL	Final Mass
0 min	0	0	0	0
5 min	0.70	7.01	1.40	7.01
10 min	0.98	9.76	1.95	11.16

Time (min)	Average Mass	σ
0	0	0
5	8.53	2.15
10	11.53	0.53

Table A.4 Final drug release and respective standard deviation (σ) correspondent to formulation #8R, in SSF dissolution media.

n=1	Recovery Area	Mass in 10 mL	Mass in 2 mL	Final Mass	Time (min)	Average Mass	σ
0 min	0	0	0	0			
5 min	1.12	11.16	2.23	11.16			
10 min	1.04	10.44	2.09	12.67	0	0	0
n=2	**Recovery Area**	**Mass in 10 mL**	**Mass in 2 mL**	**Final Mass**	5	10.00	1.64
0 min	0	0	0	0	10	11.39	1.80
5 min	0.88	8.84	1.77	8.84			
10 min	0.83	8.35	1.67	10.12			

Table A.5 Final drug release and respective standard deviation (σ) correspondent to formulation #3C, in SSF dissolution media.

n=1	Recovery Area	Mass in 10 mL	Mass in 2 mL	Final Mass	Time (min)	Average Mass	σ
0 min	0	0	0	0			
5 min	1.84	18.40	3.68	18.40			
10 min	2.26	22.55	4.51	26.23	0	0	0
n=2	**Recovery Area**	**Mass in 10 mL**	**Mass in 2 mL**	**Final Mass**	5	12.61	8.20
0 min	0	0	0	0	10	16.89	13.21
5 min	0.68	6.81	1.36	6.81			
10 min	0.62	6.18	1.24	7.54			

Table A.6 Final drug release and respective standard deviation (σ) correspondent to formulation #4C, in SSF dissolution media.

n=1	Recovery Area	Mass in 10 mL	Mass in 2 mL	Final Mass	Time (min)	Average Mass	σ
0 min	0	0	0	0			
5 min	0.99	9.90	1.98	9.90			
10 min	1.07	10.68	2.14	12.66	0	0	0
n=2	**Recovery Area**	**Mass in 10 mL**	**Mass in 2 mL**	**Final Mass**	5	6.63	4.63
0 min	0	0	0	0	10	10.07	3.66
5 min	0.34	3.36	0.67	3.36			
10 min	0.68	6.82	1.36	7.49			

Table A.7 Final drug release and respective standard deviation (σ) correspondent to formulation #7C, in SSF dissolution media.

n=1	Recovery Area	Mass in 10 mL	Mass in 2 mL	Final Mass			
0 min	0	0	0	0			
5 min	2.07	20.72	4.14	20.72	Time (min)	Average Mass	σ
10 min	1.41	14.15	2.83	18.29	0	0	0
n=2	Recovery Area	Mass in 10 mL	Mass in 2 mL	Final Mass	5	13.38	10.38
0 min	0	0	0	0	10	14.95	4.73
5 min	0.60	6.04	1.21	6.04			
10 min	1.04	10.39	2.08	11.60			

Table A.8 Final drug release and respective standard deviation (σ) correspondent to formulation #8C, in SSF dissolution media.

n=1	Recovery Area	Mass in 10 mL	Mass in 2 mL	Final Mass			
0 min	0	0	0	0			
5 min	1.25	12.54	2.51	12.54	Time (min)	Average Mass	σ
10 min	1.37	13.69	2.74	16.19	0	0	0
n=2	Recovery Area	Mass in 10 mL	Mass in 2 mL	Final Mass	5	9.50	4.31
0 min	0	0	0	0	10	13.09	4.39
5 min	0.65	6.45	1.29	6.45			
10 min	0.87	8.70	1.74	9.99			

Table A.9 Final drug release and respective standard deviation (σ) correspondent to formulation #3P, in SSF dissolution media.

n=1	Recovery Area	Mass in 10 mL	Mass in 2 mL	Final Mass			
0 min	0	0	0	0			
5 min	1.11	11.14	2.23	11.14	Time (min)	Average Mass	σ
10 min	1.09	10.85	2.17	13.08	0	0	0
n=2	Recovery Area	Mass in 10 mL	Mass in 2 mL	Final Mass	5	8.22	4.12
0 min	0	0	0	0	10	10.67	3.41
5 min	0.53	5.31	1.06	5.31			
10 min	0.72	7.20	1.44	8.26			

Table A.10 Final drug release and respective standard deviation (σ) correspondent to formulation #4P, in SSF dissolution media.

n=1	Recovery Area	Mass in 10 mL	Mass in 2 mL	Final Mass			
0 min	0	0	0	0			
5 min	1.54	15.36	3.07	15.36	Time (min)	Average Mass	σ
10 min	1.36	13.57	2.71	16.65	0	0	0
n=2	Recovery Area	Mass in 10 mL	Mass in 2 mL	Final Mass	5	10.29	7.18
0 min	0	0	0	0	10	12.37	6.05
5 min	0.52	5.21	1.04	5.21			
10 min	0.70	7.04	1.41	8.09			

Table A.11 Final drug release and respective standard deviation (σ) correspondent to formulation #7P, in SSF dissolution media.

n=1	Recovery Area	Mass in 10 mL	Mass in 2 mL	Final Mass			
0 min	0	0	0	0			
5 min	0.36	3.60	0.72	3.60	Time (min)	Average Mass	σ
10 min	0.94	9.39	1.88	10.11	0	0	0
n=2	Recovery Area	Mass in 10 mL	Mass in 2 mL	Final Mass	5	4.29	0.98
0 min	0	0	0	0	10	12.27	3.05
5 min	0.50	4.98	1.00	4.98			
10 min	1.34	13.43	2.69	14.43			

Table A.12 Final drug release and respective standard deviation (σ) correspondent to formulation #8P, in SSF dissolution media.

n=1	Recovery Area	Mass in 10 mL	Mass in 2 mL	Final Mass			
0 min	0	0	0	0			
5 min	1.66	16.56	3.31	16.56	Time (min)	Average Mass	σ
10 min	0.83	8.33	1.67	11.64	0	0	0
n=2	Recovery Area	Mass in 10 mL	Mass in 2 mL	Final Mass	5	11.66	6.93
0 min	0	0	0	0	10	10.56	1.53
5 min	0.68	6.76	1.35	6.76			
10 min	0.81	8.12	1.62	9.47			

Table A.13 Final drug release and respective standard deviation (σ) correspondent to the pure drug substance, in SSF dissolution media.

n=1	Recovery Area	Mass in 10 mL	Mass in 2 mL	Final Mass			
0 min	0	0	0	0			
5 min	1.07	10.70	2.14	10.70			
10 min	1.03	10.30	2.06	12.44			
n=2	**Recovery Area**	**Mass in 10 mL**	**Mass in 2 mL**	**Final Mass**	**Time (min)**	**Average Mass**	**σ**
0 min	0	0	0	0	0	0	0
5 min	1.13	11.30	2.26	11.30	5	10.40	1.09
10 min	1.10	10.97	2.19	13.23	10	12.12	1.31
n=3	**Recovery Area**	**Mass in 10 mL**	**Mass in 2 mL**	**Final Mass**			
0 min	0	0	0	0			
5 min	0.92	9.19	1.84	9.19			
10 min	0.88	8.84	1.77	10.68			

Table A.14 Final drug release and respective standard deviation (σ) correspondent to the amorphous drug substance, in SSF dissolution media.

n=1	Recovery Area	Mass in 10 mL	Mass in 2 mL	Final Mass			
0 min	0	0	0	0			
5 min	1.19	11.88	2.38	11.88			
10 min	2.28	12.80	2.56	15.18			
n=2	**Recovery Area**	**Mass in 10 mL**	**Mass in 2 mL**	**Final Mass**	**Time (min)**	**Average Mass**	**σ**
0 min	0	0	0	0	0	0	0
5 min	1.59	15.91	3.18	15.91	5	11.93	3.95
10 min	1.78	17.75	3.55	20.93	10	16.03	4.53
n=3	**Recovery Area**	**Mass in 10 mL**	**Mass in 2 mL**	**Final Mass**			
0 min	0	0	0	0			
5 min	0.80	8.01	1.60	8.01			
10 min	1.04	10.38	2.08	11.98			

Table A.15 Final drug release and respective standard deviation (σ) correspondent to the commercial product, in SSF dissolution media.

n=1	Recovery Area	Mass in 10 mL	Mass in 2 mL	Final Mass
0 min	0	0	0	0
5 min	0.07	0.73	0.15	0.73
10 min	0.31	3.08	0.62	3.23

n=2	Recovery Area	Mass in 10 mL	Mass in 2 mL	Final Mass	Time (min)	Average Mass	σ
0 min	0	0	0	0	0	0	0
5 min	0.12	1.15	0.23	1.15	5	0.80	0.33
10 min	0.29	2.89	0.58	3.12	10	3.24	0.13

n=3	Recovery Area	Mass in 10 mL	Mass in 2 mL	Final Mass
0 min	0	0	0	0
5 min	0.05	0.51	0.10	0.51
10 min	0.33	3.28	0.66	3.38

From table A.16 to A.20, the obtained results for the pH shift dissolution method applied are explicit, considering the calculations explained before.

Table A.16 Final drug release and respective standard deviation (σ) correspondent to the pH shift dissolution method approach for formulation #7R.

Time (min)	Recovery Area		Mass in the volume vessel		Mass in 3 mL		Final Mass		Average Mass	σ
	n=1	n=2	n=1	n=2	n=1	n=2	n=1	n=2		
0	0	0	0	0	0	0	0	0	0	0
5	2.26	2.30	67.78	68.93	6.78	6.89	67.78	68.93	68.35	0.81
15	1.88	2.11	56.40	63.22	5.64	6.32	63.18	70.12	66.65	4.90
30	1.77	1.95	53.10	58.38	5.31	5.84	65.52	71.59	68.56	4.29
45	0.52	0.52	51.67	52.00	1.55	1.56	69.40	71.05	70.23	1.17
60	0.49	0.53	49.01	53.50	1.47	1.60	68.29	74.11	71.20	4.12
90	0.46	0.33	46.44	33.15	1.39	0.99	67.19	55.36	61.28	8.36
120	0.48	0.49	47.93	49.48	1.44	1.48	70.07	72.69	71.38	1.85
150	0.44	0.48	44.18	47.93	1.33	1.44	67.76	72.63	70.19	3.44
180	0.40	0.46	39.66	45.73	1.19	1.37	64.57	71.87	68.22	5.16

Table A.17 Final drug release and respective standard deviation (σ) correspondent to the pH shift dissolution method approach for formulation #8C.

Time (min)	Recovery Area		Mass in the volume vessel		Mass in 3 mL		Final Mass		Average Mass	σ
	n=1	n=2	n=1	n=2	n=1	n=2	n=1	n=2		
0	0	0	0	0	0	0	0	0	0	0
5	0.91	1.61	27.21	48.19	2.72	4.82	27.21	48.19	37.70	14.84
15	1.21	1.49	36.22	44.59	3.62	4.46	38.94	49.41	44.18	7.40
30	1.38	1.57	41.25	47.13	4.13	4.71	47.60	56.40	52.00	6.23
45	0.45	0.48	44.54	48.49	1.34	1.45	55.01	62.48	58.75	5.28
60	0.45	0.49	45.25	49.10	1.36	1.47	57.06	64.55	60.80	5.30
90	0.48	0.48	48.41	47.88	1.45	1.44	61.57	64.80	63.18	2.28
120	0.46	0.45	46.45	44.91	1.39	1.35	61.06	63.26	62.16	1.56
150	0.43	0.44	43.21	43.55	1.30	1.31	59.22	63.26	61.24	2.85
180	0.42	0.44	42.32	44.26	1.27	1.33	59.62	65.27	62.45	3.99

Table A.18 Final drug release and respective standard deviation (σ) correspondent to the pH shift dissolution method approach for formulation #7P.

Time (min)	Recovery Area		Mass in the volume vessel		Mass in 3 mL		Final Mass		Average Mass	σ
	n=1	n=2	n=1	n=2	n=1	n=2	n=1	n=2		
0	0	0	0	0	0	0	0	0	0	0
5	1.38	1.60	41.54	48.05	4.15	4.81	41.54	48.05	44.80	4.60
15	1.69	1.58	50.77	47.26	5.08	4.73	54.93	52.07	53.50	2.02
30	1.79	1.49	53.59	44.70	5.36	4.47	62.82	54.24	58.53	6.07
45	0.48	0.44	47.82	44.05	1.43	1.32	62.41	58.06	60.23	3.08
60	0.50	0.44	49.73	44.31	1.49	1.33	65.76	59.63	62.70	4.33
90	0.51	0.72	50.74	71.67	1.52	2.15	68.26	88.33	78.29	14.19
120	0.47	0.43	47.38	43.12	1.42	1.29	66.42	61.92	64.17	3.18
150	0.48	0.43	47.88	42.84	1.44	1.29	68.34	62.94	65.64	3.82
180	0.47	0.42	46.65	42.31	1.40	1.27	68.54	63.69	66.12	3.43

Table A.19 Final drug release and respective standard deviation (σ) correspondent to the pH shift dissolution method approach for the commercial product not triturated, i.e., coated and dispersible tablet.

Time (min)	Recovery Area		Mass in the volume vessel		Mass in 3 mL		Final Mass		Average Mass	σ
	n=1	n=2	n=1	n=2	n=1	n=2	n=1	n=2		
0	0	0	0	0	0	0	0	0	0	0
5	0.58	0.72	17.34	21.49	1.73	2.15	17.34	21.49	19.42	2.93
15	1.91	1.73	57.43	51.91	5.74	5.19	59.16	54.05	56.61	3.61
30	2.35	2.25	70.39	67.55	7.04	6.76	77.87	74.89	76.38	2.11
45	0.58	0.60	58.21	59.88	1.75	1.80	72.73	73.98	73.35	0.88
60	0.62	0.61	61.85	61.18	1.86	1.84	78.11	77.07	77.59	0.74
90	0.60	0.58	59.65	58.50	1.79	1.75	77.76	76.22	76.99	1.09
120	0.52	0.55	52.07	54.65	1.56	1.64	71.98	74.13	73.05	1.52
150	0.53	0.52	52.99	52.24	1.59	1.57	74.46	73.36	73.91	0.78
180	0.52	0.54	52.04	54.23	1.56	1.63	75.10	76.92	76.01	1.29

Table A.20 Final drug release and respective standard deviation (σ) correspondent to the pH shift dissolution method approach for the commercial product triturated, i.e., powder.

Time (min)	Recovery Area		Mass in the volume vessel		Mass in 3 mL		Final Mass		Average Mass	σ
	n=1	n=2	n=1	n=2	n=1	n=2	n=1	n=2		
0	0	0	0	0	0	0	0	0	0	0
5	2.10	2.43	63.11	72.95	6.31	7.29	63.11	72.95	68.03	6.96
15	1.97	2.13	59.03	64.01	5.90	6.40	65.34	71.30	68.32	4.22
30	1.62	1.93	48.58	57.96	4.86	5.80	60.80	71.65	66.23	7.68
45	0.47	0.48	46.62	47.99	1.40	1.44	63.70	67.48	65.59	2.68
60	0.49	0.47	49.22	47.45	1.48	1.42	67.69	68.38	68.04	0.49
90	0.43	0.46	42.69	45.81	1.28	1.37	62.63	68.17	65.40	3.91
120	0.44	0.45	43.58	45.31	1.31	1.36	64.81	69.04	66.93	2.99
150	0.42	0.43	41.88	42.78	1.26	1.28	64.42	67.87	66.14	2.44
180	0.41	0.41	40.95	41.48	1.23	1.24	64.74	67.85	66.29	2.20

B. XPS Analysis

Figure B.1 SEM micrograph correspondent to the physical mixture (blend drug:polymer in the same proportion used to produce the formulations, 60:40 % wt.) at a magnification of 1 500x.
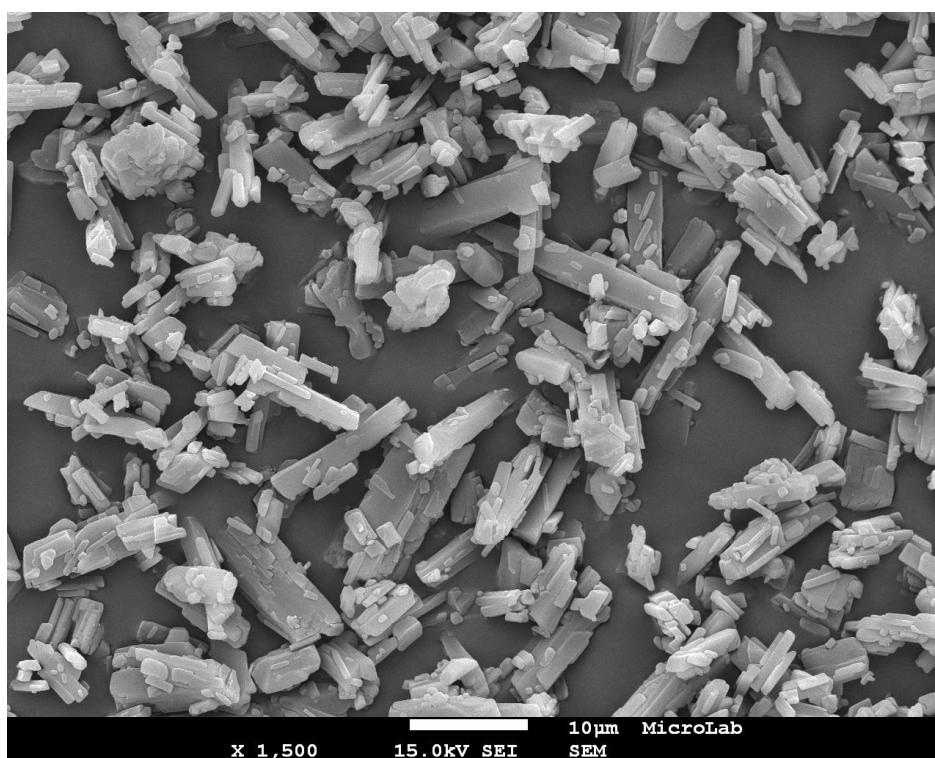

Figure B.2 SEM micrograph correspondent at the model pure drug at a magnification of 1 500x.